IDENTIFICATION OF EG5 AS A MIND BOMB1-ASSOCIATED PROTEIN AND THEIR ROLES IN CENTROSOME DUPLICATION

By

Lisa A. Lukaesko

A DISSERTATION

Presented to the Neuroscience Graduate Program

and the Oregon Health & Science University

School of Medicine

in partial fulfillment of

the requirements for the degree of

Doctor of Philosophy

August 2007

School of Medicine
Oregon Health & Science University

CERTIFICATE OF APPROVAL

This is to certify that the Ph.D. dissertation of
Lisa A. Lukaesko
has been approved by:

Dr. Wenbiao Chen, advisor

Dr. Jan Christian, Committee chair

Dr. Hua Lu, Committee member

Dr. Matthew Thayer, Committee member

TABLE OF CONTENTS

LIST OF TABLES AND FIGURES

ACKNOWLEDGEMENTS

First of all, I would like to thank my advisor, Wenbiao Chen, for the opportunity to work in his laboratory. His enthusiasm for diverse areas of science has created a stimulating scientific environment to work, which has contributed to my development as a scientist.

My sincere appreciation goes to my past and present committee members, Jan Christian, Hua Lu, David Ransom, Bruce Schnapp, and Matthew Thayer for their advice and encouragement. I am especially indebted to Jan Christian, who I could always trust to provide a honest opinion and advice during difficult times.

My sincere gratitude goes to the present and the past NGP directors, Peter Gillepsie and Ed McCleskey, not only for their dedication to the NGP program, but also for their support and advice throughout the years. I would not be writing this today without them.

I would like to thank those who have contributed to the work presented in this thesis: Corey Bystrom for mass spectrometry analysis, Aurelie Synder for confocal work on mitotic spindles in the retina, Patricia Gallagher for the generous gift of the Mind bomb antibody, and Uwe Wolfrum for his kind donation of Centrin-3 antibody.

To Chen lab members past and present, I would like to thank for all of the helpful feedback that I received during our discussions and for making the laboratory a pleasant place to work.

Endless thanks to my friends, without your kindness, graduate school would have been more difficult. I would like to thank my friends of Tae Kwon Do for their encouragement and camaraderie. Despite the nature of the sport, you are the sweetest people I know. Special thanks goes to Mandy M. and Scott H. who go out of their way to be dear friends. Their home is always a warm place to visit after a challenging day in the laboratory. I am indebted to my dear friend, Viviana D., for not only for the many ways she has helped me during graduate school, but also for being a generous and caring friend. I could fill pages with all the ways that I am grateful for our friendship.

I would like to thank my best friend and husband, Juan, for his endless love, patience, and support during this process. He was always there to give encouragement and hugs, even during the toughest times.

To my mother and father, I would like to express appreciation for all their sacrifices so I could have the luxury of an education. It is through their faith in me and my endeavors that this is possible. Finally, I would like to thank my Grandma and Pops, who taught me that in everything I do I should work hard and with integrity.

ABSTRACT

Mind bomb1 is a newly identified RING finger type E3 ubiquitin ligase with only a few known associated-proteins. Using a proteomic-based approach, I identified an array of associated-proteins of Mind bomb1, including the plus-ended kinesin Eg5. In this dissertation, I characterize in more detail the interaction between Mind bomb1 and Eg5. Mind bomb1 and Eg5 can co-immunoprecipitate, an association that requires the N terminal region of Mind bomb1. Furthermore, Mind bomb1 can promote the monoubiquitination of Eg5. Both Eg5 and Mind bomb1 co-localize at the centrosome and alteration of their levels or activity cause centrosome defects. Specifically, Eg5 inhibition and Mind bomb overexpression can both cause excess centrosomes and centrioles. Conversely, Mind bomb1-silencing can reduce the number of centrosomes produced in normal and Aphidicolin-induced centrosome duplication. Moreover, Eg5 overexpression can rescue Mindbomb1-induced centrosome overproduction. Together, these data indicate that Mind bomb1 and Eg5 function in the same pathway to ensure the proper number of centrosomes. This novel finding of two critical regulators of the centrosome contributes to our understanding of how centrosome number is maintained.

CHAPTER ONE

Introduction and Background

Death-Associated Protein Kinase (DAPK), a regulator of apoptosis [7]. Despite extensive efforts, a comprehensive understanding of Mib1 is lacking. One way to reveal other functions of Mib1 is to identify additional interacting-proteins of Mib1.

To this end, I initiated a proteomic-based screen to identify co-purifying proteins of Mib1 by mass spectrometry. This dissertation examines the relationship between Mib1 and one of the proteins identified, Eg5. A member of the kinesin-5 class of plus-end directed kinesins. Eg5 has been proposed to regulate bipolar spindle

Introduction

The Notch pathway is a highly conserved pathway that regulates a wide array of cellular processes, including stem cell self-renewal, cell proliferation, and cell fate specification [1, 2]. Notch signaling is initiated when the Notch receptor interacts with one of its ligands, Delta, Serrate, or Lag2, collectively referred to as DSL [1]. Ligand-binding promotes two cleavage events in the Notch receptor and ultimately leads to the translocation of the intracellular domain of the receptor into the nucleus, where it promotes transactivation of Notch target genes, such as *her4* [1]. Although much is known about the Notch signal transduction cascade, little is known about the regulation of DSL. Recently, Mind bomb1 (Mib1), a RING finger E3 ubiquitin ligase, was found to regulate DSL ligands by promoting their ubiquitination and in many instances internalization [3-6]. This ubiquitination is essential for activation of Notch signaling. Consequently, *mib1* mutants lack many cell types and die during embryonic development. In addition to regulation of DSL ligands, Mib1 also regulates other proteins involved in different cellular processes. For example, Mib1 also regulates the Death-Associated Protein Kinase (DAPK), a regulator of apoptosis [7]. Despite extensive efforts, a comprehensive understanding of Mib1 is lacking. One way to reveal other functions of Mib1 is to identify additional interacting-proteins of Mib1.

To this end, I initiated a proteomic-based screen to identify co-purifying proteins of Mib1 by mass spectrometry. This dissertation examines the relationship between Mib1 and one of the proteins identified, Eg5. A member of the kinesin-5 class of plus-end directed kinesins. Eg5 has been proposed to regulate bipolar spindle

formation [8]. Although the role of Eg5 in spindle formation has been extensively investigated, clear, mechanistic proof of its spindle function is currently unavailable [9]. The function of Eg5 is not limited to the spindle as Eg5 could also have a role at the centrosome. Eg5 inhibition studies found centrosome disorganization and separation defects [10, 11]. However, the role of Eg5 at the centrosome has not been sufficiently investigated.

Interestingly, I found that Mib1 and Eg5 could regulate centrosome numbers. Centrosomes are classically thought to be the microtubule-organizing center of the cell [12]. The centrosome consists of a pair of centrioles surrounded by pericentriolar matrix (PCM) [13]. This pair of centrioles is duplicated, so that only a single pair is passed on to both the mother and daughter cell during cytokinesis [14]. This process of duplication occurs only once per cell cycle, during S phase [15]. However, it is unclear exactly how centrosome duplication is controlled, as few regulating-proteins are known.

As excess centrosomes have been observed in a large number of solid tumors and hematological malignancies, a better understanding of centrosome duplication is necessary to determine whether it contributes to or is the consequence of cancer [16, 17]. The finding that Eg5 and Mib1, as described in this dissertation, are two critical regulators of centrosome duplication contributes to our understanding of this process.

This dissertation is broken down into the following chapters: the remainder of Chapter One gives an overview of Notch signaling and describes what is currently known about Mib1 function including the current findings for the second known

substrate of Mib1, DAPK. Also covered in this chapter are the currently known mechanistic and cellular functions of Eg5. Since a role for Eg5 and Mib1 in centrosome duplication will be described in Chapter Three of this dissertation, current knowledge of centrosome duplication and its implications to tumorigenesis will be discussed.

Chapter Two reports the results of the proteomic screen for Mib1-interacting proteins. It will describe the biochemical interaction between Mib1 and one of its identified substrates, Eg5, including the finding that Eg5 is monoubiquitinated by Mib1. It will also address the significance of this monoubiquitination by examining whether Mib1 promotes Eg5 relocation. Also included is the characterization of the zebrafish *eg5* hypomorphic mutant that was generated through insertional mutagenesis. These *eg5* mutants, along with previously characterized *mib1* null insertional mutants, were used to address whether Eg5 and Mib1 share common roles in spindle formation or Notch signaling.

Chapter Three describes a novel role of Eg5 and Mib1 in regulating centrosome numbers. Evidence is presented that shows that both Eg5 and Mib1 are localized to the centrosome and regulate centrosome amplification. The consequence of this centrosome defect on spindle formation and pericentriolar protein localization will be described.

Chapter Four summarizes the findings of the first three chapters and describes the significance of Mib1 mediated monoubiquitination of Eg5. In addition, the greater

implications of Mib1 and Eg5 mediated centrosome regulation and future directions will be discussed.

Background

Mib1 mutants have defects in cellular specification

The highly conserved Notch signaling pathway regulates a diversity of cellular processes, including cellular specification, proliferation, and apoptosis [1]. The primary components of the pathway are the receptor Notch and its transmembrane ligands, Delta, Serrate/Jagged, and Lag2 (DSL) [1]. Binding of Notch to DSL promotes two proteolytic cleavage events, releasing an active form of Notch, the Notch intracellular domain [18]. The Notch intracellular domain translocates to the nucleus, where it coordinates with the DNA binding protein CSL (CBF1/RBPjK, Su(H), Lag1) and the co-activator Mastermind, to promote transcription of genes involved cellular specification, including the bHLH transcription factor, *her4* [19]. Although much is known about transduction pathways downstream of Notch, little is known about the regulation of DSL ligands.

Recently, the E3 ubiquitin ligase, Mib1, was found to regulate the activity of Notch. In two independent mutagenesis screens in zebrafish, the *mib1* mutant was discovered and had a phenotype suggestive of a Delta-Notch signaling pathway defect [20, 21]. The Notch signaling pathway is best known for its role in cell fate specification during neurogenesis [22]. Mutants of the Notch signaling pathway have defects in the relative abundance of primary and secondary neurons in the nervous

system [22]. Similarly, *mib1* mutants have an excess of primary neurons at the expense of secondary neurons and glia, which could suggest that *mib1* is a component of the Notch signaling pathway [4, 5]. Since these initial studies, Mib1 was found to function not only during neurogenesis, but also in many developmental processes, such as development of the lateral line hair cells [19], hematopoiesis [23], differentiation of the pronephros [24], retina specification [25], and specification of the intestinal epithelium [26].

Mib1 encodes an E3 ubiquitin ligase

After the initial discovery of the Mib1 mutant, the *mib1* gene was cloned and found to encode an E3 ubiquitin ligase, a component of the ubiquitination reaction. The ubiquitination reaction involves a sequential series of ubiquitinating enzymes: the E1 activating-enzyme, the E2 conjugating-enzyme, and the E3 ubiquitin ligase [27]; (Figure 1.1). In the final step of this process, the ubiquitin is transferred to its substrate mediated by the E3 ubiquitin ligase. E3 ubiquitin ligases are a crucial part of the ubiquitin reaction as they contain domains involved in substrate recognition [27]. It is the ability of E3 ubiquitin ligases to recognize substrates that confers specificity to the ubiquitination reaction. Therefore, the study of E3 ubiquitin ligases, like Mib1, is important for the understanding of specificity of the ubiquitination reaction.

Mib1 contains several conserved protein domains: a ZZ zinc finger and two conserved Mib1-specific domains in the N terminal region, six to eight ankyrin repeats in the center of the protein, and most notably three RING domains in the C terminal region [5]. RING fingers, consisting of eight histidine or cysteine residues that

coordinate zinc in a cross-brace arrangement, are characteristic of the RING finger type of E3 ubiquitin ligases [28] [27]. Unlike other types of E3 ubiquitin ligases, the RING finger type lack catalytic activity and are not directly involved in the transfer of ubiquitin to the substrate protein [27, 29]. Crystallography of several RING finger E3 ubiquitin ligases with E2-conjugating enzymes show that the RING finger directly interacts with the E2-conjugating enzyme [29-33]. Therefore, it was proposed that the E3 ubiquitin ligases act as scaffolds to bring the substrate in close proximity to E2-conjugating enzyme to promote direct transfer of ubiquitin from E2-conjugating enzyme to the substrate [29, 34, 35]. One identifying feature of RING finger type of E3 ubiquitin ligases is self-ubiquitination activity, a feature that Mib1 possesses [5].

Substrates of Mib1

As E3 ubiquitin ligases play an essential role in substrate recognition, E3 ubiquitin ligases are often described in terms of the substrates that they regulate. The identity of a potential substrate of Mib1 was revealed by phenotypic analysis of *mib1* zebrafish mutants. The phenotype of *mib1* null mutants was very similar to that of the *delta* mutants; therefore, it was proposed that Mib1 could regulate Delta [4, 5]. Indeed, immunoprecipitation experiments showed an association between Delta and Mib1. Furthermore, *in vivo* ubiquitination assays demonstrated Mib1 promoted the ubiquitination of the Notch ligand Delta [4, 5]. *In vitro* ubiquitination assays also found Mib1, along with E2 and E1, is sufficient to ubiquitinate Delta, which suggests that Mib1 functions as a single protein type E3 ubiquitin ligase and not a multicomponent E3 ubiquitin ligase [5].

Ubiquitin ligases can modify their substrates by a number of structurally distinct ubiquitin modifications. The substrate can be conjugated by a single ubiquitin, monoubiquitination, or by one of approximately seven structurally distinct lysine-linked ubiquitin chains, polyubiquitination [36]. These distinct ubiquitin modifications can potentially signal diverse outcomes for the substrates. The most well studied ubiquitin modification is the $Lysine^{48}$-linked polyubiquitin [37]. Modification of a substrate with the $Lysine^{48}$-linked polyubiquitin can target the substrate to the proteasome for degradation [37]. Moreover, polyubiquitin chains linked through $Lysine^{11}$ and $Lysine^{29}$ have also been shown to target its protein substrates to the proteasome [37-40]. Conversely, ubiquitin modifications can signal nonproteolytic events and regulate localization, activity, or interactions of a substrate [36]. The most highly studied of these non-proteolytic ubiquitin modifications is monoubiquitination, which can regulate a number of cellular processes such as endocytosis, protein trafficking, transcription, and histone function [36]. $Lysine^{63}$-linked polyubiquitin chains can also promote proteasome-independent events such as endocytosis, protein trafficking, inflammatory response, and DNA repair [41-45].

The type of ubiquitin modification that Mib1 conjugates on Delta could reveal the significance of their interaction. In an ubiquitination assay, used to determine the ubiquitin modification of Delta by Mib1, ubiquitin laddering of Delta was observed on a Western blot [5]. This laddering was interpreted to be polyubiquitination. However, as Mib1 migrates close to Delta, this laddering could also be from Mib1 self-ubiquitination [5]. Therefore, it is currently unknown the type of modification that

Mib1 conjugates on Delta. More extensive studies are necessary to determine the answer to this important question.

Mib1 mediated endocytosis of DSL Ligands

As discussed in the previous section, the type of ubiquitin modification conjugated on a substrate determines diverse outcomes for a substrate. Although it is unknown the type of ubiquitin that Mib1 conjugates on DSL ligands, the consequence of its interaction is suggested by evidence in the literature. Previously, it was shown that DSL ligands need to be endocytosed to be able to fully activate Notch [3, 46]. Furthermore, endocytosis of DSL ligands require Epsin, a protein that recognizes ubiquitin modifications of extracellular membrane proteins and promotes clathrin-mediated endocytosis by causing the extracellular membrane to bend [47, 48]. Taken together, this evidence would suggest the ubiquitin-mediated endocytosis of DSL ligands is required for their activation. Since Mib1 promotes ubiquitination of DSL ligands, it could be possible that it could promote endocytosis of DSL ligands as well.

The possibility of Mib1 mediated endocytosis of DSL ligands was addressed in Drosophila and in tissue culture. Mib1 loss- and gain- of- function experiments found that Mib1 is necessary and sufficient for endocytosis and degradation of Serrate [6, 49-51]; (Figure1.2). These results support the theory of a Mib1 mediated endocytosis and degradation of Serrate [3-6, 51]. However, examination of Mib1 mediated endocytosis of Delta gave conflicting results. Overexpression of Mib1 in both vertebrate tissue culture cells and *Drosophilia* wing discs showed enhanced

extracellular membrane depletion of Delta, suggestive of enhanced endocytosis. However, the wing discs of *Drosophila* loss-of-function *mib1* mutants showed no difference in the level of Delta at the extracellular membrane compared to wild type [3-6, 51]. Furthermore, *Drosophila* loss-of-function *mib1* mutants also did not exhibit enhanced endocytosis of Delta as demonstrated by lack of uptake of a Delta antibody in an antibody uptake assay [51]. Although, Mib1 gain-of-function experiments in *Drosophila* support Mib1 mediated degradation of Delta, no degradation of Delta was observed by overexpression of Mib1 in HEK-293 cells. The necessity of Mib1 for degradation of Delta was addressed in Drosophila by overexpression of a Mib1 RING finger deletion construct, which could act as a dominant negative for endogenous Mib1 [6]. Upon overexpression of this deletion construct, a increase in the levels of Mib1 at the extracellular membrane of the wing disc was observed [6]. However, an increase in Mib1 levels in loss-of-function or null Mib1 mutants has yet to be described. Taken together, these results suggest that Mib1 can promote endocytosis and in some tissues, degradation, of Delta, but Mib1 may not be necessary for these processes in all tissues.

One explanation for this apparent discrepancy between Mib1 loss-of- and gain-of-function experiments is the existence of a paralog of Mib1, Mind bomb2 (Mib2) [52]. Mib2 could possibly substitute for Mib1 in the loss-of-function experiments. The amino acid sequences of Mib1 and Mib2 have 36% identity and 52% similarity [52]. The protein domains and their organization of Mib2 are nearly identical to Mib1, except Mib2 has only two RING finger domains as opposed to three RING fingers

domains of Mib1 [52]. Unlike *mib1*, which is abundantly expressed in zebrafish embryos, the expression of *mib2* in embryos is weak [52]. However, Mib2 is abundantly expressed in the mouse adult tissues of the heart, liver, kidney, and brain [52]. Most importantly, *mib2* can rescue the neurogenic and vascular defects of *mib1* zebrafish mutants [52]. Furthermore, it was shown that Mib1 and Mib2 share the same substrate, DeltaC [53]. Both Mib1 and Mib2 can both immunoprecipitate and promote internalization of DeltaC in Cos7 cells [53]. However, not all substrates are shared, since only Mib1 can regulate DeltaD [53].

DAPK is also a substrate of Mib1

Understanding Mib1 regulation is further complicated by the discovery of an additional substrate for Mib1. This substrate, DAPK, was found to interact with the human homolog of Mib1 [7]. DAPK, a serine-threonine kinase, regulates apoptosis and acts as a tumor suppressor in early stages of tumor development. [7]. DAPK responds to multiple triggers, including IFN-γ, Fas, TNFα, ceramide, TGFβ, or oncogene-induced proliferation, then promotes apoptotic or autophagic cell death through caspase-dependent and -independent pathways [54]. Mib1, through ubiquitination and degradation of DAPK, antagonizes its pro-apoptotic function [55]. The fact that Mib1 is capable of regulating substrates with uniquely, different cellular functions demonstrate that we are just beginning to understand the function of Mib1.

Proteomic Approach to Identifying Mib1-Associated Proteins

Despite significant advances made in understanding the function of Mib1, there are limitations because few Mib1-interacting proteins are known. One method to identify novel interacting proteins is by proteomics. Proteomic methods have become an efficient method for identification of protein complexes because of improvements made in purification of protein complexes, development of highly sensitive mass spectrometric techniques, and advances in bioinformatics analysis making it a simpler and more accessible method to identify novel protein interactions [56-58].

Epitope-tag affinity purification, in combination with mass spectrometry, is the most widely used method to purify protein complexes [59, 60]. In particular, a few epitope tags (such as FLAG, GST, and His) are often used, as there small size is unlikely to interfere with the biological function of the purified proteins. FLAG affinity purification particularly offers some significant advantages since the 3X FLAG peptide, used for elution of purified complex, is the most effective and purest method for elution [59].

The most significant advance in proteomics was the development of the gentler ionization techniques for mass spectrometry, Electrospray (ESI) and Matrix-Assisted Laser Desorption Ionization (MALDI) [58]. These techniques ionize molecules and transfer them to the gaseous phase without excessive fragmentation. Prior to development of ESI and MALDI, ionization was done by chemical ionization or fast atom bombardment; these methods are too harsh for fragile biomolecules [57, 58]. The advent of these gentler and less expensive ionization techniques has made mass

spectrometry widely available to biochemists [57, 58]. For these reasons, I decided to use mass spectrometry to identify associated-proteins of Mib1.

Eg5 may function in mitotic spindle formation

As described in Chapter Two, I took a proteomics approach to identify novel interacting-proteins of Mib1. One of the proteins identified in the screen was Eg5, a member of the kinesin-5 subclass of kinesins [8]. This subclass of plus-end-directed kinesins share high homology (about 50-60%) within their N-terminal motor domains, but share virtually no homology in their stalk and tail domains. Rotary shadow electron microscopy of the family member KRP130, suggested the kinesin-5 family forms homotetramers with a pair of motor domains at each opposing end [8]; (Figure1.3).

The best-described function of Eg5 is its regulation of the mitotic spindle. Before the function of Eg5 at the mitotic spindle can be described, an introduction to the structure and function of the mitotic spindle is necessary.

During mitosis, the bipolar microtubule-based structure, the mitotic spindle, is formed whose main function is to separate chromosomes [61]. The microtubules at the mitotic spindle are usually assembled at the centrosome, located at polar ends of the cell [62, 63]. The mitotic spindle consists of an array of antiparallel microtubules with minus ends of the microtubules focused at the polar ends and plus ends of the microtubules directed towards the equator [64]. The spindle consists of two major populations of microtubules: the kinetochore microtubules, which dock with

kinetochores of chromosomes, and interpolar microtubules, which interact with interpolar microtubules from the opposite pole [64]. The interpolar microtubules are dynamic, that are characterized by microtubule assembly at the spindle equator and microtubule disassembly at the pole, the centrosome [64]. At the same time, interpolar microtubules slide slowly toward the pole [64]. This sliding must be coordinated with the dynamically instability of spindle microtubules to promote poleward translocation of spindle microtubules, a state called poleward flux [64]. This poleward translocation of the interpolar microtubules will also drive poleward translocation of the associated kinetochore microtubules and their attached chromosomes apart during anaphase [64].

Eg5 may function in the poleward translocation of interpolar microtubules. Eg5 localization to the antiparallel radial array of the mitotic spindle is consistent with this function [65]. Furthermore, Eg5 inhibition studies also suggest Eg5 functions at the mitotic spindle. Inhibition of Eg5 activity or expression causes a single mitotic spindle to form around a central pole, a monastral spindle [66, 67]. Therefore, it was proposed that the opposing motor domains of Eg5 tetramers interact with antiparallel microtubules of the mitotic spindle [65]. Through this interaction, Eg5 could generate a force that promotes poleward translocation of spindle microtubules during poleward flux [68]. Alternatively, Eg5 could promote stabilization of these microtubules [68]. The monostral spindle generated by Eg5 inhibition could be caused by failure of Eg5 to either slide or stabilize spindle microtubules, which leads to a collapse of the dynamic spindle microtubules [69, 70].

Whether Eg5 promotes either sliding or stabilization of spindle microtubules would depend on the mode of Eg5 movement along microtubules [68]. There are two major modes of movement for kinesins: processive and non-processive [71]. A non-processive motor will dissociate shortly after a single step; a processive motor has sustained contact taking multiple step along a microtubule before dissociating [71]. For Eg5 to promote antiparallel sliding, it would have to function as a processive motor, since this would require sustained contact with the antiparallel microtubules [9].

To understand the function of Eg5 at spindle microtubules, its processivity would need to be known. Whether Eg5 is a processive motor is under intensive investigation and debate. Initial measurements of Eg5 movement, based on the number of ATP molecules consumed per microtubule contact, suggested that Eg5 was a nonprocessive motor [72, 73]. These estimates are imprecise as assumptions are made about the rate of dissociation of ATP [74]. A more precise measurement of Eg5 processivity was provided by optical trapping experiments. Two independent studies using this method, found that Eg5 was able to take about 8 step runs with a step size of 8.1 nm before dissociation, measurements expected for a processive motor [75, 76]. However, these optical trapping experiments only examined the dimeric forms of Eg5, native tetrameric forms could significantly differ in their processive properties [68]. Furthermore, these studies only measure the function of a single motor protein. If Eg5 cooperates with multiple motor proteins it function could also differ [77]. Therefore,

the question whether Eg5 is a processive motor awaits the development of more sophisticated techniques.

Although a definitive answer to whether Eg5 promotes stabilization or sliding of spindle microtubules would depend on its processivity, some evidence of Eg5-promoted sliding is supported by a study by Shirasu-Hiza et al [78]. The study Eg5-generated poleward movement independent of dynamic behavior of interpolar microtubules requires stabilization of spindle microtubules [78]. To that effect, Shirasu-Hiza et al. stabilized the isolated bipolar spindle microtubules with Taxol [78]. Upon addition of partially purified Eg5, they noticed poleward movement of the spindle microtubules, which suggests that Eg5 promotes microtubule-sliding [78].

Eg5 may regulate the centrosome

While much research has focused on how Eg5 organizes the mitotic spindle during mitosis, several groups found that Eg5 may have an additional role in centrosome regulation. Whitehead et al. found that Eg5 may have a role in centrosome separation independent of its role in spindle stabilization [10]. Injection of an Eg5 interfering antibodies into interphase cells that contain unseparated centrosomes, caused a prometaphase block and monopolar spindles [10]. However, if the antibody was injected into cells containing separated centrosomes, initial spindle formation was not blocked, but later in mitosis the spindle collapsed [10]. These results suggest that Eg5 may be essential during two phases critical during spindle formation: the

separation of centrosomes required for bipolar spindle formation and maintenance of the structure of a formed bipolar mitotic spindle.

Studies of the *S. cerevisiae* ortholog of Eg5, Cin8p, provided a potential mechanism for the role of Eg5 in centrosome separation. In Cin8p mutants, separation of the yeast analogous structure of the centrosome, the Spindle Pole Body (SPB), was inhibited. The SPB contains an electron-dense bridge structure that serves as the site of its duplication and eventually joins the resultant SPBs together [79]. Crasta et al. found in *S. cerevisiae* bundling deficient mutants of Cin8p, the bridge connecting these two SPBs failed to break [11]. They proposed that Cin8p generates force required for SPB separation [11]. Additional work by de Gramont et al. determined the consequences of failed SPB separation in Cin8p mutants, including abnormal orientation and number of astral microtubules, microtubules that projects from the spindle to the cortex and function to orient the mitotic spindle and the nucleus [80]. To that effect, de Gramont et al. also noted abnormal nuclear positioning in Cin8p mutants [80].

Further evidence for a role of Eg5 at the centrosome was provided by the observation that inhibition of Eg5 caused centrosome disorganization. This disorganization was characterized by a diffuse localization of the key centrosomal proteins, ninein, and Cep250 [10, 81]. However, the cause of this abnormal distribution of centrosomal proteins was not explained.

Taken together, these studies suggest that Eg5 may have a role at centrosome independent of its role at the mitotic spindle. However, the exact function of Eg5 at the centrosome has not been investigated.

Centrosome structure

Centrosomes are classically thought to be the Microtubule Organizing Center (MTOC) of the cell, a region where cytoplasmic interphase microtubules and mitotic spindle microtubules are assembled [62]. The structure of the centrosome is just beginning to be understood, but it is known to be composed of a pair of microtubule-containing barrel shaped structures, centrioles, that are surrounded by filamentous matrix, the pericentriolar material (PCM) [82]; (Figure 1.4A). The mature centriole is composed of nine triplets of complete 13 protofilament microtubules and two incomplete 10 or 11 protofilament microtubules [13]. The centriole has a polarized organization. The proximal end of the lumen contains a cartwheel like disc structure, but the distal end contains an undefined electron dense structure [13]. This polarized nature of the centriole is also exhibited by the outer surface of the centriole. At the proximal end of the outer surface resides immature centrioles, procentrioles, whereas the distal end has appendages [13]. There are functional differences between the proximal and distal ends. The proximal end is the exclusive site of new centriole formation and the distal end is the site for primary cilia formation and microtubule nucleation [62].

The PCM surrounds the centriole, although it is preferentially localized to the mature centriole. The PCM contains two major components: ring complex and lattice-like filaments [83]. The ring complex contains γ-tubulin, the template for microtubule nucleation. γ-tubulin forms a complex with a major component of the lattice-like network, Pericentrin. Although the significance of this Pericentrin-γ-tubulin complex is still being investigated, it is thought to be essential for microtubule nucleation [84].

Much still remains to be learned about the composition and structure of the centrosome. Large-scale proteomic screens have recently identified many previously unknown components of the centrosomes [85, 86]. Further characterization of these components may elucidate not only how the centrosome is structured, but could also reveal how the centrosome is regulated.

Centrosome duplication cycle

The centrioles of the centrosome must be duplicated to ensure that the single pair of centrioles is passed on to the mother and daughter cell during cytokinesis [12]. Failure of centrioles to properly segregate during cytokinesis can result in abnormal mitotic spindle assembly during mitosis [87]. The centrosome duplication cycle temporally corresponds to the DNA replication cycle and consists of three main stages: (1) centriole disengagement, (2) centriole duplication, and (3) separation of the centrosomes [88]; (Figure1.4B). After cytokinesis, each centrosome contains a mother and daughter centriole oriented orthogonally to each other by a poorly defined cohesive structure that joins them at their proximal ends [13]. The centrosome cycle

begins in early G1 when the cohesive structure dissolves, a process called disengagement, which results in loss of the orthogonal arrangement of the mother-daughter centriole pair [12]. The mother and daughter centriole are then joined by a microtubule-based intercentriolar bridge at their proximal ends [89, 90]. Beginning at the G1/S phase transition, centrioles duplicate creating new centrioles, called procentrioles [12]. These procentrioles grow orthogonal to both of the mother and daughter centrioles and will continue to elongate until G2 [12]. The development of these procentrioles creates a total of four centrioles contained within two centrosomes. After the intercentriolar bridge connecting the mother and daughter centrioles breaks, the two centrosomes will separate to opposite poles of the cell [90]. This separation ensures that during cytokinesis each cell will inherit a single centrosome, containing a one pair of centrioles, during cytokinesis.

Regulation of centrosome duplication

Because centrosomes must duplicate to form precisely one centrosome per cell cycle, control mechanisms must exist to regulate this process. Currently, there are four major theories of how the process of centrosome and centriole duplication is regulated.

One theory describes centriole duplication as a templated process in which the mother centriole acts as a template for the formation of precisely one centriole, the procentriole. The close proximity of the procentriole to the mother centriole suggests that this could be a possibility [12]. Specific template or seed structures, neighboring the mother centrioles, were observed in duplication of structures analogous to the

centriole, the spindle pole body and basal body [91-93]. But the existence of seed structures in centriole duplication has yet to be proven. However, upon removal of the mother centriole, formation of procentrioles is prevented [87, 94]. This experiment demonstrates not only the requirement of the mother centriole for duplication, but may further suggest that the mother centriole may serve as a seed structure [87, 94].

A second theory, proposed by Tsou and Sterns, suggests that the process of centriole disengagement could be required for centrioles to duplicate [95]. As described above, a cohesive structure joins the orthogonally arranged mother and daughter centrioles. At the beginning of G1 phase, this structure is lost in a process called disengagement. Tsou and Sterns found that disengagement of the centrioles is necessary for centriole duplication and requires Separase, a protease well-known for its role in sister chromatid separation [95, 96]. Tsou and Stearns demonstrated the requirement of centriole disengagement for centriole duplication with an *in vitro* system consisting of purified centrosomes and *Xenopus* egg extracts [95]. When these purified centrosomes were combined with egg extracts containing an inhibitor of Separase, centrioles were not disengaged and were unable to duplicate [95]. They proposed that cohesion of centrioles during their development prevents extraneous centrosome duplication and the process of disengagement itself was a "licensing mechanism" required for centriole duplication [95]. Although this model is intriguing, some issues will need to be addressed. In particular, it will need to be established whether Separase acts directly on the centriole to cause disengagement. Furthermore,

it would also interesting determine what mechanism prevents centriole overduplication once the centrioles have been disengaged.

A third theory of regulation of centrosome duplication implicates the requirement of centrosomes to split to inhibit further centrosome duplication [97]. Parental centrioles are linked by the microtubule-based intercentriolar bridge [89, 90]. This intracellular bridge tethers parental centrioles and in many cells, keeps them in close proximity usually through most of S phase [90]. The coiled-coil protein, C-Nap1, acts to anchor this intracellular bridge to the proximal ends of centrioles [98]. Phosphorylation of C-Nap1 by NIMA-related kinase, Nek2A, displaces C-Nap1 from the centriole, which promotes splitting of the centrioles [97]. Centriole splitting is required for centriole migration to opposite poles of the cell in preparation for mitosis. If Nek2A activity is inhibited by expression of a dominant-negative construct, centrosomes fail to split and monoastral spindles form [97]. Furthermore, expression of this dominant-negative Nek2a caused excess centrosomes [97]. This result suggests that centriole splitting is required to cease centrosome duplication.

The fourth theory of centrosome duplication suggests the existence of "candidate licensing molecules" which regulate centrosome duplication [12]. As centrosome duplication corresponds to be cell cycle, candidate licensing molecules would have to be tightly regulated in a temporal or spatial manner to coordinate with the cell cycle. One proposed licensing-molecules is BRCA1, an E3 ubiquitin ligase, whose gene is linked to familial breast cancer. BRCA1 localizes to the centrosome during mitosis where it promotes ubiquitination of γ-tubulin [99-101]. Overexpression

of a mutant γ-tubulin, which lacks the lysine sites required for ubiquitination, promotes centrosome overduplication [102]. Therefore, it was proposed that ubiquitination of γ-tubulin by BRCA1 was required to prevent centrosome overduplication [102]. As ubiquitination of γ-tubulin does not cause degradation, it was proposed that this ubiquitination may serve as a signal to mark centrosomes post-duplicated centrosomes, thereby preventing reduplication [99].

Another promising candidate licensing factor is a member of the Polo-like kinases of serine-threonine kinases, SAK (also called PLK4); [103-105]. SAK/PLK4 is required for centrosome duplication, as both SAK/PLK4 RNAi in S2 cells and a SAK/PLK4 hypomorphic mutation in *Drosophila* lead to loss of centrosomes and centrioles [104-106]. Furthermore, overexpression of SAK/PLK4 in U2OS cells promotes centrosome overduplication [107]. Interestingly, SAK/PLK4 is expressed and localized at centrosomes only during mitosis [108]. Levels of SAK/PLK4 peak at the anaphase and dramatically drop at G1 [108]. As the disappearance of SAK/PLK4 corresponds to when centriole disengagement occurs, SAK/PLK4 could possibly function to prevent disengagement.

An additional potential licensing factor is Nucleophosmin (NPM), a nucleolar phospho-protein. During S to G2 transition, NPM is mostly associated with the granular region of the nucleolus, but beginning in mitosis NPM associates with the centrosome [109]. The shuttling of NPM between the nucleolus and the centrosome is regulated Ran/Crm1 which recognizes the nuclear export signal (NES) of NPM [110]. Mutations in the nuclear export signal motif of NPM prevented its localization to the

centrosome thereby reducing centrosome duplication [109]. Conversely, silencing NPM with siRNA results in excessive centrosomes [109]. It was proposed that the release of NPM from the centrosome during mitosis, licenses centrosome duplication to occur, providing a spatial mechanism to regulate centrosome duplication. Despite the promise of NPM as a centrosome "licensing factors", it is unclear how NPM might regulate centrosome duplication, as its effectors are unknown.

Although significant advances have been made in understanding centrosome duplication, we still know very little about this process. Whether centrosome duplication is dependent on a template, centriole disengagement, centriole splitting, or a "licensing factor" for its regulation will require further investigation and may depend on finding additional molecular players.

Restriction of centrosome duplication to S phase

It has been known for some time that centrosome duplication is restricted to S phase. For example, centrosome duplication continues when sea urchin eggs were blocked in S phase, but not when blocked in M phase [111]. Similarly, when CHO cells or U20S were blocked at S phase with Hydroxyurea or Aphidicolin, respectively, the centrosomes continue to duplicate [112, 113]. However, the mechanism that restricts centrosome duplication to S phase is under considerable debate. The temporal relationship between the DNA replication cycle and centrosome cycle suggests they are regulated similarly. Indeed, Cdk2 paired with either Cyclin E or Cyclin A, known regulators of DNA replication, are able to promote centriole duplication [114-118].

Some evidence suggests that Cdk2 promotes centrosome duplication through nucleophosmin (NPM), a proposed licensing factor for centrosome duplication [119]. Cdk2-cyclin E phosphorylates NPM during mitosis, promoting its release from the centrosome, and allowing centrosome duplication to proceed [120].

The centrosome duplication cycle may also be controlled independently of the cell cycle using a centrosome intrinsic mechanism. Evidence of a centrosome intrinsic control was demonstrated in experiments performed by Wong and Stearns [121]. Since centrosomes duplicate in S phase they wanted to determine whether an activating factor is present in S phase cytoplasm [121]. To examine this, cells containing duplicated or unduplicated centrosomes were fused to cells at different stages of the cell cycle [121]. When cells with duplicated G2 centrosomes were fused to S phase cells they were unable to re-duplicate the centrosomes [121]. This result suggests that a centrosome-activating factor is not present in S phase cytoplasm. An alternative mechanism is that an inhibitory factor is present at G2 that prevents extraneous duplication. To investigate whether an inhibitory factor exists, Wong and Stern fused cells with unduplicated centrosomes to G2 cells. However, they found that G2 cytoplasm did not prevent centrosome duplication [121]. These results suggest that centrosome duplication is regulated by some intrinsic factor.

From these studies, it is unresolved whether cell-cycle regulators or an intrinsic centrosome regulator controls centrosome duplication. However, it is clear that centrosome duplication must be controlled. For in the absence of these control

mechanisms, centrosomes overduplicate. As discussed in the following section, aberrant centrosome duplication has implications to tumorigenesis.

Centrosome duplication in tumor development

In most instances, centrosomes direct the formation of the mitotic spindle. When there is overduplication of centrosomes, multipolar spindles can often result, leading to failed chromosome segregation and ultimately DNA aneuploidy [122]. Excess centrosomes and DNA aneuploidy are often observed in a large number of solid tumors and hematological malignancies [17].

It has been speculated that centrosome overduplication promotes aneuploidy, since excess centrosomes has been observed at the earliest stages of malignant progression before aneuploidy [122-129]. This idea is not a new one, as Theodor Boveri in 1901 proposed that properties of malignant tumors, such as aneuploidy, could arise from centrosome defects [130, 131]. However, only recently is there evidence to support centrosomal-promoted carcinogenesis. Human cervical cancer, which is associated with excessive centrosomes, is often linked to infection with high risk Human Papillonavirus (HPV), HPV-16 and HPV-18. One study found that in neonatal human keratinocytes infected with the HPV oncoprotein E7, excessive centrosomes were present early in neoplastic progression prior to development of aneuploidy [132-134].

Additional evidence of centrosome promoted tumorigenesis is provided by a study of the early breast tumor lesion, ductal carcinoma in situ (DCIS). In this study,

excessive centrosomes were observed in these early lesions prior to aneuploidy [124]. Further support for a centrosome-mediated tumorigenesis is demonstrated by BRCA1, a gene mutated in about one half of familial breast cancers including women with DCIS [135, 136]. As described above, BRCA1 regulates centrosome duplication and is proposed to be a centrosome-licensing factor.

Although evidence suggests centrosome overduplication promotes aneuploidy, experiments with Aurora A suggests otherwise [137]. Overexpression of the candidate oncogene, Aurora A in mouse embryo fibroblasts results in cell division failure and polyploidy before excess centrosome accumulation [137]. This result suggests that excessive centrosome may reflect one of the cellular abnormalities associated with tumorigenesis, but is not the cause of aneuploidy and tumorigenesis.

Most of the evidence that examines the relationship between centrosome duplication and DNA aneuploidy in tumorigenesis is correlative. A definitive answer to whether excess centrosomes drives tumorigenesis awaits a better understanding of the molecular mechanisms governing centrosome duplication. As additional molecular players required for centrosome duplication become known, we will become closer to understanding the complex process of centrosome duplication.

ATP
ADP+PPi
Ub
E1
E2
E3
E2
substrate
Lysine 48
Degradation
(Proteasome)
substrate
Lysine 63
Protein Trafficking
Inflammatory response
DNA Repair
Endocytosis
substrate
Endocytosis
Protein Trafficking
Gene expression/silencing

Figure 1.1 Ubiquitination and the significance of ubiquitin modifications

The process of ubiquitination involves a sequential series of ubiquitinating enzymes. The first of these enzymes, the E1 ubiquitin-activating enzyme (E1), activates ubiquitin in an ATP-dependent process. The activated ubiquitin is transferred from E1 onto the active-site cysteine of an E2 ubiquitin-conjugating enzyme (E2), where it forms a thioester bond. In the last step of this process, the E3 ubiquitin ligase (E3) transfers ubiquitin to the lysine residue of a substrate. Different types of structural distinct ubiquitin modifications can be transferred to a substrate. The type of ubiquitin modification conjugated to a substrate can signal different outcomes for a substrate. This figure shows an example of the three most common types of ubiquitin modifications: Lysine 48-linked polyubiquitin chains, Lysine 63-linked polyubiquitin chains, and monoubiquitin. Lysine 48-linked polyubiquitin chains promote proteasome-mediated degradation, whereas Lysine 63-linked polyubiquitin chains and monoubiquitins promote proteasome-independent processes.

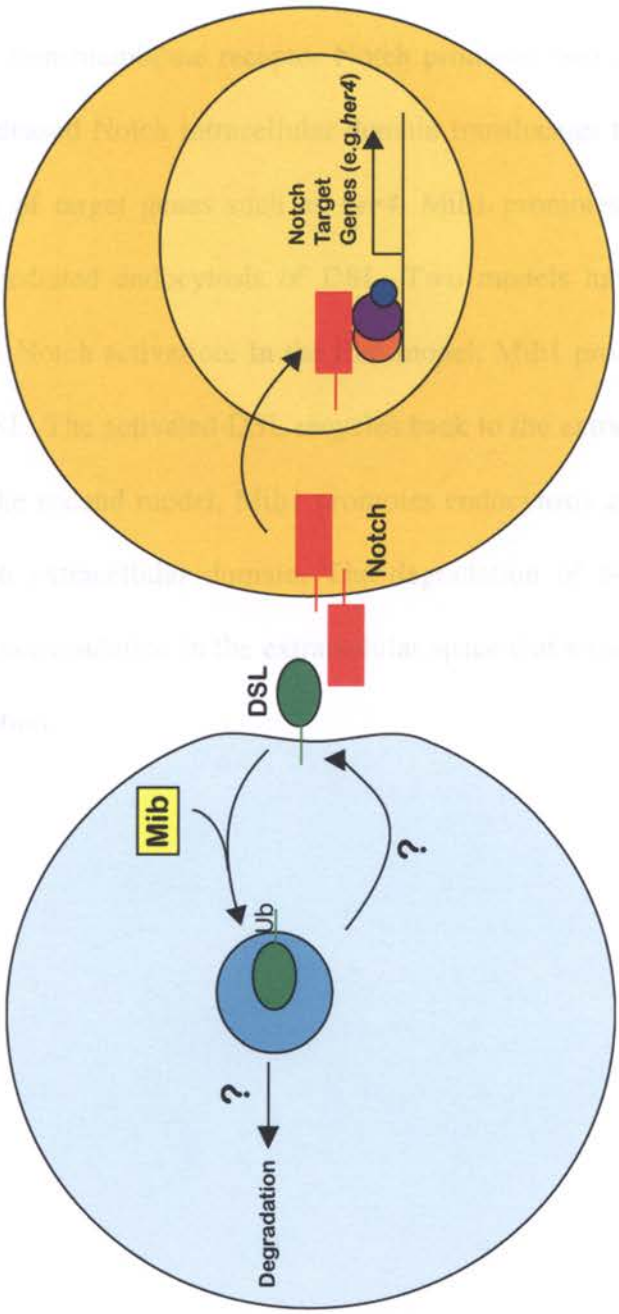
Notch Target Genes (e.g. her4)
Notch
DSL
Mib
Ub
?
?
Degradation

Figure 1.2 Regulation of the Notch signaling pathway by Mib1

DSL binding to the transmembrane receptor Notch promotes two cleavage events in the receptor. The released Notch intracellular domain translocates to the nucleus and promotes activation of target genes such as *her4*. Mib1 promotes Notch activation through ubiquitin-mediated endocytosis of DSL. Two models have been proposed how Mib1 promotes Notch activation. In the first model, Mib1 promotes endocytosis and activation of DSL. The activated DSL recycles back to the extracellular surface to activate Notch. In the second model, Mib1 promotes endocytosis and degradation of DSL and the Notch extracellular domain. The degradation of Notch extracellular domain prevents its accumulation in the extracellular space that would be inhibitory to further Notch activation.

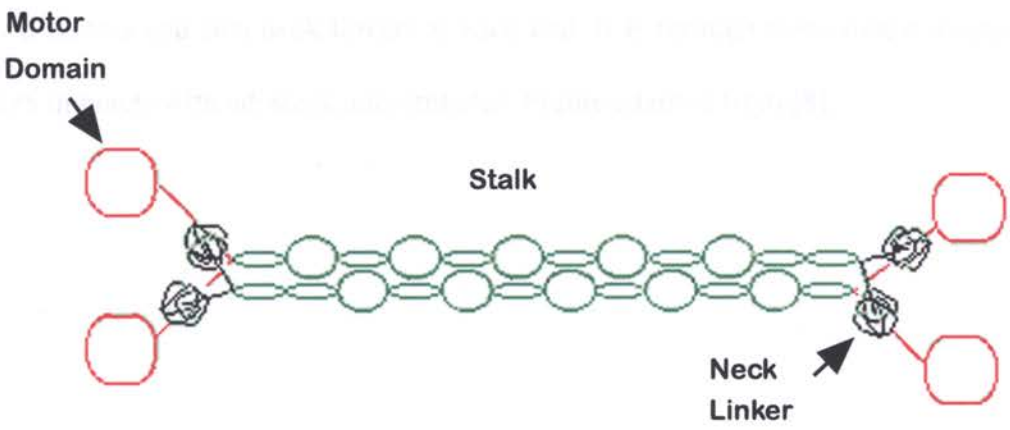
Motor
Domain
Stalk
Neck
Linker

Figure 1.3 Proposed structure of the kinesin-5 family member, Eg5

Eg5 is a plus-end-directed homotetrameric kinesin that forms tetramers through dimerization of its coiled-coil stalk domain. This dimerization creates a molecule with two motors and two neck linkers at each end. It is through these motor domains that Eg5 interacts with adjacent microtubules. Figure adapted from [8].

A.

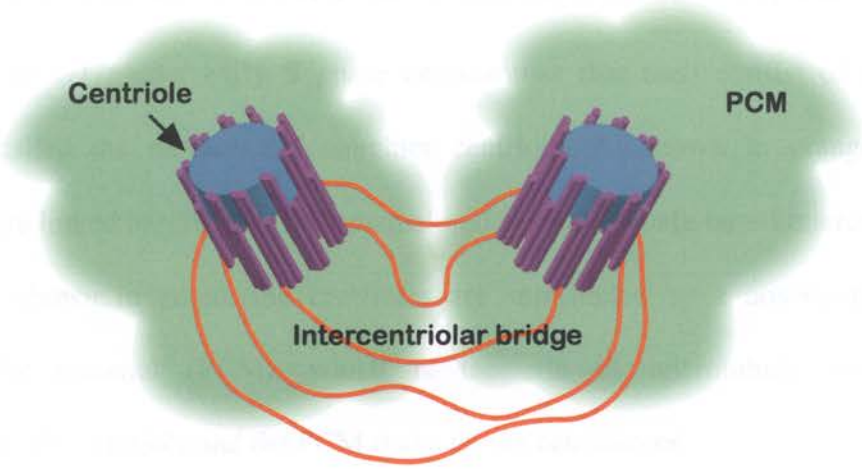
Centriole
PCM
Intercentriolar bridge

B.

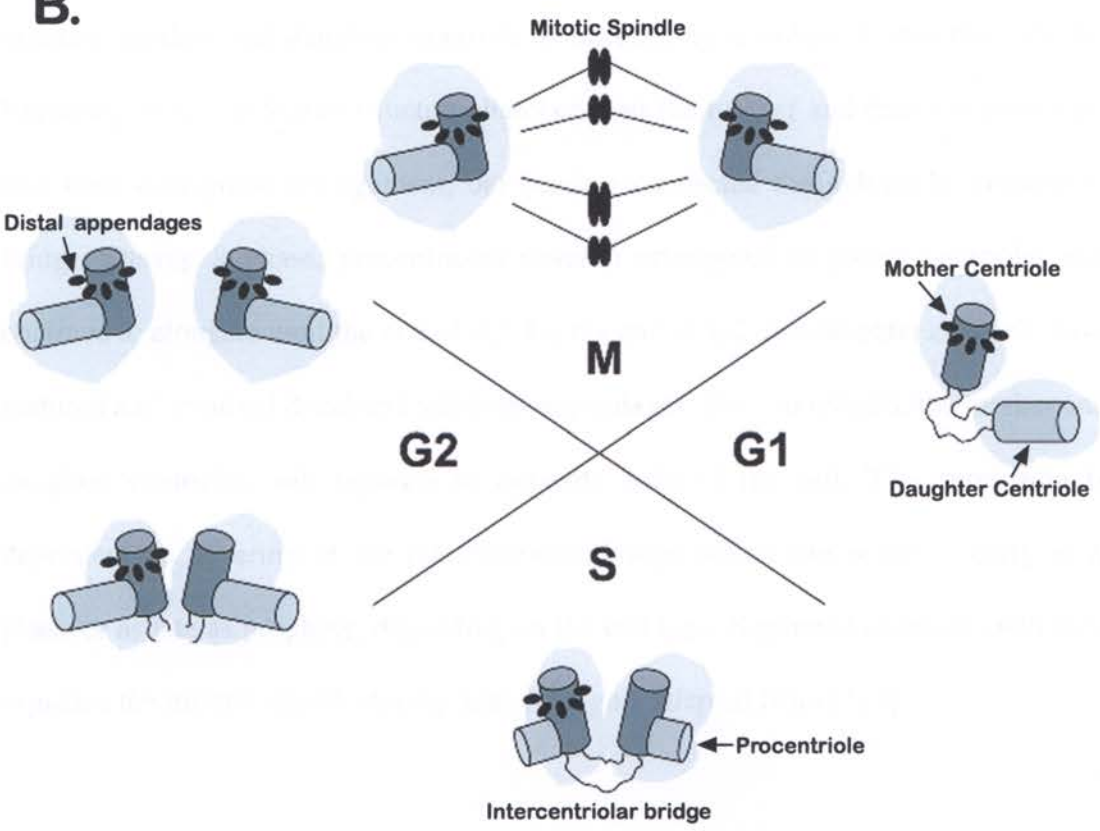
Mitotic Spindle
Distal appendages
Mother Centriole
M
G2
G1
S
Daughter Centriole
Procentriole
Intercentriolar bridge

Figure 1.4 Ultrastructure of the centrosome and the centrosome duplication cycle

(A) Two late G1 phase/ early S phase centrosomes that each consist of a single centriole, called the mother and daughter centriole. As shown in orange, these centrioles are linked together at the proximal end by microtubule-based intercentriolar bridge. As shown in green, the centrioles are surrounded by a non-membranous pericentriolar material (PCM), which is the site of microtubule nucleation. Collectively, the centriole and the PCM make up the centrosome.

(B) The centrosome cycle. The centrosome cycle temporally corresponds to the DNA replication cycle. After cytokinesis, the centrosome consists of an orthogonally oriented mother and daughter centriole connected by a cohesive structure. At the beginning of G1, cohesive structure dissolves and the mother and daughter centrioles lose their orthogonal arrangement, but become connected through an intercentriolar bridge. During S phase, procentrioles develop orthogonal to parent centrioles and continue to elongate until the end of G2. By the end of G2, the daughter centriole have matured and acquired distal and subdistal appendages. Prior to mitosis, the mother and daughter centrioles will separate to opposite ends of the cell. This separation is dependent on severing of the intercentriolar bridge which can occur as early as S phase or as late as prophase, depending on the cell type. Separated centrioles will help organize the mitotic spindle during mitosis. Figure adapted from [123].

CHAPTER TWO

Characterization of the

Mind bomb1-Associated Protein Eg5

Introduction

Ubiquitination is a post-translational modification in which an 8 kD ubiquitin protein is added to its substrate protein [5, 29, 138]. There are a number of structurally different types of ubiquitin modifications: monoubiquitination and approximately seven different types of polyubiquitination [36]. The consequence for the substrate depends on the type of ubiquitin modification [139]. For example, modification by a single ubiquitin promotes endocytosis or protein trafficking, whereas modification by polyubiquitin, such as the lysine 48-linked ubiquitin chain, promotes proteasome-mediated degradation [36, 139]. The process of ubiquitination consists of an enzymatic reaction cascade involving an E1 activating-enzyme, an E2 conjugating-enzyme, and an E3 ubiquitin ligase [140]. E3 ubiquitin ligase is a key component of this reaction, as it selects substrates for ubiquitin modification, thereby conferring specificity of the reaction [37]. Together, the use of distinct ubiquitin modifications and the specificity of E3 ubiquitin ligase make ubiquitination a versatile post-translational modification [36, 139]. Therefore, it is not surprising that ubiquitination can also regulate numerous cellular pathways, including a pathway important for this dissertation, the Notch signaling pathway [139].

As outlined in Chapter One, the Notch signaling pathway is an evolutionary conserved pathway that regulates a wide range of cellular functions, such as specification, proliferation, and apoptosis [1, 141]. The core components of the Notch signaling pathway are the transmembrane receptor, Notch, and its transmembrane ligands, DSL (Delta, Serrate or Lag2). DSL ligand-binding promotes two proteolytic

cleavages in the Notch receptor, leading to the release of Notch intracellular domain [1]. Once cleaved, the Notch intracellular domain translocates to the nucleus, where in cooperation with the DNA binding protein CSL and its co-activator Mastermind, promotes transcription [1].

There are several known E3 ubiquitin ligases that regulate the Notch pathway (e.g. Sel-10, Deltex, Su(dx) and Neuralized); most of these are involved in regulating the Notch receptor [18]. Recently, an additional E3 ubiquitination ligase, Mib1, was found. Mutations in the *mib1* gene in zebrafish cause defects resembling those observed in Notch-signaling pathway mutants [20, 21, 142, 143]. Significantly, Mib1 was found to regulate DSL ligands [5, 138]. Although much is known about how Notch and its downstream processes are regulated, little is known about the regulation of Notch activation by Delta [49]. Mib1 was found to promote ubiquitination and extracellular membrane depletion of the DSL ligands, Delta and Serrate [3, 5, 6, 138, 144, 145]. The necessity of Mib1 for DSL ligand regulation appears to be tissue- and species-specific [3, 5, 6, 138, 144, 145]. Surface depletion of DSL ligands suggests that Mib1 promotes endocytosis, though currently there is no direct evidence for this involvement. However, such a role would be consistent with previous observations that endocytosis is required for DSL ligand-Notch signaling [3, 46, 50]. A direct mechanism for Mib1 mediated endocytosis of DSL ligands has not been demonstrated.

Mib1 also regulates another substrate, one that is not involved in the Notch signaling pathway. This substrate, DAPK, regulates apoptosis and is a potential tumor suppressor [7]. In response to multiple triggers, including IFN-γ, Fas, TNFα,

ceramide, TGFβ, or oncogene-induced proliferation, DAPK induces apoptotic or autophagic cell death through caspase-dependent and -independent pathways [54]. Some authors have proposed that DAPK may act as a tumor suppressor to sensitize cells to apoptosis during tumorigenesis [54]. Mib1 was found to promote ubiquitin-mediated degradation of DAPK, inhibiting its pro-apoptotic functions [7]. Mib1 regulation of these distinct substrates, DSL ligands and DAPK, reveals that Mib1 has a complex role in the cell.

To advance the understanding of Mib1 function and its regulation, I used a proteomic approach to identify interacting-proteins of Mib1 through mass-spectrometry. In this chapter, I report on the results of that proteomic screen. I describe in detail the interaction between Mib1 and one of the associated-proteins identified, Eg5. Here, I report that Mib1 promotes monoubiquitination of Eg5. As monoubiquitin modifications can promote translocation of proteins, I examine whether Mib1 is necessary for localization of Eg5 to the mitotic spindle and whether Mib1 is essential for mitotic spindle formation. Finally, I examine *eg5* and *mib1* zebrafish mutants for shared defects in Notch signaling and spindle formation.

Materials and Methods

Cell Culture and Transfection

HEK-293 and HeLa cells were maintained in high glucose DMEM containing 10% heat-inactivated fetal calf serum (Gibco BRL) and 100 U penicillin/streptomycin

at 37°C in 5% CO_2. Cells were transiently transfected with a 2:1 ratio of LIPOFECTAMINE 2000: DNA in antibiotic-free media, according to manufacture's instructions (Invitrogen). Media was changed 6 hours after the application of the DNA-lipid complex with normal culture media.

siRNA transfection

STEALTH-siRNA duplexes that target human MIB1 (MIB1HSS126396) and a low GC content random siRNA control were obtained from Invitrogen.

The sequence for the MIB1 siRNA duplex is as follows:

AAUACUGGAAUAUUCCCACUUGAGA.

HEK-293 or HeLa cells were transfected with 100 nM of the siRNA duplexes with LIPOFECTAMINE 2000 according to manufacturer's instructions. The media was replaced 6 hours after the addition of the complexes with normal culture media.

Protein Purification and Mass Spectrometry

HEK-293 cells were stably transfected with 2XFLAG-Mib1-pcDNA3 or pcDNA3 as a control, washed with 1X PBS, lysed in CelLytic M buffer (SIGMA), pelleted to remove cellular debris, and purified over a FLAG-Agarose column (SIGMA). After extensive washes with Wash buffer (50 mM Tris-Cl, pH7.4 and 150 mM NaCl), bound proteins eluted off the column by competition with 200 ng/μL of 3XFLAG peptide (SIGMA) in Wash buffer. Elutants were concentrated in an Amicon Ultra 4 column and eluted with wash buffer. Concentrated elutants were run on a 4-

12% Bis-Tris gradient gel in 1X MOPS. The gel was then fixed in 50% ETOH, 8% phosphoric acid and stained with Bio-Safe Coomassie blue (Bio-Rad). Bands that were in the 2XFLAG-Mib1 lane, but not in the control lane, were extracted with a Leap 2DiDx spotcutter for further analysis. Tryptic digests were prepared and analysed on a LC/MS/ MS (Applied Biosystems QStar XL) at the OHSU Proteomics Shared Resource. Peptides identified by mass spectrometric analysis were identified with MASCOT. Putative interacting-proteins were identified with the Global Proteomics Machine (GPM). Only those proteins scoring a confidence value of 95% or greater were considered for further analysis.

Immunoprecipitation

Twenty-four hours after transfection, cells were lysed in a buffer containing Protease Complete Inhibitor (Roche), an EDTA-free lysis buffer was used for ubiquitination assays (50 mM Tris-Cl, pH8, 150 mM NaCl, 10% Glycerol, 1% NP40), or a NP40/Tris IP buffer (20 mM Tris-Cl pH 8, 1% NP-40, 137 mM NaCl, 10% Glycerol, 2 mM EDTA, 10 mM NaF) for all other immunopreciptations. In all experiments, 500 μg of lysates were pre-cleared in Protein G-Sepharose (GE Healthcare), then immunoprecipitated with one of the following antibodies: rabbit anti-Eg5 (Cytoskelton), mouse anti-HA (Covance), or mouse anti-Myc (a gift from Monika Davare). Immunoprecipitates were washed four times with the appropriate lysis buffer then lysed with Laemelli buffer.

Fish Lines and Maintenance

mib ^{Hi904}, *eg5*^{Hi3112A}, and *eg5*^{Hi486} *Danio rerio* insertional mutants used in this study were derived from TAB lines obtained from the Hopkins Lab at MIT [142, 143]. Adult fish and juveniles were raised on an Aquatic Habitats system with a 14- to 10-hour light-dark cycle. Embryos were raised at 28 °C in 0.3X Danieau's media supplemented with penicillin/streptomycin. Embryos were staged as hours post-fertilization [146]. Prior to use in experiments, all embryos were anesthetized with Tricaine [147].

Western blotting Analysis

Samples were denatured in Laemelli buffer, and then run on a 4-12 % Bis-Tris Criterion XT gel in 1X MOPS XT buffer. The gel was then transferred to PDVF membrane in Towbin buffer, according to standard protocols. Membranes were blocked then incubated overnight at 4°C with the following primary antibodies: mouse anti-V5 (Sigma), mouse anti-GFP (Invitrogen), mouse anti-Myc (Gift of Monika Davare), mouse anti-βActin (Sigma), and Rabbit anti-Eg5 (Cytoskelton). After incubation in HRP-conjugated secondaries (GE Healthcare), membranes were processed with ECL (Western Lightning, Perkin Elmer) and exposed to X-ray film for development.

In situ Hybridization

To reduce pigment formation in embryos, 0.005% 1-phenyl-2-thiourea (PTU) was added in Danieau's media when embryos were at 22 hpf. At the stated timepoints, embryos were fixed with 4% paraformaldehyde in 1X PBS (pH 7.4). DIG-labeled sense and antisense RNA probes were generated against the full-length zebrafish Eg5 (accession number BC048061) using DIG-labeling mix (ROCHE). *In situ* hybridizations were performed according to standard methods and developed with NBT/BCIP substrate [147]. Embryos were mounted in 3% Methyl Cellulose and photographed using a Zeiss M^2-Bio microscope equipped with a halogen lamp and a cooled CCD camera (Axio CAM HR). Images were processed with AxioVision software and Photoshop.

Immunocytochemistry

HEK-293 and HeLa cells plated on poly-D-lysine coated coverslides were fixed in methanol at 20 °C for 10 minutes, washed with 1X PBS, blocked with 10% goat serum in 1X PBS, pH 7.4, and subsequently incubated overnight in primary antibody diluted in 3% goat serum at 4 °C. After 3 washes in 1X PBS, cells were incubated in goat anti-mouse or goat anti-rabbit Alexa- 488 or 568 conjugated secondary antibodies (Invitrogen) at 1:1000 for 1 hour at room temperature. After final 3 rinses in 1X PBS, cells were stained with Hoechst 33342 and mounted in Prolong

Gold (Invitrogen). The following primary antibodies were used: mouse anti-α-tubulin (Sigma), rabbit anti-Eg5 (Cytoskeleton) and mouse anti-HA (Covance).

Immunohistochemistry

Embryos were fixed in 4% paraformaldeyde in 1X PBS for 2 hours. Washed in PBST, then infiltrated in sequentially in 15% and 30% sucrose for 1 hour each. Embryos were embedded in OCT and cryosectioned to 12 microns. Sections were blocked in 5% goat serum, 1% BSA, 0.2% Triton X-100 for 2 hours, then incubated in primary antibodies overnight at 4°C. Sections were washed in 1% goat serum, 1% BSA, then incubated in Alexa-488 or –568 conjugated secondary antibodies for 1-2 hours. Sections were washed 3 times in 1X PBS, then mounted in n-propyl gallate mounting media (1% n-propyl gallate, 100 mM Tris-Cl pH8, 50% glycerol). The following primary antibodies were used: rabbit anti-phospho Histone3 (Cell signaling), mouse anti-Zrf1 (ZIRC), Mouse anti-Islet-1 (ZIRC), mouse anti-HuC/D (Invitrogen), rabbit anti-PKCα (Cell signaling) and mouse anti-GAD-67 (Covance).

Microscopy

Most of the immunofluorescent-labeled samples were imaged under a Plan Apochromat 63X/1.4NA oil-immersion lense on a Zeiss Axioplan2 equipped with Hamamatsu CCD camera and the Openlab image acquistion program. Mitotic spindles were imaged on a Nikon Eclipse TE300 microscope equipped with a Bio-Rad 1024 ES

confocal imaging system using the 568 nm line of the krypton/argon laser (MMI Core facility).

Results

Proteomic screen to identify interacting-proteins of Mib1

To identify potential interacting-proteins and substrates of Mib1, lysates from HEK-293 cells stably transfected with 2X FLAG-tagged Mib1-pcDNA3 or the control pcDNA3 were purified over a FLAG agarose column. After extensive washing, Mib1 and its associated-proteins were eluted off the column by competition with a 3X FLAG peptide and elutants run on 4-12 % Bis-Tris gradient gel. Protein bands that were present in the 2XFLAG-Mib1 lane, but not in the control lane, were extracted and analyzed by mass spectrometry to determine the identity of the isolated proteins (Figure 2.1).

The identified Mib1-associated proteins are involved in a wide array of cellular functions: ubiquitination, translation, transcription, cytoskeletal structure, methylation, centrosome regulation and spindle formation (Table 2.1). As expected, one of the identified proteins has functions related to ubiquitination, Ubiquitin-specific protease 9. Ubiquitin-specific protease 9 is a deubiquitinating enzyme that is involved in the removal of ubiquitin from a protein substrate [148]. The mutant of *fats facets*, the *Drosophila* homolog of ubiquitin-specific protease 9, has a neurogenic phenotype. *Fat facets* was found to genetically interact with Epsin and promote Delta signaling in

Drosophila ommatidia [149]. Other lab members pursued characterization of this protein. Interestingly, two of the identified proteins, serine-threonine protein kinases, NDR1 and NDR2, have recently been found to regulate centrosome duplication [150]. In this screen, I did not identify Delta. This is not unexpected as Delta is a transmembrane protein, and membranes were not purified for this study.

A small subset of proteins identified by mass spectrometry were selected for small-scale co-immunoprecitations with Mib1: NDR1, NDR2, Arginine Methyltransferase 4, Fats-facets, and Eg5 and were found to be interacting-proteins of Mib1 (data not shown and Figure 2.2).

Mib1 associated with Eg5 and promotes its ubiquitination

As preliminary evidences suggested a strong association between Eg5 and Mib1, I decided to focus my attention on their interaction. Eg5 is a member of the kinesin 5 subclass of plus-ended kinesins [9]. Kinesins of subclass all share a homotetrameric structure with motor domains at each end [8]. It was proposed that Eg5 functions to stabilize and slide the spindle through interaction of its motor domains with the antiparallel microtubules of the mitotic spindle [151]. To verify that Eg5 associates with Mib1, I performed co-immunoprecipitations on lysates of HEK-293 cells. A reliable antibody to immunoprecipitate endogenous expressed Mib1 is not available, so I relied on the expression of a Myc-tagged Mib1. Immunoprecipitation of myc-tagged Mib1 was able to pull down endogenous Eg5 (Figure 2.2A). Likewise,

immunoprecipitation of an endogenous Eg5 was also able to pull down Mib1 (Figure 2.2A). Therefore, I conclude that Mib1 is associated with Eg5.

To determine the Eg5 interaction site on Mib1, I prepared three myc-tagged Mib1 deletion proteins: one lacking the N-terminal half of Mib1 (MibΔN), another lacking the ankyrin repeats (MibΔM), and a third lacking all of the Ring-finger domains (MibΔC) (Figure 2.2D). The deletion constructs were immunoprecipitated with Myc antibody and examined for the presence of Eg5 by Western blot analysis. Eg5 could interact with all of them except MibΔN (Figure2.2C). It was shown previously that the N-terminal region of Mib1 is required for interaction with Delta and Serrate, hence, this region may contain the substrate-recognition site of Mib1 [5, 6].

As Mib1 is an E3 ubiquitin ligase, I investigated whether it could promote ubiquitination of Eg5. HEK-293 cells were transfected with Mib1-myc, Eg5-V5-His, and HA-Ubiquitin and harvested 24 hours later. Immunoprecipitation of ubiquitin revealed two distinct Eg5 bands, suggesting that Eg5 is modified by multiple mono-ubiquitins (Figure 2.3). Furthermore, control-transfected cells also contain a monoubiquitinated band, which could indicate ubiquitin modification of Eg5 by endogenous Mib1.

Taken together, these results indicate that Eg5 interacts with Mib1 through its N terminal region. It is through this interaction that Mib1 promotes ubiquitination of Eg5.

Mib 1 did not cause relocation of Eg5 from the mitotic spindle

Eg5 has a dynamic localization pattern during the cell cycle. During interphase, Eg5 is localized in the cytoplasm along with interphase microtubules, but throughout mitosis, it is localized along the mitotic spindles along the spindle poles [151-153]. Since ubiquitination can affect the subcellular distribution of proteins, I was interested to see whether Mib1 could affect the localization of Eg5 to the mitotic spindle [140]. 3XHA-Mib1 was expressed in HEK-293 cells and cells examined 48 hours post-transfection by immunolabeling with Eg5 and HA. However, Eg5 showed normal localization at the spindle in all 100 mitotic spindles examined (Figure 2.4). Similar results were obtained with transfection periods of 24 and 72 hours and in comparable experiments in HeLa cells (data not shown).

I then asked whether silencing Mib1 with siRNA could affect the localization of Eg5 to the spindle. To verify the effectiveness of Mib1 siRNA, Mib1 siRNA and FLAG-Mib1 were co-transfected in HEK-293 cells, then the expression of FLAG-Mib1 was examined by Western blot analysis of 48 hours post-transfection lysates. At 48 hours, there was a significant decrease in the levels of Mib1 in Mib1 siRNA-transfected cells, relative to control siRNA-transfected cells, which suggests the siRNA effectively silences Mib1 expression (Figure 2.5B). This Mib1 RNAi or control siRNA was transfected into HEK-293 cells to examine the necessity of Mib1 in Eg5 localization. To mark mitotic spindles and transfected cells, cells were also transfected with α-tubulin-GFP. These transfected HEK-293 cells were then examined 48 hours post-transfection for Eg5 spindle localization. One hundred mitotic spindles

were examined as determined by α-tubulin-GFP expression. However, Eg5 appropriately localized to the spindle in Mib siRNA-transfected cells (Figure 2.5A). Similar results were observed at 24 and 72 hours post-transfection and in comparable experiments in HeLa cells (data not shown). Taken together, these results demonstrate that Mib1 does not affect the spindle localization of Eg5.

Alteration of Mib1 expression did not cause mitotic spindle defects

Although Mib1 did not appear to have a role in promoting Eg5 localization to the spindle, it is possible it could regulate Eg5 function independent of its localization. It was previously observed when Eg5 was inhibited or its expression silenced, microtubules do not organize into bipolar spindles during mitosis. Instead, the spindles form an array of microtubules organized about a single pole, termed monastral spindles [67, 154]. Therefore, I examined whether normal spindle formation was disrupted if Mib1 expression levels were altered. HEK-293 cells were transfected with Mib1-eGFP, and α-tubulin and immunofluorescence was used to examine spindles 48 hours post-transfection. One hundred spindles for each timepoint were examined, but no abnormal spindles were observed (Figure 2.6B). Similar results were seen at 24 and 72 hours post-transfection and in comparable experiments in HeLa cells (data not shown). These results suggest that Mib1 is not essential for spindle formation.

I also examined whether silencing Mib1 using siRNA could disrupt normal spindle formation. HEK-293 or HeLa cells (data not shown) were co-transfected with Mib1 siRNA or control siRNA along with mRFP, a marker for transfection. I

inspected 100 spindles of transfected cells at each timepoint and did not find any abnormal spindles (Figure 2.6A). For this reason, I conclude that Mib1 does not regulate spindle formation in HEK-293 and HeLa cells.

Characterization of the *eg5*^{Hi3112a} zebrafish mutant

Although shared function in spindle development of Eg5 and Mib1 was not seen in cell cultures, it is possible that there are similarities *in vivo*. Two retroviral insertions in the *eg5* locus, Hi486 and Hi3112A, were previously generated in during a large-scale insertional mutagenesis at the Hopkins lab [143, 155]. These viral insertions are located within the first intron of the gene [143, 155]; (Figure 2.7A). These insertions reduced Eg5 transcript levels. Furthermore, this gross phenotype of a curved body shape was linked to a reduced transcript level, but no further characterization was performed [143, 155].

Therefore, further analysis of these mutants was necessary. Since the phenotype exhibited by zebrafish with the Hi486 insertion produced a mild phenotype, only the Hi3112A insertion will be discussed for the remainder of this chapter. Based on quantitative RT-PCR analysis, the Hi3112a insertion caused a 50.75% reduction in the level of Eg5 transcript (Figure 2.7B). An elevated number of cells exhibiting acridine orange uptake, a marker for apoptotic/necrotic cells, was observed in *eg5*^{Hi3112A} mutant embryos [156]. A slight elevation in the number of dying cells was observed in *eg5*^{Hi3112A} mutant beginning at 24 hpf (hours post-fertilization) and by 48 hpf there was a significant elevation in the number of dying cells (data not shown). By

30 hpf, there was tail curvature, a smaller head, and smaller eyes were noticeable. Pericardial edema, heart atrophy, brain disorganization, and underdeveloped gut were obvious by 56 hpf. The above described phenotypes persist throughout the remainder of their development. The *eg5*^{Hi3112a} mutants do not survive past 6 dpf (days post-fertilization). Interestingly, he *eg5*^{Hi3112a} mutants look remarkably similar to the phenotype of *mib1*^{Hi904} insertional mutant described previously in our lab (Figure 2.7C, D); [5].

_eg5_ transcripts were expressed in regions similar to _mib1_

An *in vivo* interaction between Eg5 and Mib1 would require that the transcripts be localized in similar regions within the embryo. Using *in situ* hybridization, I examined the expression of pattern of *eg5* throughout early development. *eg5* was ubiquitously expressed throughout a gastrulating embryo at 6 hpf (Figure 2.8). However, at 18 hpf, transcripts of *eg5* become increasingly restricted to neurogenic regions. By late neurogenesis at 48 hpf, *eg5* transcripts were highly restricted to neurogenic regions especially at the midbrain-hindbrain boundary. This *eg5* localization is similar to previously described *mib1* expression patterns. *mib1* transcripts are initially ubiquitous, but become restricted to neurogenic regions as embryos proceed through neurogenesis [5]. These *in situ* hybridization findings provide evidence for an interaction between Eg5 and Mib1 *in vivo*.

Zebrafish eg5^{Hi3112A} mutants had monastral spindles, but *mib^{Hi904}* had normal bipolar spindles

In *Drosophila*, the mutant for the Eg5 ortholog, KLP61F, was observed to have monastral spindles. As my study is the first *in vivo* characterization of *eg5*, I investigated whether there were similar mitotic spindle defects to those observed in *Drosophila* KLP61F mutants [157, 158]. Fourty-eight hpf zebrafish embryos were examined for defects in the mitotic spindles of retina. The later developing retina was selected for observation to avoid rescue of zygotic mutations from maternally provided yolk transcripts [159, 160]. Using an antibody against α-tubulin, bipolar mitotic spindles were observed in wild type embryos localized primarily to the proliferative region of the retina at this stage, called the ciliary marginal zone (Figure 2.9A). *eg5^{Hi3112A}* mutants, in contrast, had predominantly monastral spindles that were not restricted to the ciliary marginal zone, but located throughout the retina (Figure 2.9B). Furthermore, these spindles were oriented randomly and not aligned in the usual parallel orientation to the apical membrane. The monastral spindle phenotype of these eg5^{Hi3112A} mutants is consistent with phenotypes observed in the *Drosophila* KLP61F mutant. However, it is a novel finding that cells with abnormal spindles are not restricted to the ciliary margin or the apical membrane, but instead localize throughout the retina.

In cell culture, alteration of Mib1 expression levels did not cause spindle defects, but is possible that Mib1 could have a spindle defect *in vivo*. To this end, the mitotic spindles of 48 hpf *mib^{Hi904}* mutant retinas were examined for defects. Unlike

the *eg5*^{Hi3112A} mutant, no mitotic spindle deformities were observed in the *mib*^{Hi904} retinas (Figure 2.9C). These results suggest the Mib1 is non-essential for spindle formation in the retina.

_eg5_^{Hi3112A} had an elevated number of mitotic cells, but _mib1_^{Hi904} had a normal number of mitotic cells

To assess the consequence of this abnormal spindle development in *eg5*^{Hi3112A} mutants on mitotic progression, the retinal cells of these mutants were examined using the mitotic marker, phospho-Histone 3 (pH3). It was previously observed in the retina of wild type zebrafish, that proliferation levels are highest at 27 hpf and are maintained roughly at the same level until 36 hpf, at which point proliferation declines until 48 hpf [161]. Comparison of the numbers of pH3-positive cells of the *eg5*^{Hi3112A} and wild type embryo retinas revealed that at 29 hpf the levels of mitotic levels were about equal. However, at 36 hpf and 48 hpf *eg5*^{Hi3112A} mutants had significantly more mitotic cells. There are two possible explanations for the higher levels of pH3-positive cells in *eg5*^{Hi3112a} mutants. The first possibility is that *eg5*^{Hi3112A} cells are arresting in mitosis leading to an accumulation of mitotic cells. Alternatively, the elevated number of mitotic cells could suggest an enhanced proliferation rate (Figure 2.10).

I also examined whether *mib1*^{Hi904} mutants also had an alteration in the number of mitotic cells. Once again, pH3 labeling was used to a mark cell proliferation of the developing retina. However, no major differences in the number of pH3-positive cells were found in *mib1*^{Hi904} mutants compared to wild type embryos (Figure 2.10). Taken

together, I can conclude that *mib1*^{Hi904} mutants do not have an elevation in the number of mitotic cells like that observed in *eg5*^{Hi3112A} mutants.

Cellular specification defects were not observed in eg5^{Hi3112A} mutants

mib1^{Hi904} mutants exhibit neuronal specification defects, the overproduction of primary neurons and progenitors at the expense of secondary neurons and glia [5, 138, 162]. In the hindbrain of *mib1*^{Hi904} mutants there are an overall increase in the numbers of differentiated neurons, but a decrease in later-born, hindbrain commissural neurons and branchiomotor neurons. These results could suggest a premature neuronal differentiation. Since *eg5* transcripts are highly expressed in the nervous system, it is possible that *eg5*^{Hi3112A} mutants could have neurogenic defects similar to the *mib1*^{Hi904} mutants. I examined the number of differentiated neurons in *eg5*^{Hi3112A} hindbrains using the pan-neuronal marker, HuC/D (Figure 2.11). Previously, *mib*^{Hi904} mutants were observed to have elevated numbers of HuC/D positive cells in their hindbrain relative to wild type embryos. However, no appreciable differences were observed in the number of HuC/D-positive cells in the hindbrains of wild type and *eg5*^{Hi311A} mutants. In prior studies, the hindbrain of *mib*^{Hi904} mutants was observed to have a reduction in the number and disorganization of the later-born hindbrain commissural neurons, branchimotor neurons, and glia [163]. Using the antibodies Zn5, Islet1, and Zrf1, which respectively mark the commissural neurons, branchimotor neurons, and glia, no apparent differences in *eg5*^{Hi3112A} mutants were observed when compared to wild type (Figure 2.11). These results would suggest that Eg5 is not essential for cellular specification in the hindbrain.

It is possible is that *eg5*^{Hi3112A} mutants were rescued by maternally provided transcripts, thus occluding any early defects present in the hindbrain. An alternative region to examine for cellular specification defects is the retina, which undergoes specification at a later time period compared to the hindbrain [164]. It was previously observed in our laboratory that *mib*^{Hi904} mutants fail to produce the amacrine and bipolar cells of the retina. Furthermore, *mib*^{Hi904} mutants were also observed to have a significant reduction in the number of double cone photoreceptors [25]. For these reasons, I decided to survey the retina for specification defects using markers of ganglion, amacrine, bipolar, horizontal, and double cone photoreceptors. However, no change in the relative numbers of these cell-types was observed in the Eg5 mutants compared to the wild type embryos. A gross interlayer disorganization was observed, but the overall laminar organization was preserved. Therefore, I can conclude that *eg5*^{Hi3112A} mutants do not have the same retinal specification defects that were observed in *mib*^{Hi904} mutants.

Discussion

Ubiquitination regulates a wide diversity of cellular events. This diversity is generated, in part, by the selection of specific substrates by E3 ubiquitin ligases. Here, I examined proteins that may interact with the RING-finger E3 ubiquitin ligase Mib1. Previously, the only known interacting-proteins of Mib1 were DSL ligands and DAPK, regulators of Notch signaling and apoptosis, respectively. In this study, I identified a number of potential substrates involved in centrosome regulation, mitotic spindle development, methylation, and transcriptional/translational regulation.

Identification of Eg5 as a substrate for Mib1

In this study, I further characterize one of the identified proteins, the kinesin Eg5. I found that Mib1 could promote monoubiquitination of Eg5. Monoubiquitination has been linked to regulation of endocytosis, transcription, and DNA repair. The ability of monoubiquitination to regulate these diverse cellular processes is just beginning to be understood. However, monobiquitination may be as important as phosphorylation in modulating diverse cellular events [36]. As Mib1 mediated monoubiquitination of Eg5 is the only known monoubiquitination of a motor protein, I can only speculate how this modification regulates Eg5. However, some hints of Eg5 regulation may be provided by its other known modifications. Eg5 and other members of the kinesin-5 subclass of kinesins, contain a highly conserved sequence, the bimC box, in their tail domain [8]. Threonine 937 located with the bimC box, can be phosphorylated *in vitro* by p34cdc2 [165]. If this threonine is mutated to a non-phosphorylatable alanine, Eg5 fails to localize to the spindle [165]. Furthermore, phospho-specific antibodies designed against bimC box, showed that the phosphorylated form of Eg5 is highly localized to the spindle and only during mitosis [81]. This evidence suggests a cell cycle-dependent phospho-regulation of Eg5 localization. For Eg5 to bind spindle microtubules, a conformational change in Eg5 would be necessary [166]. However, hydrodynamic analysis of the phosphorylated and non-phosphorylated forms of Eg5 revealed no differences in their conformational states [65]. This suggests that another factor is required for phosphorylation-dependent microtubule binding. Examples from other ubiquitin-modified proteins have shown

that in some instances phosphorylation is required prior to ubiquitination [167, 168]. Taken together, phosphorylation of Eg5 by p34cdc2 may prime the site for Mib1 ubiquitination, which then facilitates Eg5 spindle binding.

One implication of this type of ubiquitination is suggested by a recent study on ubiquitin regulation of growth coactivator SRC-3. SRC-3 was ubiquitinated in two phases in a phosphorylation-dependent manner [169]. In the first phase, SRC-3 is multi-monoubiquitinated which regulates SRC-3 activity. In the second phase, the monoubiquitin transition to polyubiquitin leading to degradation of SRC-3 [169]. A similar modification could occur for Eg5. If ubiquitination was required for the localization of Eg5 to the spindle, a bi-phasic mode of ubiquitination might regulate the tight temporal event of spindle formation. Monoubiquitination of Eg5 would promote its localization to the mitotic spindle during mitosis, and then Eg5 is polyubiquinated at the end of mitosis promoting its degradation.

Explanation for absence of spindle deformities observed in Mib1 experiments

If regulation by Mib1 is critical for an Eg5 interaction with the spindle, how is the lack of spindle defects in Mib1 mutants explained? Since the time of these studies, a paralog of Mib1, called Mib2 was found [145]. Mib2 and Mib1, are nearly identical in their domain organization [145]. More importantly, there is overlap in the substrates that Mib1 and Mib2 regulate [53, 145]. Both Mib1 and Mib2 were able to promote ubiquitin mediated endocytosis of Delta C. *In vivo* proof of Delta C as a substrate of Mib2 will be necessary, as these studies relied on overexpression of Mib2. However,

not all substrates are shared because as Delta D is regulated solely by Mib1. In my studies of Mib1 siRNA-silenced cells, Mib2 may compensate for Mib1 loss and this may explain why Mib1-mediated spindle defects were not observed.

eg5^{Hi3112A} mutants had spindle defects, but did not have specification defects

In this study, I also characterized the *in vivo* functions of the *eg5* using a zebrafish hypomorph mutant, *eg5*^{Hi3112A}. Mutants of the *Drosophila* ortholog of Eg5, KLP61F, have monastral spindles instead of bipolar spindles. Similarly, *eg5*^{Hi3112A} mutants have monastral spindles at 48 hpf. Unlike the mitotic spindles observed in wild type retinas these mitotic spindles were not restricted to the ciliary margin, but located throughout the retina. Interestingly, monastral spindles of *eg5*^{Hi3112A} mutants were oriented in multiple orientations relative to the apical margin. A current model for cell specification proposes that the plane of cell division, dictated by the mitotic spindle orientation, determines inheritance of cell fate determinants and ultimately dictates cell fate [170]. This mechanism of cell fate determination may occur in the zebrafish retina. One study in zebrafish retina found that the plane of cell division changes from central-peripheral to circumferential during neurogenesis [171]. This change in plane is correlated with cell fate determination of these cells [171]. However, cell fate specification of the retina and the hindbrain was normal in *eg5*^{Hi3112A} mutants. These results suggest that spindle orientation may not dictate cell fate determination in the zebrafish retina and hindbrain. An underlying assumption is that the monopolar cells divide and survive to differentiation. However, these cells may die

and the differentiated cells are descendants if progenitors with a normal mitotic spindle.

An interesting observation, although currently inexplicable, is that mitotic cells of *eg5*^{Hi3112A} mutants were located throughout the retina. Normally, in a developing retina, the nucleus and cytoplasm of the cell are connected to the apical membrane with only a membrane process connecting at the basal membrane [171]. However, in the *eg5*^{Hi3112A} mutants the dividing cell bodies were located in the basal region as well as the apical region. One possible explanation is the apical attachment is lost, therefore, the cells migrate throughout the retina. Whether these result from a secondary defect remains to be seen.

I did not observe cellular specification defects in the retina and hindbrain of *eg5*^{Hi3112A} mutants, although it is possible that Eg5 could affect specification in other regions. The role of Mib1 in specification is not limited to the CNS, as recent work found *mib1* mutants had specification defects in the gut epithelium [26]. *eg5*^{Hi3112A} mutants were observed to have underdeveloped intestines and this region could be explored for specification defects. Furthermore, development of gut epithelium occurs at 3 dpf, when maternal contributions are negligible.

The identification of Eg5 as an interacting-protein of Mib1 creates a new perspective on the diversity of proteins that Mib1 can regulate. Mib1 was found to regulate the monoubiquitination of Eg5. These findings have provided the groundwork for Chapter 3 to which I now turn.

Protein classification	Protein Name	Accession number
Centrosome	Serine-Threonine kinase, NDR1	NCBI:NM_007271
	Serine-Threonine kinase, NDR2	NCBI:NM_015000
Motor Protein	Eg5	SWISS-PROT:P52732
Signaling	CDK5 RAP3	SWISS-PROT:PP1553
	TAK1	NCBI:O43318
Ubiquitination	Ubiquitin-Specific Protease 9, Fat facets related	TRM:Q8WWT3
Methylation	Arginine N-Methyltransferase 5	SWISSPROT:O14744
	Methylsome protein 50	SWISSPROT:Q9BQA1
Transcription/ Translation	Motor neuron complex-interacting protein1, Gemin-2	SWISSPROT:014893
	Nuclear Ribonucleoprotein K	SWISSPROT:Q07244
	Nuclear Ribonucleoprotein H	SWISSPROT:P31943
	Helicase-like protein 2	SWISSPROT:O00571
	Polyadenylate-binding protein 3	SWISSPROT:Q9H361
	Eukaryote translation initiation factor 4B	SWISSPROT:P23588
	Nucleolin 20	SWISSPROT:P19338
	Ribosomal Protein S4	SWISSPROT:P46781
	Ribosomal Protein S7	SWISSPROT:P23821
	Ribosomal Protein L24	SWISSPROT:P38663
	Ribosomal Protein S7	SWISSPROT:P23821
	Ribosomal Protein L4	SWISSPROT:P36578
Cytoskeletal	Integrin β-6 precursor	ENSP00000297130
	Spectrin, alpha chain	SWISSPROT:Q13813
	Apolipoprotein 20 A-I precursor	SWISSPROT:P02647
	Alpha-tubulin 1	SWISSPROT:P05209
	Beta-tubulin 5	SWISSPROT:P05218
	Beta-tubulin, class II subtype	TRM:Q8IWR2
	Vimentin	SWISSPROT:P08670
Chaperone	Heat Shock Protein 70	SWISSPROT:P042264

Table 2.1 Mib1-associated proteins identified in proteomic screen

Mib1-associated proteins that scored an identification confidence value >95% by MASCOT are shown. Proteins are classified according to their known biological function. The accession numbers for each of identified proteins from NCBI, SWISS PROT, and TRM are shown.

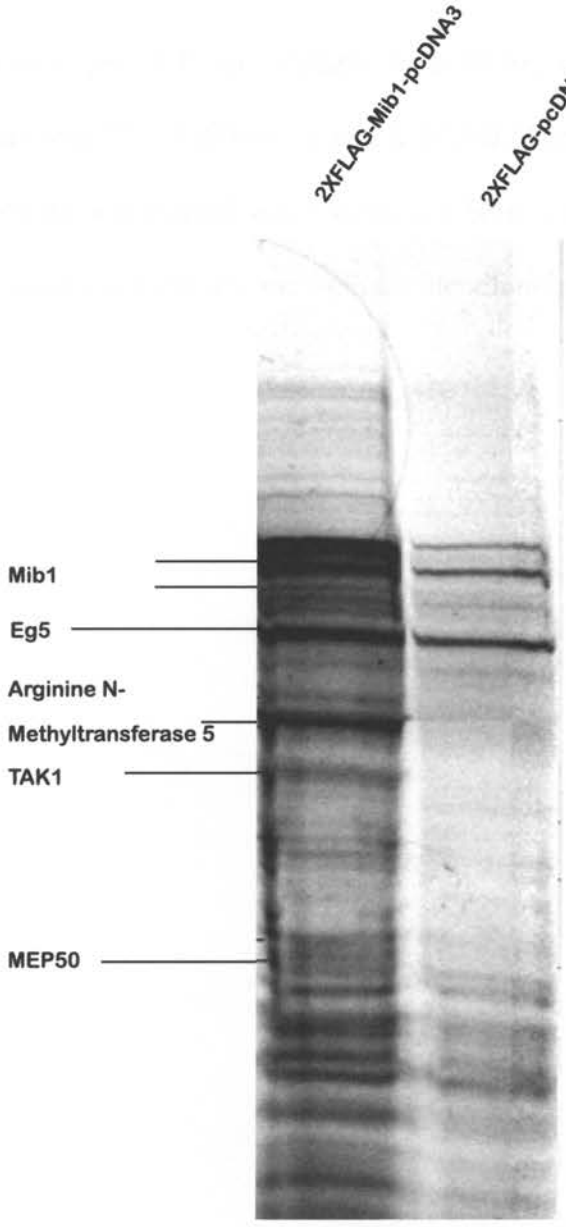
2XFLAG-Mib1-pcDNA3
2XFLAG-pcDNA3
Mib1
Eg5
Arginine N-
Methyltransferase 5
TAK1
MEP50

Figure 2.1 Affinity purification of 2X FLAG-Mib1 associated proteins

A representative gel of FLAG elutants from FLAG affinity columns bound to cell lysates, containing 2X FLAG-Mib1 or 2X FLAG. The elutants were separated on 4-12% Bis-Tris gel and stained with Coomassie blue. Lines point to bands selected for analysis by mass-spectrometry and indicate identified proteins.

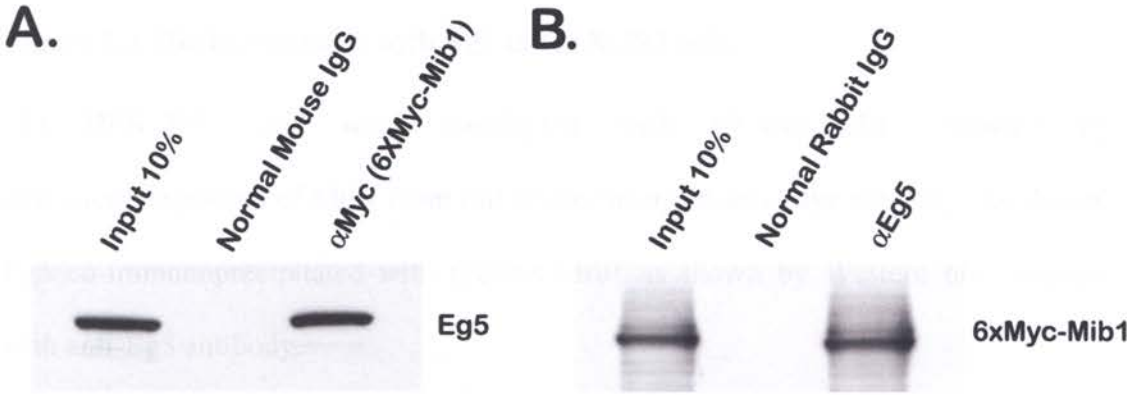
A.
Input 10%
Normal Mouse IgG
αMyc (6XMyc-Mib1)
Eg5
B.
Input 10%
Normal Rabbit IgG
αEg5
6xMyc-Mib1

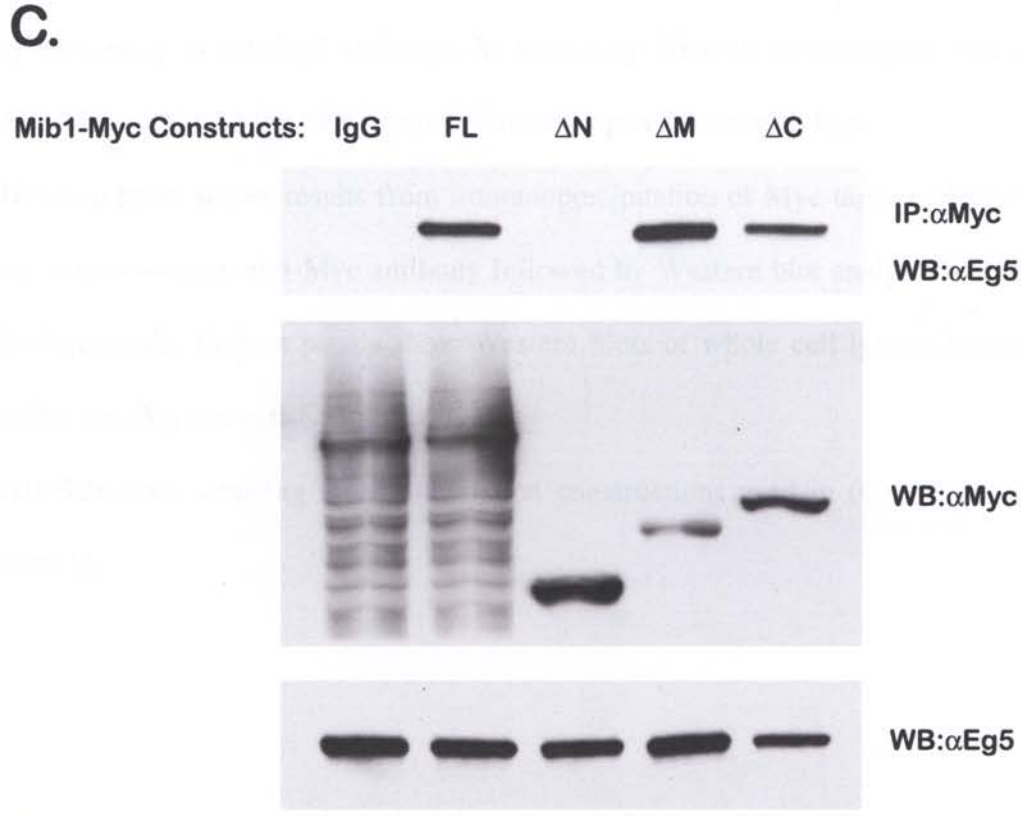
C.
Mib1-Myc Constructs: IgG FL ΔN ΔM ΔC
IP:αMyc
WB:αEg5
WB:αMyc
WB:αEg5

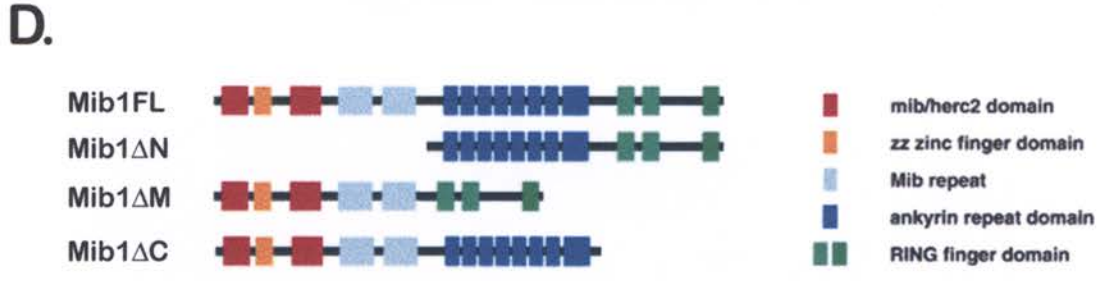
D.
Mib1FL
Mib1ΔN
Mib1ΔM
Mib1ΔC
mib/herc2 domain
zz zinc finger domain
Mib repeat
ankyrin repeat domain
RING finger domain

Figure 2.2 Mib1 associated with Eg5 in HEK-293 cells

(A) HEK-293 cells were transfected with 6XMyc-Mib1 followed by immunoprecipitation of Mib1 from cell lysates using an anti-Myc antibody. As shown, Eg5 co-immunoprecipitated with 6XMyc-Mib1 as shown by Western blot analysis with anti-Eg5 antibody.

(B) Eg5 was immunoprecipitated from 6XMyc-Mib1-transfected HEK-293 cell lysates using an anti-Eg5 antibody. As shown by Western blot analysis with an anti-Myc antibody, 6XMyc-Mib1 could co-immunoprecipitate with Eg5.

(C) Top panel shows results from immunoprecipitation of Myc-tagged Mib1 deletion constructs with an anti-Myc antibody followed by Western blot analysis with an anti-Eg5 antibody. Bottom panels show Western blots of whole cell lysates labeled with either anti-Myc or anti-Eg5 antibodies.

(D) Schematic drawing of Mib1 deletion constructions used in (C). Figure adapted from [4].

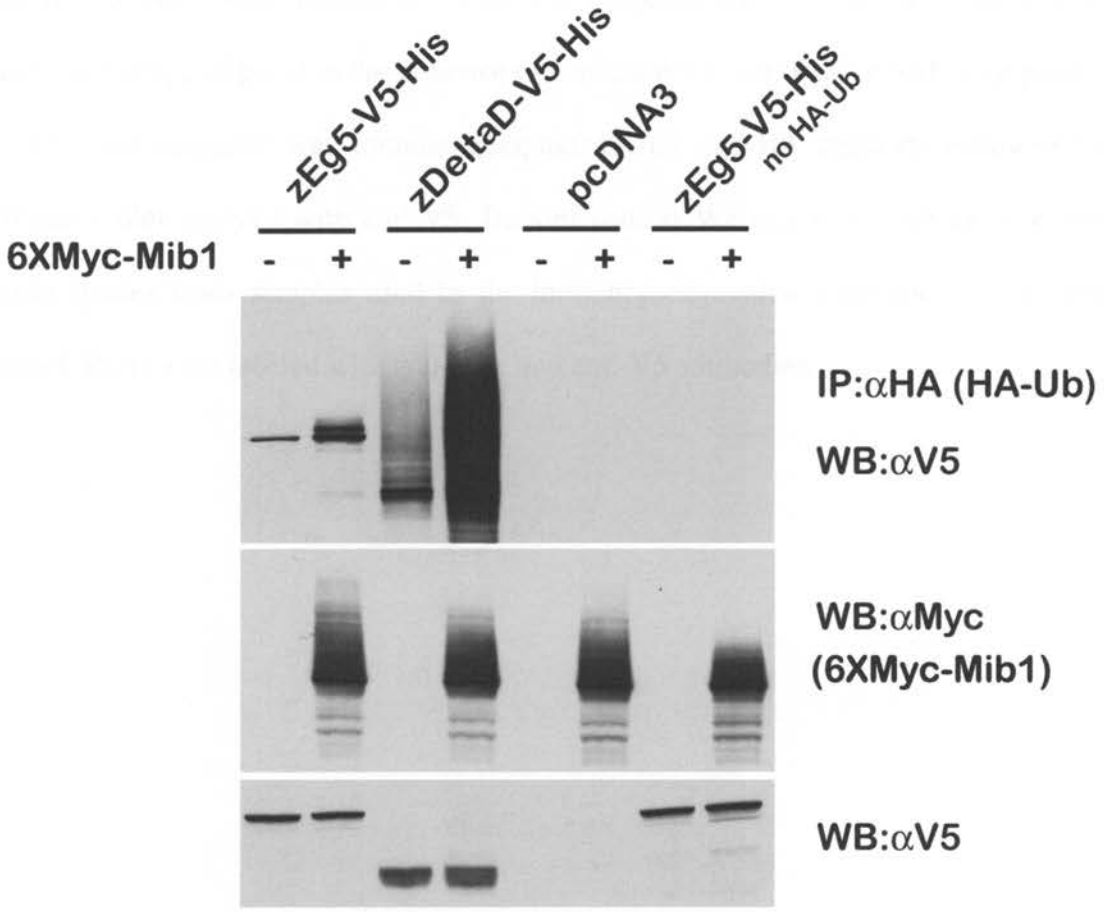
zEg5-V5-His
zDeltaD-V5-His
pcDNA3
zEg5-V5-His
no HA-Ub
6XMyc-Mib1
- + - + - + - +
IP:αHA (HA-Ub)
WB:αV5
WB:αMyc
(6XMyc-Mib1)
WB:αV5

Figure 2.3 Mib1 enhanced ubiquitination of Eg5 in HEK-293 cells

HEK-293 cells were transfected with HA-ubiquitin and V5-tagged constructs as indicated at top of panel in the presence (+) or absence (-) of 6XMyc-Mib. Top panel) HA-tagged ubiquitin was immunoprecipitated with anti-HA antibody followed by Western blot analysis with anti-V5. Bottom panels) Western blot analysis of whole cells lysates from samples used in the immunoprecipitation experiment in the top panel. Blots were labeled with anti-Myc and anti-V5 antibodies.

3XHA-Mib1
pcDNA3
αHA
αEg5
Hoechst
Merge

Figure 2.4 Overexpression of Mib1 did not affect Eg5 mitotic spindle localization

HEK-293 were transfected with 3XHA-Mib1 or pcDNA3 for 48 hours and detected with both an anti-HA antibody (green) and anti-Eg5 antibody (red). Nuclei were stained with Hoechst 33342 (blue). One hundred transfected cells, as assessed by 3XHA-Mib1 expression, were examined for Eg5 distribution. Eg5 maintained normal spindle distribution in the presence 3XHA-Mib1.

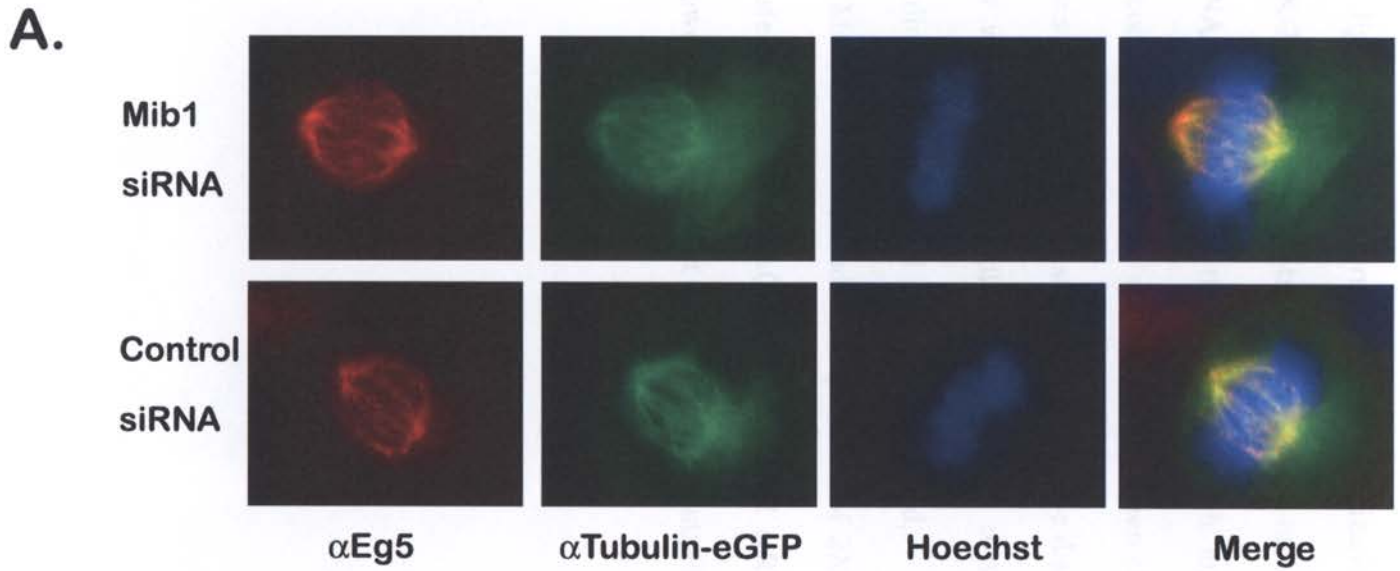
A.
Mib1
siRNA
Control
siRNA
αEg5
αTubulin-eGFP
Hoechst
Merge


B.
Control siRNA
Mib1 siRNA
2XFlag-Mib1

Figure 2.5 Silencing of Mib1 did not affect Eg5 spindle localization

(A) Eg5 maintained normal spindle localization in Mib1 siRNA-transfected cells. HEK-293 cells were co-transfected with α-tubulin-GFP and Mib1 siRNA or control siRNA for 48 hours, then detected with anti-Eg5 (red) and anti-GFP (green) antibodies. Cytoplasmic staining in the green channel is due to free tubulin. Nuclei were stained with Hoechst 33342 (blue). The distribution of Eg5 was examined in 100 cells with mitotic spindles, identified by α-tubulin-GFP. Eg5 maintained mitotic spindle localization in all 100 cells examined.

(B) Mib1 siRNA reduced the expression of 2XFLAG-Mib1. Hek293 cells were co-transfected with 2XFLAG-Mib1 and Mib1 siRNA or control siRNA for 48 hours, followed by Western blot analysis with an anti-FLAG antibody.

A.

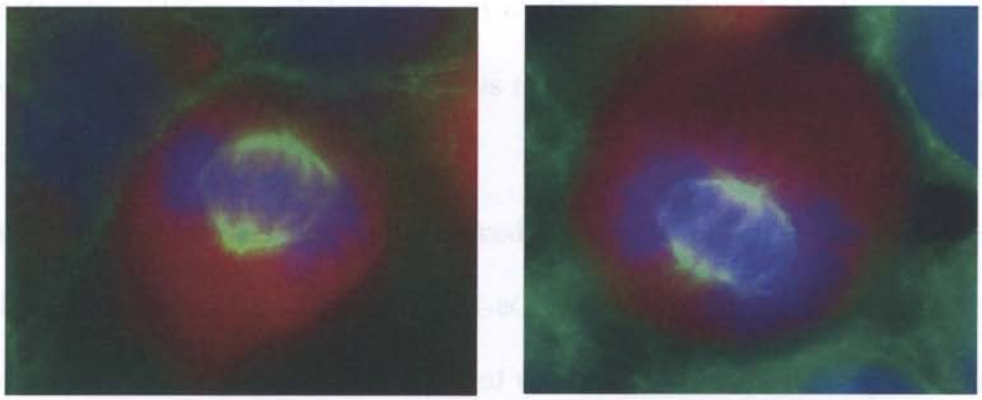

Mib1 siRNA Control siRNA

B.

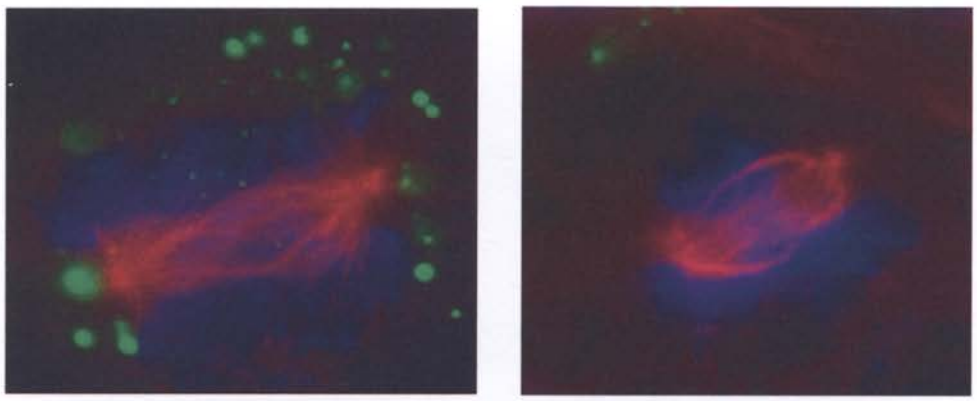

Mib1-eGFP Untransfected

Figure 2.6 Alteration of Mib1 expression levels did not affect spindle formation

(A) Normal mitotic spindles are formed in Mib1-silenced cells. HEK-293 cells were co-transfected with mRFP and Mib siRNA, or control siRNA. At 48 hours post-transfection, cells were labeled with anti-α-tubulin antibody (green) and stained with Hoechst 33342 (blue). One hundred cells expressing mRFP (red) were examined for abnormal spindle formation.

(B) Normal mitotic spindles were formed in Mib1-overexpressing cells. HEK-293 cells were either transfected with Mib1-eGFP (green) or were untransfected. At 48 hours post-transfection, cells were labeled with anti-α-tubulin antibody (red) and also stained with Hoechst 33342 (blue). One hundred cells were examined for abnormal mitotic spindle formation.

A.

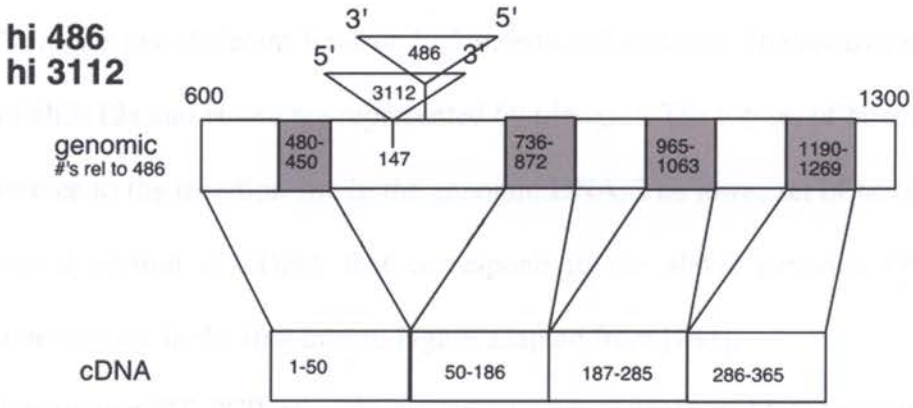
hi 486
hi 3112
3'
5'
5'
486
3'
3112
600
1300
genomic
#'s rel to 486
480-
450
147
736-
872
965-
1063
1190-
1269
cDNA
1-50
50-186
187-285
286-365

B.

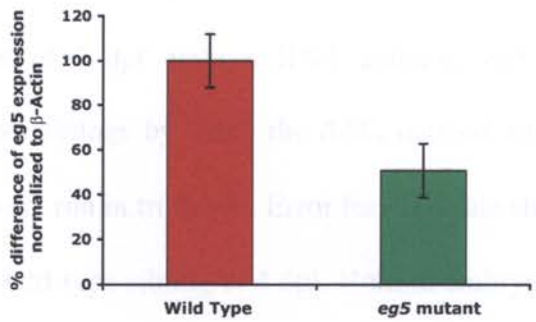
% difference of eg5 expression normalized to β-Actin
120
100
80
60
40
20
0
Wild Type
eg5 mutant

C.


eg5Hi3112a

D.

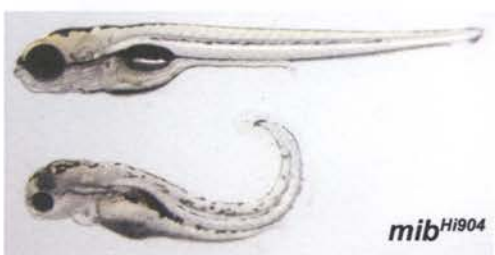
mibHi904

Figure 2.7 Characterization of *eg5*^{Hi3112A} zebrafish mutant

(A) There are two different lines of Eg5 insertional mutants. The retroviral insertion sites of Hi3112a and Hi486 are represented by triangles. The top set of boxes indicates the distance to the insertion site in the genomic DNA. The lower set of boxes indicate the cloned portion of cDNA that correspond to the above genomic DNA. Both insertion sites are in the first intron. Figure adapted from [143].

(B) Quantitative RT-PCR of *eg*^{Hi3112A} homozygous mutants at 4dpf. Quantitative RT-PCR using primers to zebrafish *eg5* or zebrafish *β-actin* was performed on cDNA prepared from a pool of 4 dpf embryo RNA extracts. *eg5* transcript levels were compared to wild type siblings by using the $\Delta\Delta C_t$ method and converted to percent difference. Samples were run in triplicate. Error bars indicate standard deviation.

(C) Top embryo is a wild-type sibling at 4 dpf. Bottom embryo is an *eg5*^{Hi3112A} mutant at 4 dpf. As shown, these *eg5*^{Hi3112A} mutants exhibit tail curvature, smaller eyes, brain disorganization, and pericardial edema.

(D) Top embryo is a wild-type sibling at 4 dpf. Bottom embryo is a *mib1*^{Hi904} mutant. *mib1*^{Hi904} mutants exhibit similar gross phenotypes compared to *eg5*^{Hi3112A} mutants.

Antisense
Sense
6hpf
18hpf
24hpf
48hpf

Figure 2.8 *eg5* expression during gastrulation and neurogenesis

Whole-mount *in situ* hybridization was performed on embryos during the developmental stages of gastrulation (6 dpf), primary neurogenesis (18 hpf), secondary neurogenesis (24 hpf), and late neurogenesis (48 hpf). Top panel shows expression of *eg5* using DIG-labeled antisense probe. Bottom panel shows the control DIG-labeled anti-sense probe used for non-specific hybridization. *eg5* was expressed ubiquitously at the gastrula stage, but becomes increasingly restricted to anterior regions as development proceeds. Intense staining is noted in the midbrain-hindbrain boundary at 48 hpf.

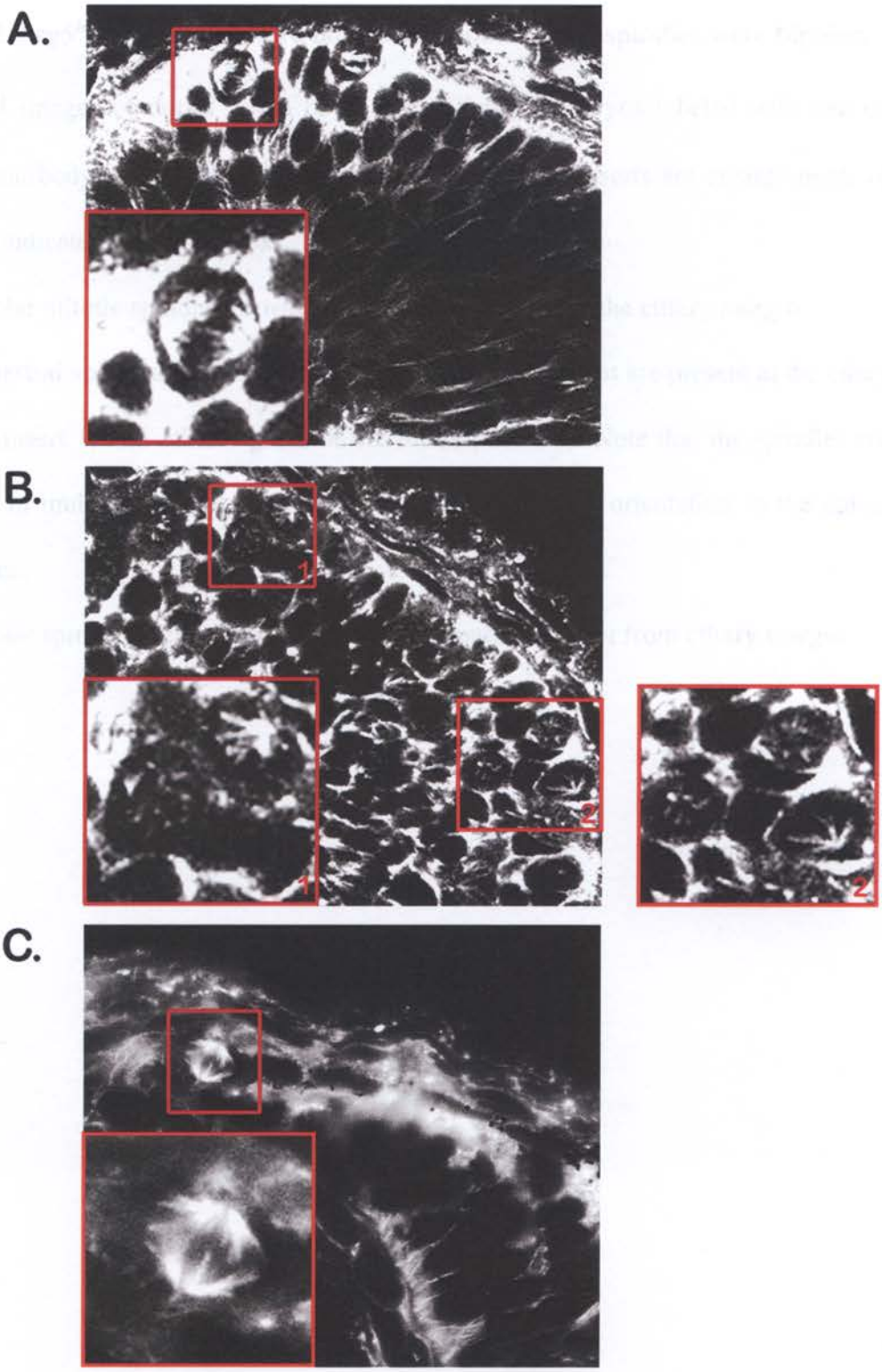
A.
B.
1
2
1
2
2
C.

Figure 2.9 *eg5*^{Hi3112a} spindles were monastral, but *mib1*^{Hi904} spindles were bipolar.

Confocal images of dorsal retina of 48 hpf zebrafish embryos labeled with anti-α-tubulin antibody to detect mitotic spindles. Dorsal is up. Inserts are enlargements of the area indicated with a red box.

(A) Bipolar mitotic spindles of wild type retinas. Insert from the ciliary margin.

(B) Monastral spindles were observed in *eg5*^{Hi3112A} mutants that are present at the cilary margin (insert 1) and other regions of the retina (insert 2). Note that the spindles are oriented in multiple directions instead of the usual parallel orientation to the apical membrane.

(C) Bipolar spindles were observed in *mib1*^{Hi904} mutants. Insert from ciliary margin.

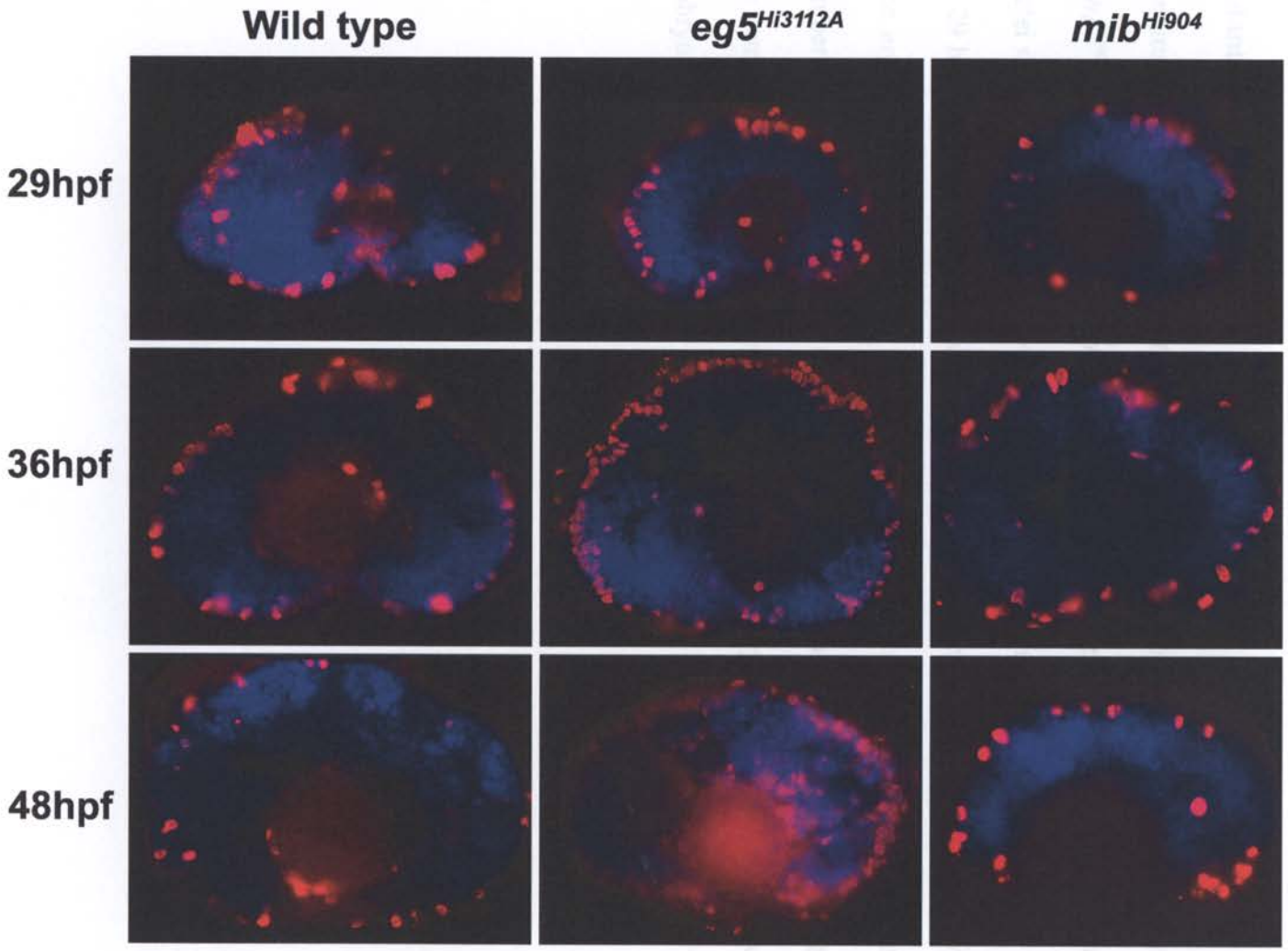
Wild type
eg5Hi3112A
mibHi904
29hpf
36hpf
48hpf

Figure 2.10 Characterization of mitotic populations in *eg5*^{Hi3112A} and *mib1*^{Hi904} mutants

Longitudinal sections of 29, 36, and 48 hpf retinas from wild-type, *eg5*^{Hi3113A} and *mib1*^{Hi904} embryos that were immunolabeled with an anti-pH3 (red) antibody and their nuclei stained with Hoechst 33342 (blue). Dorsal is up. Anterior is left.

At 29 hpf, the number of pH3 cells in eg5^{Hi3112A} mutant embryos was similar to wild type embryos. At 36 hpf and 48 hpf, eg5^{Hi3112A} mutants embryos had an elevated number of pH3 positive cells as compared to wild type embryos. At all of these stages, the number of pH3 positive cells in *mib1*^{Hi904} mutant embryos was similar to wild type embryos.

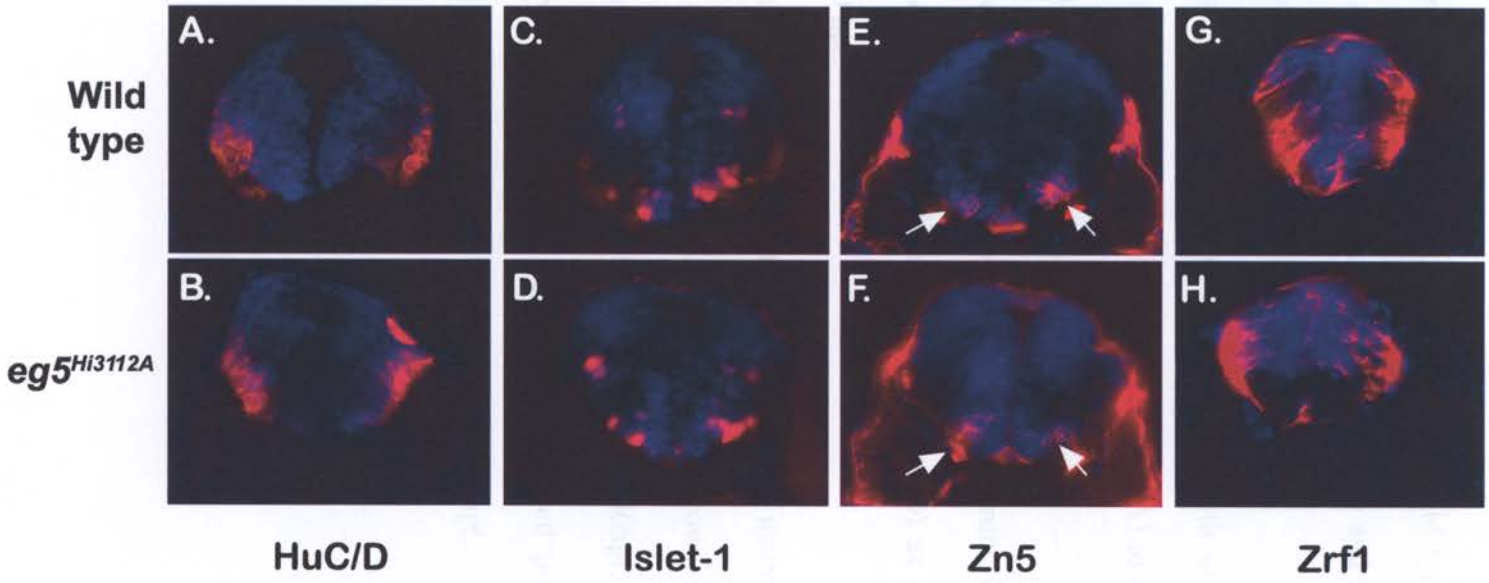
A.
C.
E.
G.
Wild type
B.
D.
F.
H.
eg5Hi3112A
HuC/D
Islet-1
Zn5
Zrf1

Figure 2.11 *eg5*^{Hi3112A} mutants did not have hind brain cell specification defects

Transverse sections through the caudal hindbrain of wild type and *eg5*^{Hi3112A} mutant embryos. Nuclei are stained with Hoechst 33342 (blue) and labeled with antibodies indicated below (red). Dorsal is up. Anterior is left.

(A, B) Comparison of differentiated cells, labeled with an antibody to the pan-neuronal marker HuC/D, of a 30hpf wild type embryo (A) to the *eg5*^{Hi3112A} mutant (B) embryo indicate a normal level of differentiation.

(C, D) The number and distribution of branchimotor neurons, labeled with anti-Islet-1 antibody, were normal in *eg5*^{Hi3112A} mutant embryos (D) as compared to wild type embryos (C) at 30 hpf.

(E, F) Similar numbers and distribution of commissural neurons in *eg5*^{Hi3112A} mutants (F), labeled with anti-Zn5 antibody and identified by arrows, indicate that these cells are specified normally like the wild type embryos (E) at 30hpf.

(G, H) Glia, labeled with anti-Zrf1 antibody, developed properly in the *eg5*^{Hi3112A} mutant (H) as compared to wild-type (G) embryos at 36 hpf.

A.

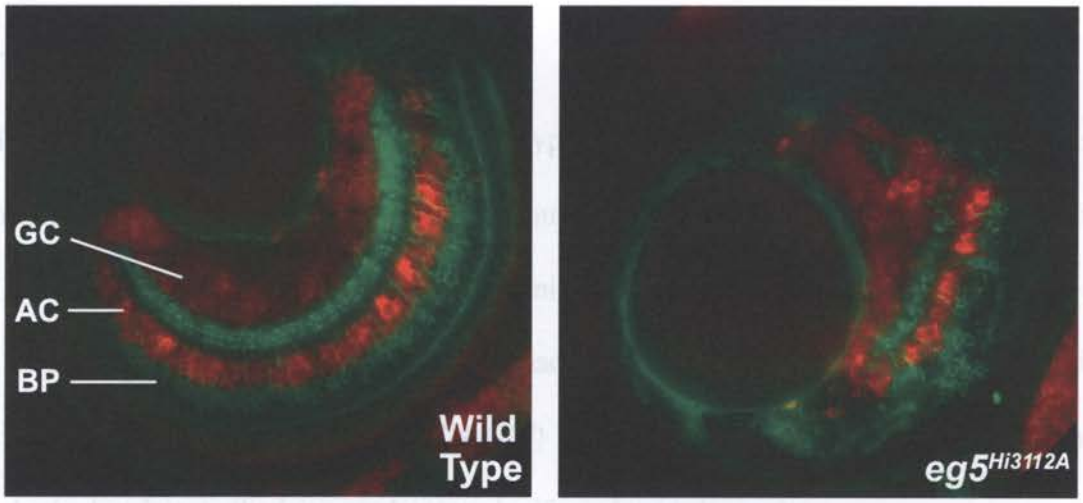

B.

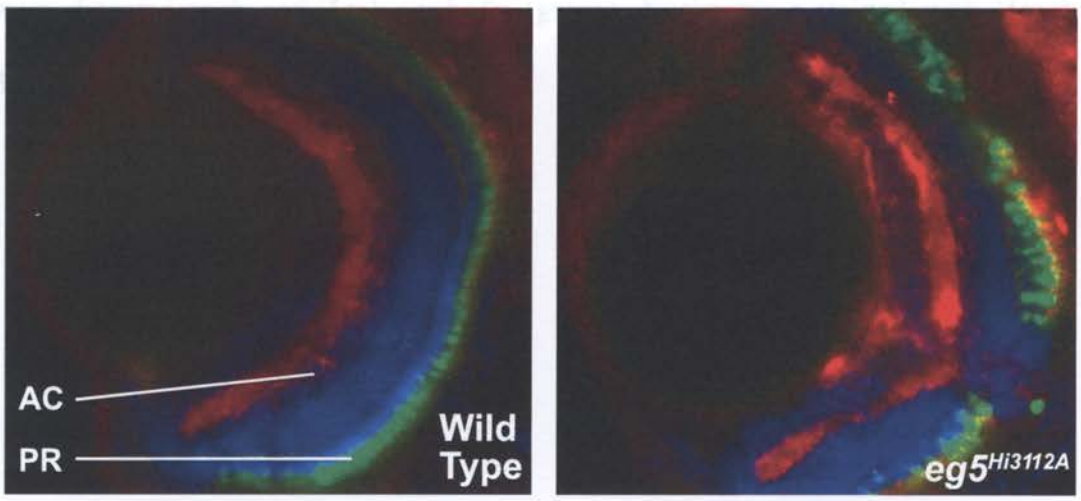

Figure 2.12 *eg5*^{Hi3112A} mutants did not have defects in cell specification in the retina

Transverse sections of 4 dpf of wild type and *eg5*^{Hi3112A} retinas. The intra-layer organization is disorganized in *eg5*^{Hi3112A} mutants, but all retinal cell types examined in (A) and (B) were present and laminar organization was maintained.

(**A**) Retinal ganglion cells (RG) and Amacrine (AC) cells were detected with anti-HuC/D antibody (red). Bipolar cells (BP) were detected with anti-PKCα antibody, which also detects the inner and outer plexiform layers (green).

(**B**) Amacrine cells (AC) were detected with anti-GAD-67 antibody (red). The anti-GAD-67 antibody also detects the inner plexiform layer. Double cone photoreceptors were detected with anti-Zpr1 antibody (green). Nuclei were stained with Hoechst 33342 (blue).

CHAPTER THREE

Antagonistic Roles of Eg5 and Mind bomb1 in Centrosome Duplication

Introduction

The centrosome is a small, non-membranous organelle that functions as the microtubule-organizing center (MTOC) of the cell [62]. It directs the assembly of the microtubule arrays in interphase and bipolar spindle during mitosis [62]. Consequently, it plays an important role in organelle positioning, cell polarity, as well as cell division [62]. Like the genome, it duplicates only once per cell cycle in S phase [12]. The resultant centrosomes are critical for the formation of bipolar mitotic spindle separation that separates sister chromatids [88]. Abnormalities in centrosome duplication can lead to severe consequences [123]. Supernumerary centrosomes, for example, are associated with numerous solid tumor and hematologic malignancies [172]. For some forms of breast and cervical cancer, centrosomal abnormalities arise prior to genomic instability and are considered as the underlying cause [17, 173, 174]. Despite the importance of the centrosome in cell biology and carcinogenesis, we have a poor understanding of how centrosome duplication is controlled.

Several motor proteins have been implicated in regulating centrosome duplication. The minus-ended motor, Dynein, was found necessary for assembly of the pericentriolar matrix proteins, pericentrin and γ-tubulin, onto the centrosome. [175, 176] The kinesin-like protein, KIFC5A, also regulates centrosome duplication as its inhibition promoted the formation of supernumerary centrosomes [177]. Finally, Goshima and Vale found that by individually siRNA silencing many of the motor proteins, spindle pole defects were observed, but did not further characterize the exact nature of these defects [178].

Eg5, a member of the kinesin-5 subclass of plus-ended kinesins, is another motor protein that could play a potential role in centrosome regulation [8]. Eg5 has a unique homotetrameric structure with two motor domains at each opposing end [69]. Because of this homotetrameric structure, it was proposed that the motor domains of Eg5 bind to antiparallel microtubules, such as those found in the mitotic spindle [179]. The significance of this binding to mitotic spindles is still under extensive investigation and debate, but it was proposed that Eg5 could promote stability and sliding of mitotic spindles [9]. Evidence for a role of Eg5 at the mitotic spindle is supported by the observation that mitotic spindles collapse when Eg5 is inhibited [66, 67].

However, some early observations suggest that Eg5 function is not limited to the formation of the bipolar spindle, but could also function at the centrosome. Whitehead and colleagues found that inhibition of Eg5 lead to a diffuse localization of the pericentrosomal proteins, Cep150 and ninein, at the centrosome, suggesting a role for Eg5 in centrosome organization [10]. Yet, the significance of this finding remained unexplored. In addition, recent studies of Cin8p, the *Saccharomyces cerevisiae* homolog of Eg5, showed that it plays an essential role at the analogous structure to the centrosome, the spindle pole body (SPB) [11]. The SPB contains of an electron dense half-bridge that serves as the site of its duplication and eventually joins these duplicated SPBs together [79]. Cin8p, through its microtubule-bundling activity, was found to generate the force necessary for severing the bridge joining them [11]. These

observations suggest further investigation of the function of Eg5 at the centrosome is necessary.

In this study, I report that the kinesin Eg5 is localized to the centrosome, where it inhibits centrosome duplication. I also report that an interacting protein of Eg5, the E3 ubiquitin ligase Mib1, promotes centrosome duplication. I provide evidence for an Eg5 and Mib1 interaction in centrosome duplication and show that these proteins are implicated in centrosomal organization and spindle formation.

Materials and Methods

Cell culture and Transfection

U2OS cells were maintained in high glucose DMEM containing 10% heat-inactivated fetal calf serum (Gibco BRL) and 100 U penicillin/streptomycin at 37°C in 5% CO_2. Cells were transiently transfected with 2:1 ratio of LIPOFECTAMINE 2000: DNA in antibiotic-free media, according to manufacture's instructions (Invitrogen). Media was replaced 6 hours after the application of the DNA-lipid complex with normal culture medium. Two μg pcDNA3, 3XHA-Mib1-pcDNA3, or 3XHA-Mib1ΔN-pcDNA3 was used in all Mib1 overexpression experiments. One-half of a μg of Eg5-V5-His was used in Mib1-rescue experiments. One μg of Centrin2-GFP was used in Mib1 co-localization experiments.

Inhibitors

A final concentration of 2 μg/mL Aphidicolin (SIGMA) and 100 μM Monastrol (Cytoskelton) were used in all experiments. Equivalent amounts of DMSO, used to dissolve the inhibitors, were used in the controls (vehicle).

Immunocytochemistry

U20S cells that were plated on poly-D-lysine coated coverslides were fixed in methanol at 20 °C for 10 minutes, washed with 1xPBS, blocked with 10% goat serum in 1X PBS, pH 7.4, then incubated overnight in primary antibody diluted in 3% goat serum at 4°C. After 3 washes in 1X PBS, cells were incubated in goat anti-mouse or rabbit Alexa-488 or 568 conjugated secondary antibodies (Invitrogen) at 1:1000 for 1 hour at room temperature. After final 3 rinses in 1X PBS, cells were stained with Hoechst 33342 and mounted in Prolong Gold (Invitrogen). The following dilutions of the following primary antibodies were used: Mouse anti-Eg5 (1:100, BD Biosciences), Rabbit anti-Eg5 (1:250, Cytoskeleton), Rabbit anti-αtubulin (1:250, SIGMA), Mouse anti-γ-tubulin (1:1000, SIGMA), Mouse anti-HA (1:1000, Covance), Rabbit anti-Mib1 (1:150, obtained from Patricia Gallagher), Rabbit anti-Centrin2 (1:1000, obtained from Uwe Wolfrum), Mouse anti-GFP (1:500, Invitrogen).

Microscopy and image analysis

Immunofluorescent-labeled samples were imaged under a Plan Apochromat 63X/1.4NA oil-immersion lenses on a Zeiss Axioplan2 equipped with Hamamatsu

CCD camera and Openlab image acquisition program. In all imaging experiments, 200 mononucleated cells were counted in 2 independent experiments. Data was analyzed by One-way ANOVA with Tukey-Kramer post-hoc multiple comparisons test. For Eg5 rescue of Mib1 experiment, the two-tailed t test was used. Statistics were done with InStat3 (GraphPad software).

Aphidicolin blocks and FACS analysis for DNA content

Cells were blocked in S phase by incubation with 2 μg/mL Aphidicolin for 24 to 48 hours. After 24 hours of Aphidicolin treatment a subset of cells were treated with 100 μM Monastrol or the vehicle, 0.1 % DMSO. Twenty-four hours later cells were trypsinized, fixed in ice-cold methanol, washed with Versene, then stained with Propidium Iodide staining solution (20 μg/mL RNase A, 20 μg/mL Propidium Iodide, and 0.01 % Triton X-100 in 1X PBS). Cells were then analyzed on a FACS Calibur (Becton Dickinson) using CellQuest analysis software. Specifically, two dot plots were generated from 10,000 events to show forward vs. side scatter and FL2-Area vs. FL2-Width. The majority of cells were gated on the forward/side scatter plot and reported in the FL2-Area/FL2-Width plot. A gate was drawn in FL2-Area /FL2-Width plot around singlets. These values were reported on a histogram that plots on the y-axis the number of counts for a given FL2 Area.

RNA extraction and Quantitative RT-PCR

Total RNA from siRNA-transfected cells was extracted using an RNAeasy kit (Qiagen) and treated with DNaseI (Ambion). cDNA was prepared from 500 ng of RNA using the Superscript III Reverse Transcription kit and Random Hexamers (Invitrogen and Ambion). Quantitative RT-PCR was performed on a Stratagene MX Real-Time PCR machine using SYBR green PCR mix and the PCR primers designed to detect human β-Actin and human Mib1. The following PCR cycling conditions were used with reads taken at the end-point of each cycle: 95°C, 2 min; 95°C, 15 sec, 68°C, 50 sec for 40 cycles. A melting curve was obtained at the end of the run by obtaining continuous reads during a transition from 68 °C to 95 °C. The efficiency of PCR reaction with the described primer sets was determined using a dilution series of the input cDNA. Samples were run on PAGE gels to verify amplication of a single product and the absence of dimers. β-Actin normalized Mib siRNA- and control siRNA-treated samples were compared by $\Delta\Delta C_T$ method and converted to fold difference. All samples were run in triplicate.

siRNA transfection

STEALTH-siRNA duplexes that target human Mib1 (MIB1HSS126396) and a low GC content random siRNA control were obtained from Invitrogen. The sequence for the Mib1 siRNA duplex is as follows:

AAUACUGGAAUAUUCCCACUUGAGA.

Cells were transfected with 50 nM of the siRNA duplexes with LIPOFECTAMINE 2000 according to manufacturer's instructions. The media was replaced, 6 hours after the addition of the complexes. For the Mib1 siRNA rescue of Aphidicolin-induced centrosome duplication experiments, cells were allowed to recover for 2 hours, then a 1000X stock of Aphidicolin was added at a final concentration of 2 μg/mL.

Western blotting analysis

siRNA transfected cells were lysed in 100 μL of NP40-Tris Lysis buffer (20 mM Tris-Cl pH8, 1% NP-40, 137 mM NaCl, 10% Glycerol, 2 mM EDTA, 10 mM NaF) containing Protease Complete Inhibitor (Roche). As determined by a Bio-Rad protein assay, 50 μg of the total protein, were denatured in Laemelli buffer, then run on a 4-12% Bis-Tris Criterion XT gel in 1X MOPS XT buffer. The gel was then transferred to PDVF membrane in Towbin buffer, according to standard protocols. Membranes were blocked then incubated overnight at 4°C with an antibody recognizing the endogenous human Mib1 (1:1000, obtained from Patricia Gallagher) and an antibody recognizing β-Actin (1:20,000, Sigma)

Results

Eg5 was localized to the centrosome

Previous studies described only the localization of Eg5 to spindle poles and mitotic spindles [151]. As Eg5 was described to have a role in centrosomal organization, I wanted to determine the location of endogenous Eg5 [10, 11]. U20S cells were immunolabeled with a monoclonal antibody generated against the stalk region of Eg5 (BD Biosciences). This region is thought to be specific to Eg5, and antibodies against this region are unlikely to recognize other Kinesin-5 family members. Immunofluorescent labeling of U2OS cells revealed discrete localization of Eg5 in the proximity of the nucleus (Figure 3.1A). A similar immunolabeling pattern was observed using a different Eg5 polyclonal antibody (Cytoskeleton); (data not shown). As the intense, proximal nuclear staining of Eg5 was in a similar subcellular region of the centrosome, I examined whether Eg5 was localized at the centrosome. Co-immunofluorescent labeling of Eg5 with γ-tubulin, a component of the pericentriolar matrix, showed a partial overlap of these two proteins. Eg5 is localized to one end of the centrosome. Furthermore, centrosomal localization of Eg5 was observed in both single and duplicated centrosomes (Figure 3.1A).

As Eg5 had a polarized localization within the centrosome, I wished to examine its localization further. Centrioles, a microtubule-based barrel-shaped structure, are an integral component of the centrosome. Centrioles have a polarized orientation within the centrosome with a proximal and distal end [180]. The EF-hand protein, Centrin, localizes exclusively to the distal end of the lumen of centrioles,

making them a good marker of localization of proteins within the centrosome [181]. Immunofluorescent labeling with an antibody against Centrin found that Eg5 did not co-localize with the distal centriole marker, Centrin, but instead surrounded the Centrin at one end (Figure 3.1B). Therefore, I determined that Eg5 localizes to one end of the centrosome and this region is most likely the proximal end of the centriole.

Inhibition of Eg5 activity promoted excess numbers of centrosomes

Considering that Eg5 was localized at the centrosome, I examined whether inhibition of Eg5 would affect the centrosome organization or function. I used a highly specific and potent inhibitor of Eg5, Monastrol, to treat U20S cells for various durations and then I examined the cells with the centrosomal marker γ-tubulin. Monastrol inhibits Eg5 activity by inhibiting ADP release, leading to decreased microtubule binding [182-184]. The number of cells with excess centrosomes in Monastrol-treated cells was increased compared to vehicle-treated cells (Figure 3.2A). The number of mononucleated cells containing greater than two centrosomes was quantified in both groups (Figure 3.2C). As compared to vehicle treatment, Monastrol treatment promoted excess numbers of centrosomes in a duration-dependent manner (14.25±1.77% vs. 2.25±1.06% for 24 hours of treatment, $P<0.01$; 29.75±3.18% vs. 2.75±0.354% at 48 hours of treatment, $P<0.001$; 35.75±3.18% vs. 0.75±0.353% at 72 hours of treatment, $P<0.001$).

The excess centrosomes observed could be from an increase in the number of centrioles or fragmentation of the pericentriolar matrix. To distinguish between the

two possibilities, I examined treated cells for an increase in the number of centrioles with the centriolar marker, Centrin, in conjunction with pericentriolar matrix marker, γ-tubulin, by immunofluorescence. In Monastrol-treated cells I observed an excess of centrioles that corresponded with γ-tubulin staining (Figure 3.2B). Quantification of mononucleated cells containing excessive centrioles (≥5) also revealed a marked elevation with longer Monastrol treatments (Figure 3.2C) (19.5±3.54% vs. 3.75±1.06% at 24 hours of treatment, $P<0.01$; 22.75±2.47% vs. 7.5±2.12% at 48 hours of treatment, $P<0.01$; 25.5±2.12 vs. 5.75±1.06% at 72 hours of treatment, $P<0.001$). These results show that excess centrosomes observed in Monastrol-treated cells is due an increase in the number of centrioles.

Eg5 inhibition promoted excess centrosome formation during S phase

An excess of centrosomes observed could result from centrosome overduplication, centrosome splitting, or by disrupting cytokinesis. Centrosome splitting and duplication occur in S phase, whereas cytokinesis occurs after mitosis. To distinguish between these possibilities, U2OS cells were arrested at the G1/S boundary with Aphidicolin, a DNA polymerase α inhibitor. After a 24 hour block with Aphidicolin, there was a significant block at G1/S boundary as determined by FACS analysis for DNA content (Figure 3.3A). This block was maintained for at least 48 hours. This blockade was further verified by the addition of Monastrol to cells that were pre-treated with Aphidicolin for 24 hours. Ordinarily, Monastrol induces a block in M phase, but in Aphidicolin-treated cells the S phase block was maintained.

Using this treatment paradigm, the number of cells with excess centrosomes after pre-treatment with Aphidicolin for 24 hours followed by treatment with Monastrol or the vehicle for an additional 48 or 72 hours were counted (Figure 3.3B). Although Aphidicolin treatment itself was able to increase centrosome number, I observed an additional significant elevation in the number of Aphidicolin-blocked cells with excess centrosomes when treated with Monastrol compared to the vehicle (13±1.06% vs. 5.5±1.06% for 24 hours of treatment, $P<0.01$ and 45.5±3.54% vs. 35.5±1.77% for 48 hours of treatment, $P<0.01$).

Mib1 co-localized with Eg5 at the centrosome

As described in Chapter Two, Mib1 associated with Eg5 and promoted its monoubiquitination. In addition, Mib1 was found to associate with several other centrosomal proteins. Therefore, I wanted to examine whether Mib1 associates with Eg5 at the centrosome.

First, it was examined whether Mib1 was localized to the centrosome using an antibody against the pericentriolar matrix component, γ-tubulin, as a marker in U2OS cells. Mib1 was observed to co-localize with γ-tubulin and also detected in regions extending outside of γ-tubulin-defined boundaries (Figure 3.4A). This localization pattern cells occurred in cells with both single and duplicated centrosomes. The pattern of Mib1 staining is suggestive of centrioles. Examination of Mib1 localization in cells expressing a GFP-tagged version of the centriolar marker, Centrin2, found that Mib1 was expressed in a pattern similar to centrioles (Figure 3.4B). However, Mib1

did not co-localize with centrioles, but instead enveloped a region surrounding the centrioles.

Finally, as Mib1 has a centrosome distribution similar to Eg5, I examined whether the two proteins co-localize. As predicted, Mib1 co-localized with Eg5 at the centrosome (Figure 3.5).

Mib1 promoted excess centrosomes and centrioles

As Mib1 co-localized with Eg5 at the centrosome, I wanted to ask whether Mib1 could also induce centrosome defects. Using a transient transfection approach, I asked whether overexpression of a 3XHA-tagged version of human Mib1 could affect centrosome numbers. Like the endogenous protein, 3XHA-Mib1 was appropriately localized to the centrosome (Figure 3.6A). Similar to the phenotype observed following inhibition of Eg5, Mib1 overexpression also promoted centrosome amplification. Mib1-overexpressing cells, and control cells transfected with pcDNA3, were quantified for excessive centrosomes (≥3) as revealed with γ-tubulin immunofluorescent labeling (Figure 3.6B). Beginning at 48 hours post-transfection, a significant elevation in the number of Mib1-expressing cells with centrosome amplification as compared to control was observed (14.75 ± 1.06% vs. 0.75± 0.707%, $P<0.001$), which remained after 72 hours post-transfection (19± 1.41% vs. 1.25± 0.354%, $P<0.001$). Taken together, these results suggest that Mib1, like Eg5, is able to promote excess centrosome numbers.

In Chapter Two, I determined that the N-terminal region of Mib1 was required for interaction with Eg5. Therefore, I wanted to determine whether this region of Mib1 is required to promote centrosome amplification. Therefore, I created a 3XHA-tagged N-terminal deletion of Mib1 (3XHA-MibΔN), which lacks the ZZ zinc finger, and Mib1-specific interaction domains, that are required for interaction with Eg5, but retains the ankyrin repeats and three RING finger domains. The 3XHA-MibΔN construct was ubiquituously distributed throughout the cytoplasm (Figure 3.6A). Overexpression of the 3XHA-Mib1ΔN in U2OS cells relative to control did not induce excess centrosomes at both 48 and 72 hours post-transfection (1.25±0.354% vs. 0.75%±0.707% at 48 hours and 1±0.707% vs. 1.25%±0.354 at 72 hours); (Figure 3.6B). These results indicate that the N-terminal region of Mib1 was not required for excess centrosome formation.

To determine whether Mib1, like Eg5 inhibition, promotes bona-fide centriole duplication, I examined Mib1-overexpressing cells for excessive centrioles using the centriole marker, Centrin2 (Figure 3.7). Similar to our observations with centrosomes, Mib1 could significantly promote excessive centrioles at both 48 and 72 hours post-transfection (20±4.24% vs. 4.25±1.06% at 48h, $P<0.01$ and 27.75±2.47% vs. 4.5±0.707% at 72h, $P<0.001$). In addition, the overexpression of 3XHA-Mib1 ΔN was unable to affect centriole duplication (Figure 3.7). Taken together, these results show that Mib1 promotes bona-fide centriole amplification through N-terminal region interaction with other proteins.

Mib1 was required for centrosome duplication

As overexpression of Mib1 was able to promote centrosome amplification, I wanted to determine whether the endogenously expressed Mib1 was required for centrosome amplification. The expression of endogenous Mib1 was silenced using duplexed siRNA against Mib1 (Mib1 siRNA) in U2OS cells. The efficiency of the Mib siRNA duplex against Mib1 transcripts was assessed by quantitative RT-PCR. At 72 hours post-transfection, an 87.6% reduction in the relative abundance of human Mib1 transcripts in Mib1-silenced cells as compared to control samples was observed (Figure 3.8A). The efficiency of this siRNA-silencing was further supported by Western blot analysis, which showed undetectable levels of Mib1 protein in Mib1 siRNA-transfected cell lysates (Figure 3.8B).

Mib1 siRNA was then transfected into U2OS cells and the number of centrosomes were quantified. In Mib1 siRNA-transfected cells, there were fewer cells with two centrosomes compared to control-transfected cells (54.5±4.24% vs. 76.0 ±2.12%, $P<0.01$) (Figure 3.8C). Conversely, a greater number of single centrosomes in Mib1 siRNA-transfected, as compared to control-transfected, was observed (43.5±4.24% vs. 22.25±2.47%, $P<0.01$). These results suggest that endogenous Mib1 expression is required for normal centrosome duplication.

It was previously observed that centrosomes overduplicate when arrested for a prolonged period in S phase; this property is often used to test for centrosome duplication defects [113, 118, 150]. Therefore, I tested whether Mib1-silencing could also inhibit S-phase induced centrosome duplication. Indeed, Mib1-silenced cells

treated with Aphidicolin, caused an excess of centrosomes compared to control siRNA cells. (18±3.18% vs. 39.5±5.3%, P<0.05); (Figure 3.8D). This finding suggests that Mib1 is also required for Aphidicolin-induced centrosome amplification.

Mib1 promoted excess centrosomes during S phase

As Eg5 inhibition promoted excess centrioles in the S phase, I wanted to know whether Mib1-promoted centrosome duplication also occurred in S phase of the cell cycle. Aphidicolin was added to 3XHA-Mib transfected cells and examined 72 hours later. Mib1 could promote centrosome duplication, even when cells were arrested in S phase, as Mib1 overexpressing cells had significant more cells with excess centrosomes compared to control cells (54.75±4.25% vs. 33.75±3.89%, P<0.05); (Figure 3.9).

Eg5 rescued Mib1-mediated centrosome amplification

To further address whether Eg5 and Mib1 function together in centrosome duplication, I tested whether I could rescue defects caused by overexpression of Mib1 with overexpression of Eg5. I reasoned that if inhibition of Eg5 could promote centrosome duplication, then perhaps its overexpression would rescue Mib1 overexpression defects if it works downstream. I used an Eg5-His-V5 tagged construct that localized appropriately to centrosome and mitotic spindle (data not shown), and can be ubiquitinated by Mib1 (Chapter Two). I found that 12±1.41% of cells

transfected with Mib1 had excess centrosomes, whereas 7±0.707% cells co-transfected with Mib1 and Eg5 had excess centrosomes (P=0.0465, two tailed t test); (Figure 3.10). These results suggest that Eg5 works downstream of Mib1 to counter-act Mib1 induced centrosome duplication.

Alteration of Mib1 and Eg5 levels or activity promoted abnormal spindles and Pericentrin redistribution

As the centrosome functions as the site of mitotic spindle assembly, I wanted to see how an abnormal number of centrosomes would affect spindle formation. To examine this, U20S cells were treated with Monastrol for 48 hours and examined their spindles by immunolabeling with anti-α-tubulin. Consistent with previous observations, monastral spindles were observed in these cells (Figure 3.11A). Likewise, U2OS cells were transfected with 3XHA-Mib and their spindles examined by immunolabeling with anti-α-tubulin 48 hours later. In these cells, Mib1 overexpression caused multi-polar spindles to form (Figure 3.11B). These results suggest that these cells with excess centrosomes form abnormal spindles.

Many pericentriolar components are recruited to the centrosome from a cytoplasmic pool to form a scaffold that promotes procentriole formation and microtubule assembly [185]. One well-characterized pericentriolar scaffolding protein is the coiled coil protein Pericentrin [185]. I used an antibody against Pericentrin to further assess the structure of the pericentriolar matrix. After 48 hours of treatment with Monastrol, there was a greater accumulation of Pericentrin at the centrosomes

compared to control treatments (Figure 3.11C). Similarly, Mib1-transfected cells also had greater accumulation of Pericentrin at the centrosome compared to pcDNA3-transfected cells (Figure 3.11D). Taken together, these results suggest that the change in Pericentrin distribution upon treatment with Monastrol or transfection with Mib1 reflects an enhanced Pericentrin recruitment from cytoplasmic pools. Alternatively, the seeming accumulation of Pericentrin at the centrosome may result from a disorganized pericentriolar matrix.

Discussion

Modulation of centrosome and centriole numbers by Eg5 and Mib1

In this chapter, I showed that Eg5 and its previously identified interacting-protein, Mib1, co-localized at the centrosome and contributed to centrosome and centriole duplication. My results showed that inhibition of Eg5 and overexpression of Mib1 could cause the cells to form excess centrosomes. Conversely, Mib1-silencing with siRNA inhibited centrosome duplication. Furthermore, I found that Eg5 inhibition and Mib1 overexpression promoted an excess of centrioles supporting a bona-fide centriole overduplication. I also noted that longer treatments with Monastrol led to increasing number of cells with excess centrioles and centrosomes. This upward trend in centriole and centrosome numbers could reflect the effectiveness of longer treatments or the time required for additional rounds of duplication. In Mib1-overexpressing cells, an upward trend in the number of centrosomes and centrioles was also observed, but this was not statistically significant. There was a slight

decrease in the level of expressed Mib1 at 72 hours as compared to 48 hours, which may explain an absence of time-dependent severity of centrosome amplification. This observed diminishment of Mib1 expression may be caused by self-ubiquitination and degradation, a common characteristic of RING finger type E3 ubiquitin ligases [28]. I observed that Mib1-silencing could decrease the number of centrosomes not only in normal cycling cells, but also in Aphidicolin-treated cells, suggesting that Mib1 function is required for both normal and aberrant centrosome duplication.

I also showed that Mib1-overexpressing and Eg5-inhibited cells form abnormal spindles, which suggest that excess centrosomes present in these cells can function in microtubule assembly. In the Mib1-expressing cells, the abnormal spindles were multipolar, but in the Eg5-inhibited cells, they were monastral. This apparent inconsistency between the types of abnormal spindle cells may be explained from observations in the literature. It was previously found that silencing of the novel centrosome protein CPAP by RNAi caused excess centrosomes and consequently multipolar spindles [186]. Adding an Eg5 inhibitor to CPAP-silenced cells, however, induces monopolar spindles instead of multipolar spindles [186]. Eg5 inhibition could collapse a multi-polar spindle into a monopolar spindle through destabilizing of spindle microtubules. Consequently, monopolar spindles would form in Eg5-inhibited cells regardless of the number of centrosomes.

Interaction of Mib1 and Eg5 in promoting excess centrioles and centrosomes

In this study, I showed that Mib1 and Eg5 co-localize at the centrosome. The ability of Mib1 to promote overduplication was dependent on the N-terminal region of Mib1, a region where Eg5 interacts. Furthermore, I found that excess centrosomes promoted by overexpression of Mib1 could be inhibited by overexpression of Eg5. These results suggest that Mib1 negatively regulates Eg5 and consequently promotes excess centrosomes. As Mib1 is known to promote ubiquitination of Eg5, one hypothesis is that Mib1 inhibits Eg5 through this ubiquitination. This ubiquitination inactivates the motor and bundling activity of Eg5 and leads to aberrant centrosome amplification. The presumption of this hypothesis is the requirement of E3 ubiquitin ligase activity of Mib1 in promoting excess centrosomes. Identification of the ubiquitnated sites of Eg5 could reveal how this modification negatively impacts its function.

Possible reasons for observed changes in centrosome and centriole numbers

At least three possible defects can result in excess centrosomes and centrioles: (1) cytokinesis failure, (2) centriole splitting failure, and (3) centriole overduplication [123]. Excess centrosomes and centrioles can occur from a cytokinesis failure because centrosomes and centrioles fail to properly segregate during cell division [187, 188]. In addition, a cytokinesis failure could also increase DNA content and result in multi-nucleated cells. Because data presented in this chapter excluded multi-nucleated cells, the described centrosome amplification is unlikely to be from a cytokinesis failure.

However, data presented in this chapter was unable to determine whether centriole splitting failure or centrosome overduplication was the cause of excess centrosomes.

Failure of centriole splitting can also cause excess centrioles. Parental centrioles are connected, by a microtubule-based intercentriolar bridge, at their proximal ends. If this bridge fails to split after duplication, the parental centrioles will remain connected. This phenomenon of failed centriole splitting is best illustrated with NIMA-related kinase, Nek2, and its effector C-NAP1 [98]. C-NAP1, a coiled-coil protein, links the filamentous bridge to the proximal ends of centrioles [98]. Ordinarily, phosphorylation of C-NAP1 by Nek2A promotes the release of C-NAP1 from the centriole, causing the centriole to split [97]. However, when Nek2A is inhibited, normal centriole splitting does not occur, causing an excess of centrioles [97]. Although how failed centriole splitting induces excess centrioles is not clear, one possible explanation is that centriole splitting may be required to cease centriole duplication.

Eg5 may be required for centriole splitting. The microtubule bridge that connects two SPBs failed to break in mutants of *S. cerevisiae* Eg5 ortholog, Cin8p, which results in unseparated SPBs [79]. The splitting requires the bundling, but not motor activity of Cin8p [79]. It was suggested that Cin8p generates a force that causes the microtubule bridge to break [79]. Eg5 could use a similar mechanism to break the intercentriolar bridge that joins parent centrioles. Inhibition of Eg5 would prevent the intercentriolar bridge from breaking and allow centriole duplication to continue. As I

did not examine whether overexpression of Eg5 would induce centriole splitting, I cannot determine whether centriole splitting is the cause of the centriolar defects.

Excess centrosomes could also occur if there was a perturbation in one of the proteins that regulate centrosome duplication. Data from *C. elegans* indicate that a new centrosome is assembled by the ordered recruitment of the centrosomal scaffolding proteins SPD-2, SAS-5, SAS-6, and SAS-4 and requires the kinase activity of Zyg-1 [84]. Zyg-1 phosphorylation of SPD-2 promotes the sequential recruitment of SAS-5 and SAS-6 to the centrosome from their cytoplasmic pools [84]. At the centrosome, SAS-5 and SAS-6 form a tube-like structure. Upon this structure, SAS-4 promotes microtubule assembly that results in the formation of the pro-centriole [84]. Homologs of the scaffolding proteins SPD-2, SAS-6, and SAS-4 and others, such as Pericentrin, were found in vertebrates and are also necessary for centriole duplication [88, 185]. Although a Zyg-1 homolog has been elusive, another kinase, Plk4, is proposed to be the vertebrate functional equivalent. Interestingly, overexpression of Plk4 and SAS6 induces excess centrioles and centrosomes by simultaneously forming multiple procentrioles on the mother centriole. Eg5, through its binding at the centrosome, may play a role in limiting a single procentriole site on the mother centriole. Interestingly, in cells with overexpression of Mib1 or inhibition of Eg5, I found more aggregation of Pericentrin at centrosome. The elevated aggregation of Pericentrin may indicate overrecruitment of other centrosomal structural proteins. Future experiments will determine whether Mib1 and Eg5 perturb the centrosomal levels of these core components of centrosome duplication.

Possible mechanism for regulation of Eg5 and Mib1 at the centrosome

I observed that Eg5 and Mib1 co-localize at the centrosome. Furthermore, they localized to both single and duplicated centrosomes, indicative of G1 and S/G2 cells, respectively. As Mib1 and Eg5 were constitutively centrosomal throughout the cell cycle, how they regulate the centrosome would not depend on their subcellular localization. However, as centrosome regulation does require precise coordination with the cell cycle, Eg5 and Mib1 would have to be regulated by some other mechanism. One possibility is the E3 ligase activity of Mib1 in regulated by another cell cycle dependent protein. One candidate, as revealed by my proteomic screen, is the serine-threonine kinase, NDR1. Recently, NDR1 was found to localize to the centrosome in a cell-cycle dependent manner to regulate centrosome duplication. Furthermore NDR1-mediated centrosome duplication requires cdk2 activity [150]. Currently, the substrate for NDR1 is unknown. However, it was proposed that this unknown substrate resides at the centrosome since centrosome anchored-NDR still promotes centrosome duplication [150]. This suggests that Mib1 is a potential target of NDR1 and could provide a mechanism for a cell cycle-dependent regulation of Eg5 by Mib1

The centrosome duplication cycle is a highly regulated process that ensures that only a pair of centrosomes are available for mitotic spindle assembly [12]. Absence of a controlled centrosome duplication often results in abnormal spindle formation and aneuploidy [87]. I have unraveled Eg5 and Mib1 as two regulators that necessary for the maintenance of the appropriate number of centrosomes. The

identification of the precise function of Mib1 and Eg5 at the centrosome could promote a greater understanding of the centrosome duplication cycle.

A.

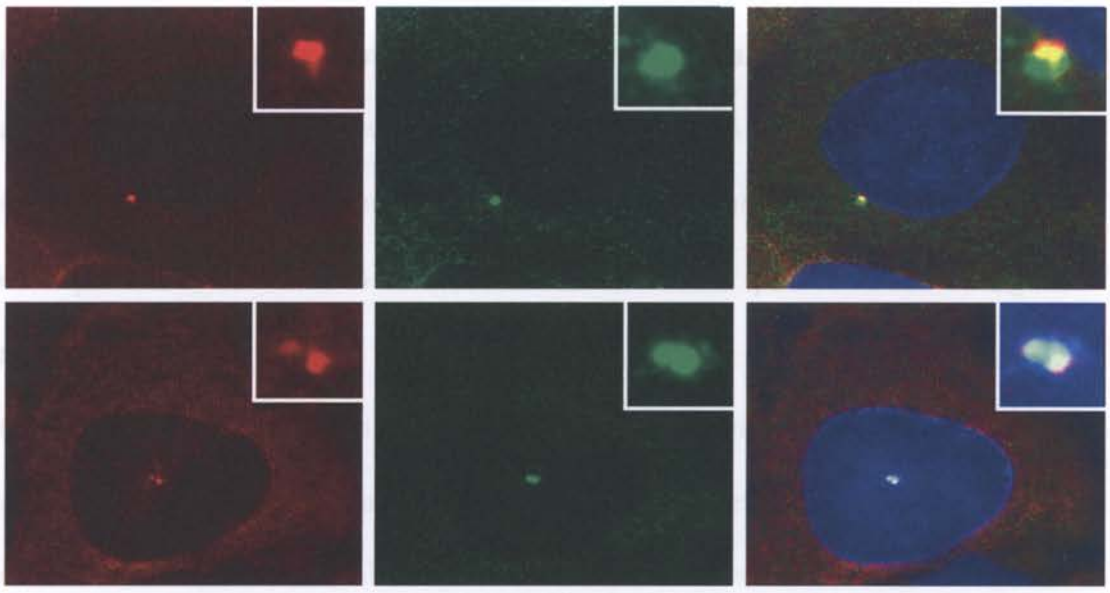

Eg5 γ-tubulin Merge

B.

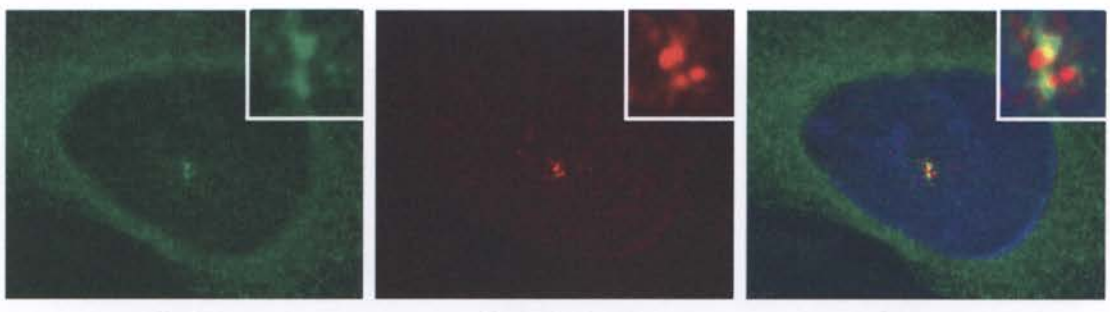

Eg5 Centrin-3 Merge

Figure 3.1 Eg5 localization at the centrosome

(**A**) Partial co-localization of Eg5 with the PCM protein, γ-tubulin. U2OS cells were processed for fluorescent immunocytochemistry using antibodies against Eg5 (red) and γ-tubulin (green). Merged image, also showing nuclei stained with Hoechst 33342 (blue), indicates a partial overlap between Eg5 and γ-tubulin in unduplicated (top row) or duplicated (bottom row) centrosomes. Inserts show portion of the images 4X magnified.

(**B**) Eg5 localizes to a region of the centrosome neighboring the centriole. U20S cells processed for fluorescent immunocytochemistry using antibodies against Eg5 (green) and Centrin-3 (red). Merged image also shows nuclei stained with Hoechst 33342 (blue). Inserts are from a portion of image magnified 4X.

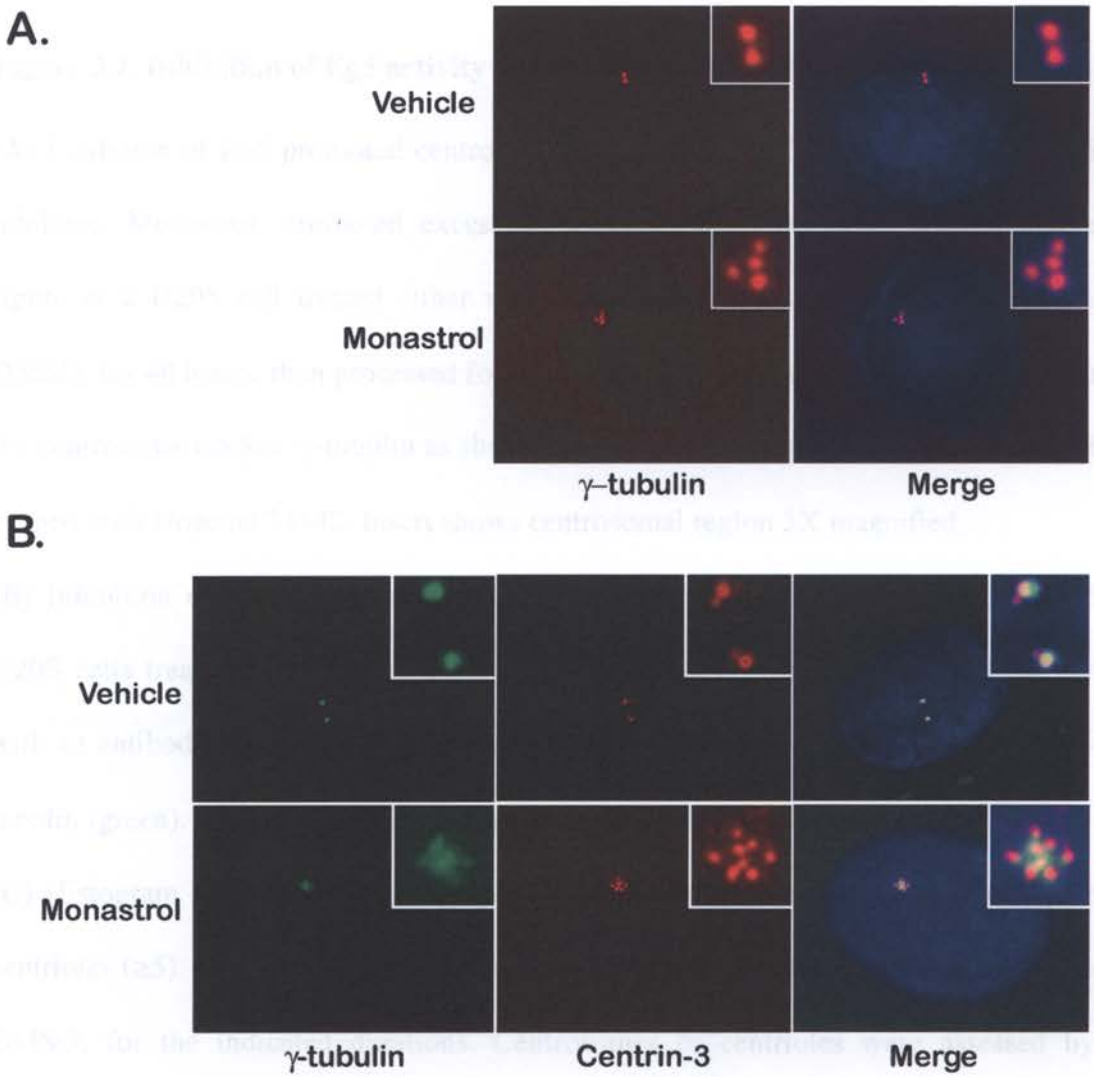
A.
Vehicle
Monastrol
γ–tubulin
Merge
B.
Vehicle
Monastrol
γ-tubulin
Centrin-3
Merge
C.
Vehicle
Monastrol
% of cells with centrosomes ≥3
**
***
***
24
48
72
Length of treatment (hours)
Vehicle
Monastrol
% of cells with centrioles ≥5
**
**
***
24
48
72
Length of treatment (hours)

Figure 3.2. Inhibition of Eg5 activity promoted excess centrosomes and centrioles

(**A**) Inhibition of Eg5 promoted centrosome overduplication. Treatment with the Eg5 inhibitor, Monastrol, promoted excess centrosomes in U20S cells. Representative figure of a U20S cell treated either with 100 μM Monastrol or the vehicle, 0.1% DMSO, for 48 hours, then processed for immunofluorescence with an antibody against the centrosome marker, γ-tubulin as shown in red. Merge images shows in blue nuclei stained with Hoechst 33342. Insert shows centrosomal region 3X magnified.

(**B**) Inhibition of Eg5 promoted centriole overduplication. Representative image of U20S cells treated as in (A) except cells were processed for immunocytochemistry with an antibody against the centriole marker, Centrin-3 (red) and an antibody for γ-tubulin (green). Insert shows centriolar region 3X magnified.

(**C**) Histogram shows the percentage of U20S cells with excess centrosomes (≥3) or centrioles (≥5). U2OS cells were treated with 100μM Monastrol or the vehicle, 0.1% DMSO, for the indicated durations. Centrosomes or centrioles were assessed by labeling with the anti-γ-tubulin or the anti-Centrin-3 antibody, respectively. Data shown in each histogram is from two independent experiments, where 200 mononucleated cells were counted in each experiment. Error bars indicate standard deviation. P values were obtained by One way-ANOVA, Tukey-Kramer post-hoc test to compare monastrol-treated to vehicle-treated cells at each given time point. P values from these comparisons are indicated on the histogram with **, $P<0.01$; ***, $P<0.001$.

A.

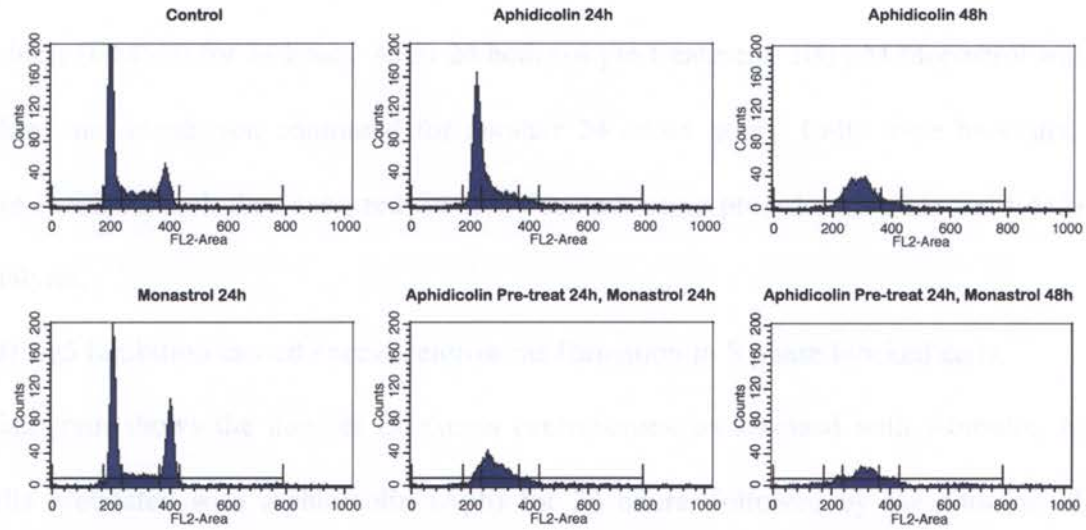
Control
Aphidicolin 24h
Aphidicolin 48h
Monastrol 24h
Aphidicolin Pre-treat 24h, Monastrol 24h
Aphidicolin Pre-treat 24h, Monastrol 48h
Counts
FL2-Area

B.

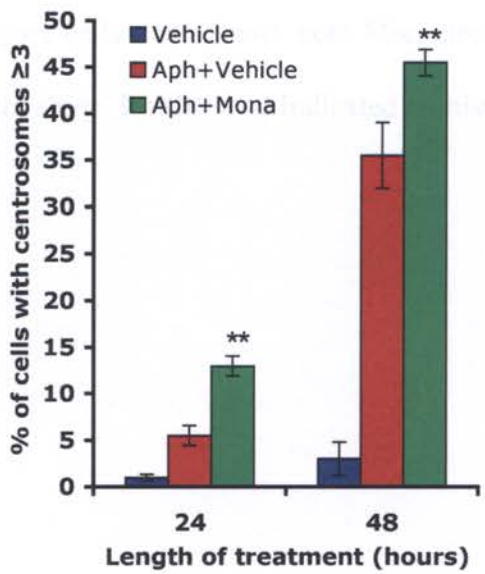
Vehicle
Aph+Vehicle
Aph+Mona
% of cells with centrosomes ≥3
Length of treatment (hours)
24
48
**
**

Figure 3.3 Eg5 inhibition caused excess centrosomes during S phase block

(A) Treatment with Aphidicolin blocked U20S cells at the G1/S boundary. Cells were pre-treated with either Aphidicolin (2 μg/mL) to block cells in S phase or with the vehicle (DMSO) for 24 hours. After 24 hours of pre-treatment, 100 μM Monastrol was added and incubation continued for another 24 or 48 hours. Cells were harvested, fixed with ethanol, then analyzed for DNA content using propidium iodide and FACS analysis.

(B) Eg5 inhibition caused excess centrosome formation in S phase blocked cells. Histogram shows the number of excess centrosomes, as assessed with γ-tubulin, in cells pretreated with Aphidicolin (Aph) for 24 hours, followed by the addition of either vehicle or Monastrol (Mona) for another 24 to 48 hours. Error bars indicate standard deviation. P values were obtained by One way-ANOVA, Tukey-Kramer post-hoc test and compare cells treated with both Monastrol and Aphidicolin to those treated with Aphidicolin alone. P values are indicated on histogram with **, $P<0.01$.

A.

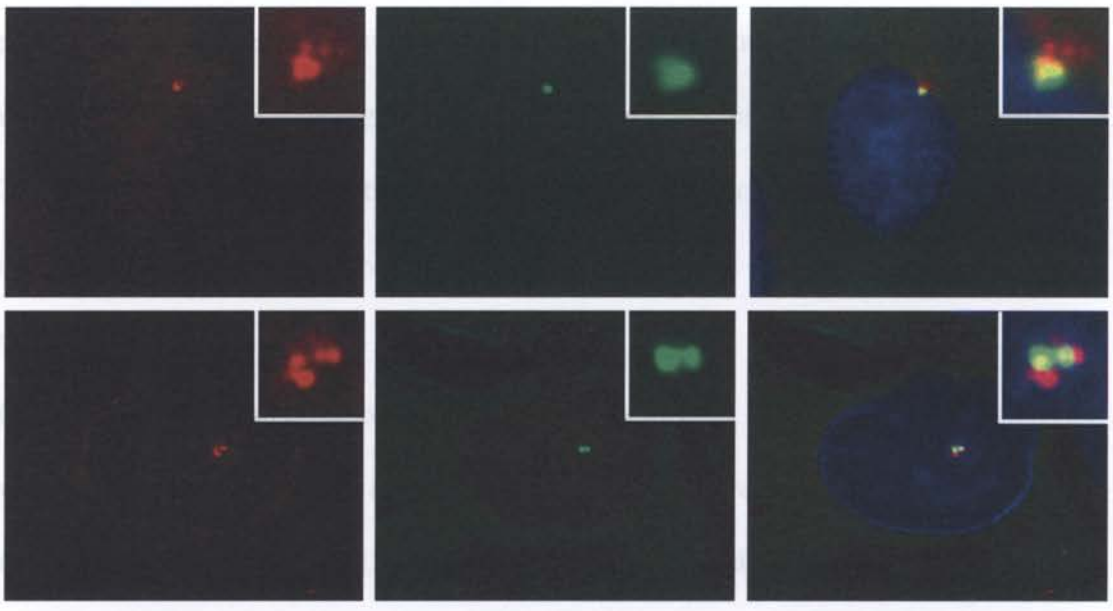

B.

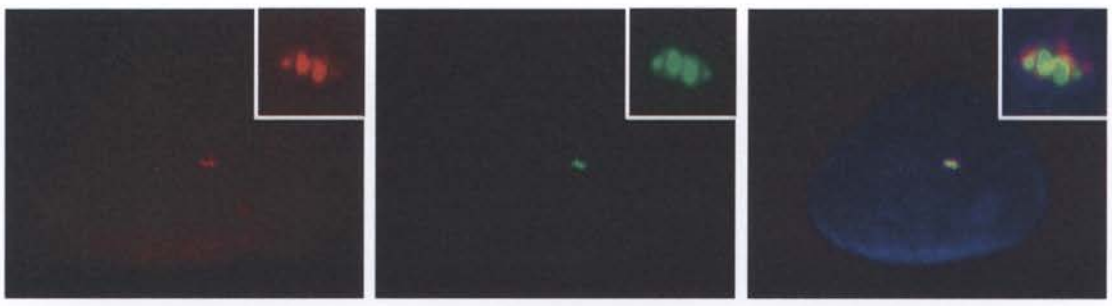

Figure 3.4 Mib1 localized to the centrosome

(A) Mib1 partially co-localized with the PCM protein, γ-tubulin. U2OS cells were processed for fluorescent immunocytochemistry using antibodies against Mib1 (red) and γ-tubulin (green). Merged images, also showing nuclei stained with Hoechst 33342 (blue), indicate a partial overlap between Mib1 and γ-tubulin in unduplicated centrosomes (top row) or duplicated (bottom row). Inserts show a portion of the image at 4X magnification.

(B) Mib1 localized to a region surrounding the centriole. U20S cells were transfected with a GFP-tagged centriole marker, Centrin-2. Cells were processed as in (A) except antibodies against Mib1 (red) and GFP (green) were used. Merged image also shows nuclei stained with Hoechst 33342 (in blue). Inserts show a portion of the image at 4X magnification.

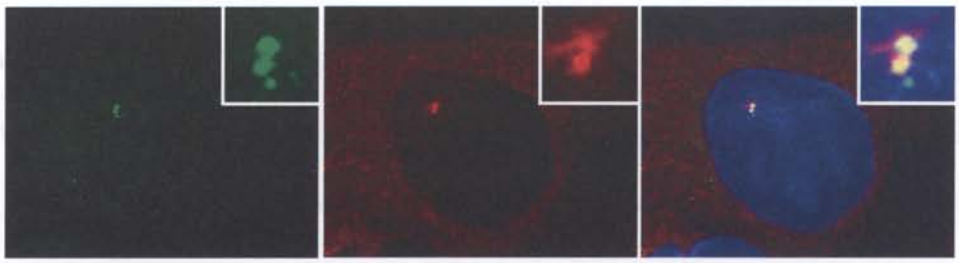

Mib1 Eg5 Merge

Figure 3.5 Mib1 co-localized with Eg5

Immunofluorescence was performed in U20S cells using antibodies against Mib1 (green) and Eg5 (red). Merged image shows co-localization of Eg5 and Mib1 (yellow). The merged image also indicates nuclear staining with Hoechst 33342 (blue). Inserts show a portion of the image magnified 4X to show detail.

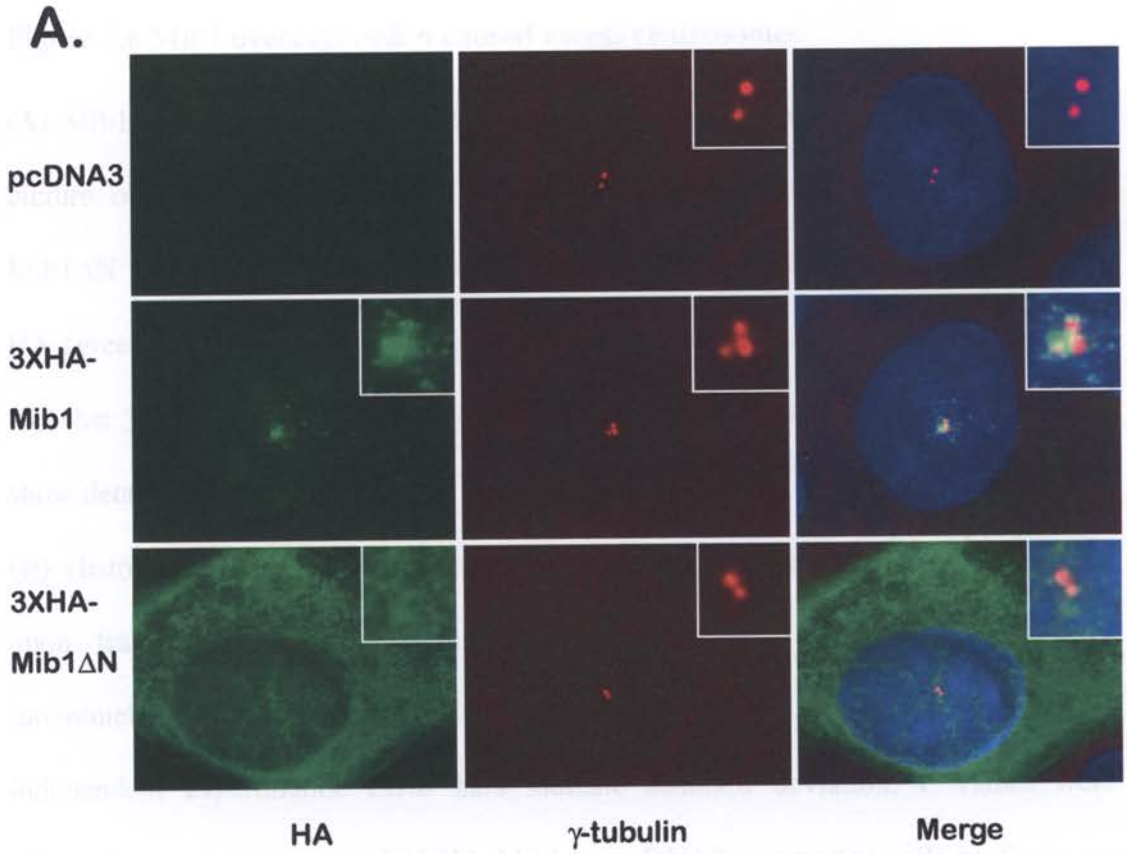
A.
pcDNA3
3XHA-
Mib1
3XHA-
Mib1ΔN
HA
γ-tubulin
Merge

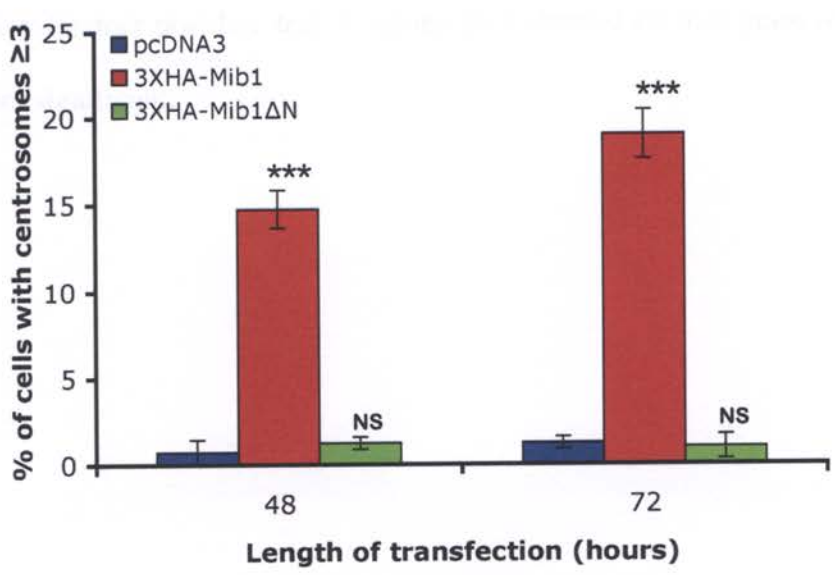
B.
% of cells with centrosomes ≥3
25
20
15
10
5
0
pcDNA3
3XHA-Mib1
3XHA-Mib1ΔN
***
***
NS
NS
48
72
Length of transfection (hours)

Figure 3.6 Mib1 overexpression caused excess centrosomes

(A) Mib1 overexpression caused excess centrosomes. Figure shows a representative picture of U20S cells transfected with pcDNA3, 3XHA-tagged Mib1, or 3XHA-Mib1ΔN for 48 hours then processed for fluorescent immunocytochemistry with an HA (green) and a γ-tubulin antibody (red). Merged image shows nuclei stained with Hoechst 33342 (blue). Inserts show a portion of the images at 3X magnification to show detail.

(B) Histogram shows the percentage of U2OS cells with excess centrosomes (≥3) upon transfection with the constructs as described in (A). The number of mononucleated cells with excess centrosomes from 200 cells was counted in 2 independent experiments. Error bars indicate standard deviation. P values were obtained from comparison of 3XHA-Mib1 to pcDNA3-transfected cells by One-way ANOVA, Tukey-Kramer post-hoc test. P values are indicated on histogram with *** <0.001; NS, not significant.

A.

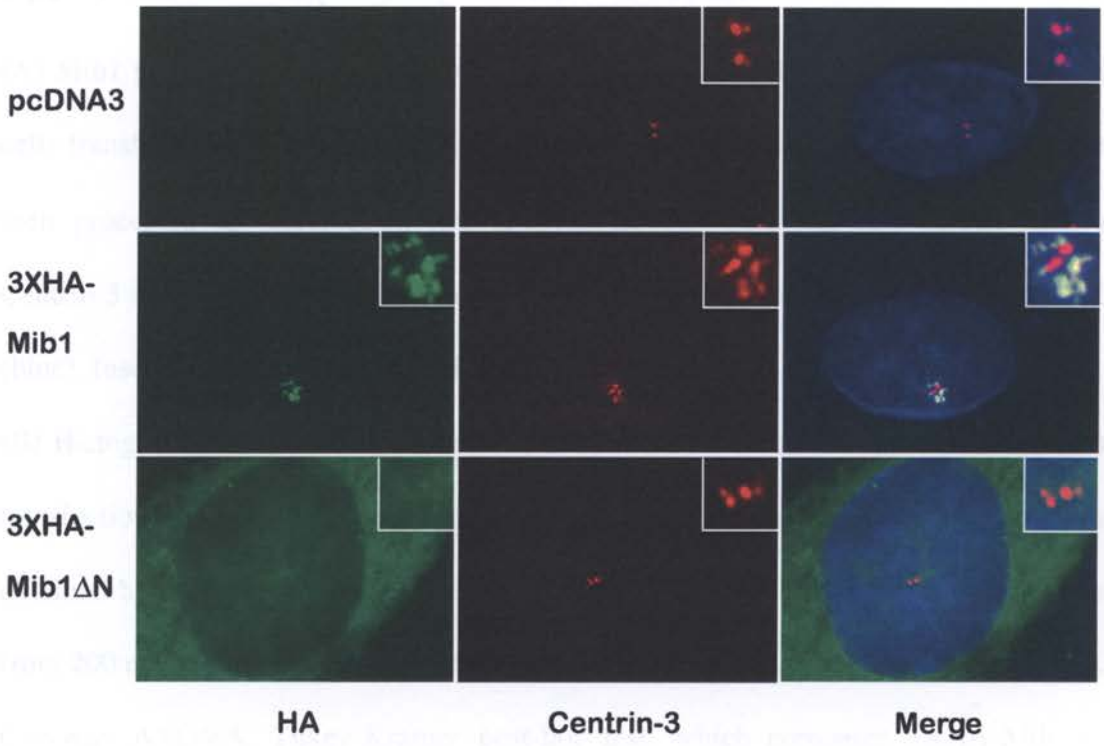
pcDNA3
3XHA-
Mib1
3XHA-
Mib1ΔN
HA
Centrin-3
Merge

B.

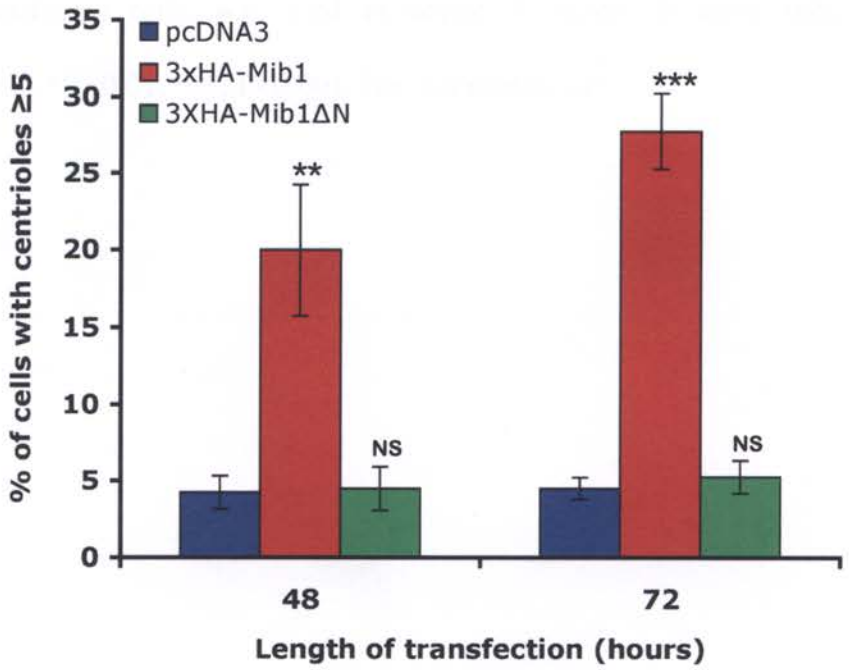
pcDNA3
3xHA-Mib1
3XHA-Mib1ΔN
% of cells with centrioles ≥5
35
30
25
20
15
10
5
0
**
***
NS
NS
48
72
Length of transfection (hours)

Figure 3.7 Mib1 overexpression promoted excess centrioles

(A) Mib1 promoted excess centrioles. Figure shows a representative picture of U20S cells transfected with pcDNA3, 3X HA-tagged Mib1, or 3XHA-MibΔN for 48 hours then processed for fluorescent immunocytochemistry with an HA (green) and a Centrin-3 antibody (red). Merged images also show nuclei stained with Hoechst 33342 (blue). Inserts show portions of the images enlarged 3X.

(B) Histogram shows the percentage of U2OS cells with excess centrioles (≥5) upon transfection with the constructs as described in (A). Data on the histogram was obtained by determining the percentage of mononucleated cells with excess centrioles from 200 cells in two independent experiments. Error bars indicate standard deviation. One-way ANOVA, Tukey-Kramer post-hoc test, which compares 3XHA-Mib- to pcDNA3-transfected cells, was used to obtain P values. P value indicated on histogram with **,<0.01; ***, P<0.001; NS, not significant.

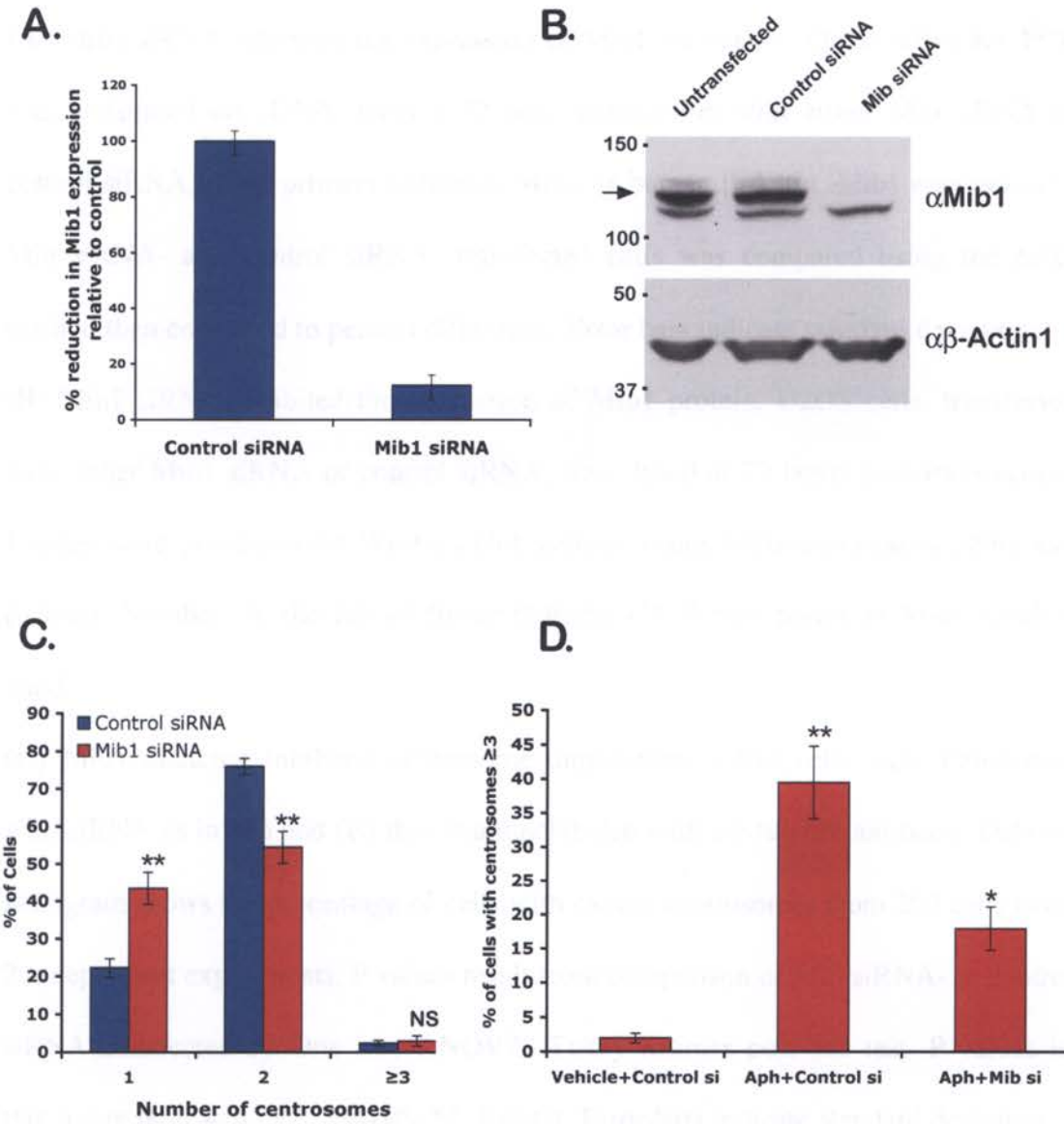
A.
% reduction in Mib1 expression relative to control
120
100
80
60
40
20
0
Control siRNA
Mib1 siRNA
B.
Untransfected
Control siRNA
Mib siRNA
150
100
50
37
αMib1
αβ-Actin1
C.
Control siRNA
Mib1 siRNA
% of Cells
90
80
70
60
50
40
30
20
10
0
**
**
NS
1
2
≥3
Number of centrosomes
D.
% of cells with centrosomes ≥3
50
45
40
35
30
25
20
15
10
5
0
**
*
Vehicle+Control si
Aph+Control si
Aph+Mib si

Figure 3.8 Mib1-silencing inhibited centrosome overduplication

(A) Mib1 siRNA inhibited the expression of Mib1 transcripts. Quantitative RT-PCR was performed on cDNA, from a 72 hour transfection with either Mib siRNA or control siRNA, using primers to human Mib1 or human β-Actin. Mib1 expression in Mib siRNA- and control siRNA- transfected cells was compared using the $\Delta\Delta C_t$ method then converted to percent difference. Error bars indicate standard deviation.

(B) Mib1 siRNA inhibited the expression of Mib1 protein. U2OS cells, transfected with either Mib1 siRNA or control siRNA, were lysed at 72 hours post-transfection. Lysates were processed for Western blot analysis using antibodies against Mib1 and β-Actin. Numbers to the left of figure indicate kD. Arrow points to Mib1 specific band.

(C) Mib1-silencing inhibited centrosome duplication. U20S cells were transfected with siRNA as in (A) and (B) then immunolabeled with a γ-tubulin antibody. Data on histogram shows the percentage of cells with excess centrosomes from 200 cells from 2 independent experiments. P values result from comparison of Mib siRNA- to control siRNA-transfected by One way-ANOVA, Tukey-Kramer post-hoc test. P values in this figure indicated by *, $P<0.05$; **, $P<0.01$. Error bars indicate standard deviation.

(D) Mib1-silencing inhibited Aphidicolin-induced centrosome amplification. Aphidicolin-arrested cells (Aph) were transfected with siRNA as in (A) and (B). Centrosomes were labeled and counted as in (C). P values indicate the affect of Aphidicolin on centrosome amplification (**) and the affect of Mib siRNA on Aphidicolin-induced centrosome amplification (*).

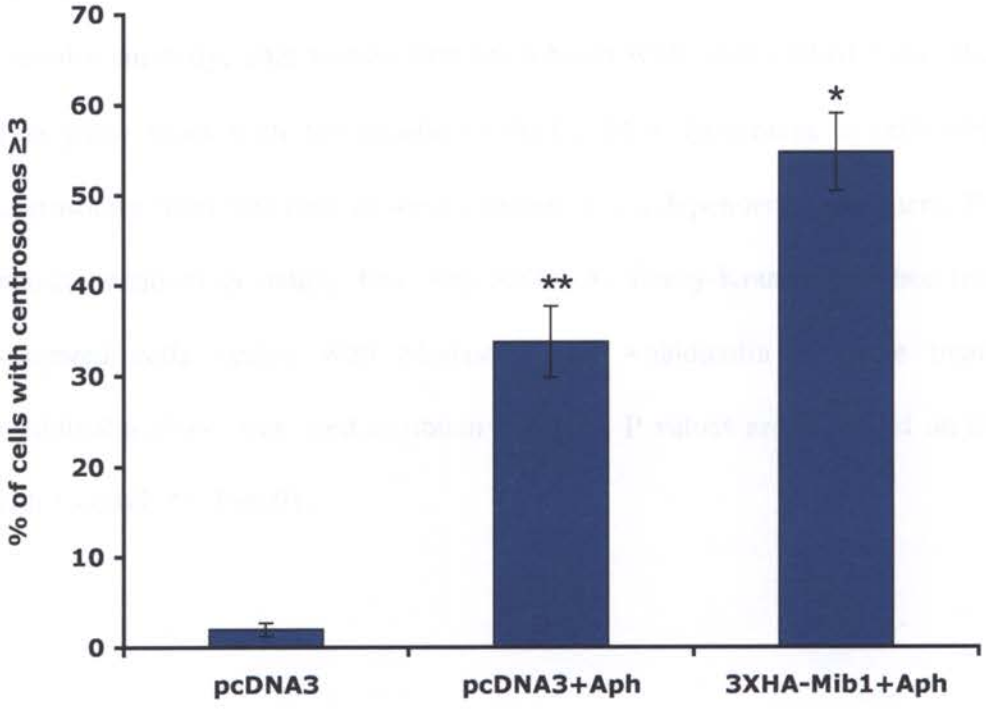
70
60
50
40
30
20
10
0
% of cells with centrosomes ≥3
**
*
pcDNA3
pcDNA3+Aph
3XHA-Mib1+Aph

Figure 3.9 Mib1 overexpression caused excess centrosomes during S phase block

Histogram shows the percentage of cells with excess centrosomes, as assessed with a γ-tubulin antibody, after transfection for 6 hours with 3XHA-Mib1 then followed by G1/S phase block with Aphidicolin (Aph) for 24 h. Percentage of cells with excess centrosomes from 200 cells in were counted in 2 independent experiment. Error bars indicate standard deviation. One way-ANOVA, Tukey-Kramer post-hoc test, which compared cells treated with Monastrol and Aphidicolin to those treated with Aphidicolin alone, was used to obtain P values. P values are indicated on histogram with *,<0.05; **, P<0.01.

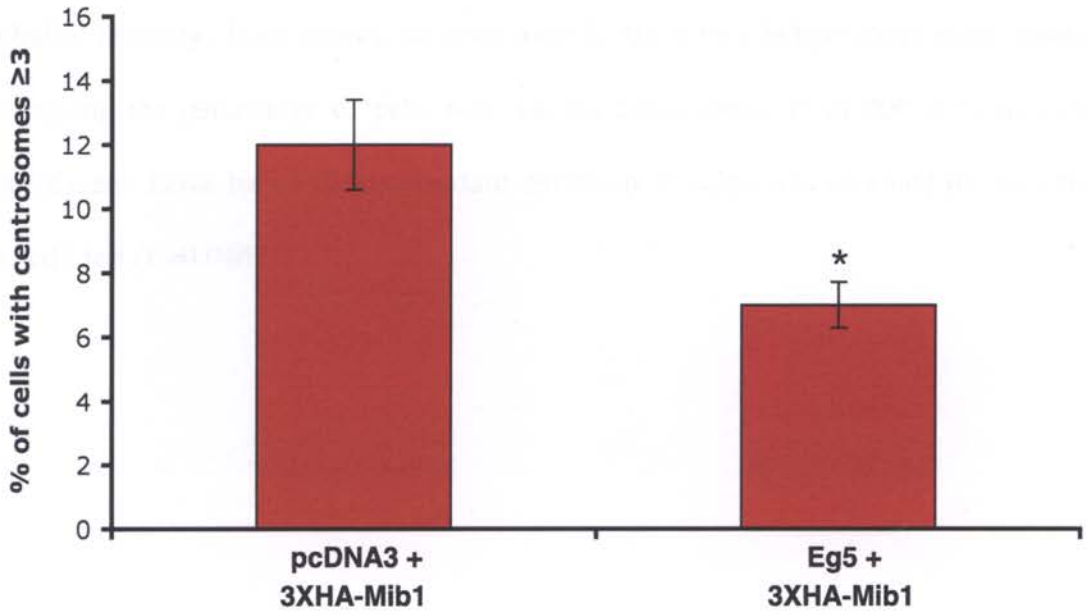
% of cells with centrosomes ≥3
16
14
12
10
8
6
4
2
0
*
pcDNA3 +
3XHA-Mib1
Eg5 +
3XHA-Mib1

Figure 3.10 Eg5 overexpression rescued Mib1-promoted centrosome amplification

U2OS cells were co-transfected with 3X HA-Mib1 and Eg5-V5-His or pcDNA3. At 72 hours post-transfection, cells were processed for immunocytochemistry using γ-tubulin antibody. Data shown on histogram is from two independent experiments, indicating the percentage of cells with excess centrosomes from 200 cells in each experiment. Error bars indicate standard deviation. P value was obtained by the two-tailed t test (P=0.0465).

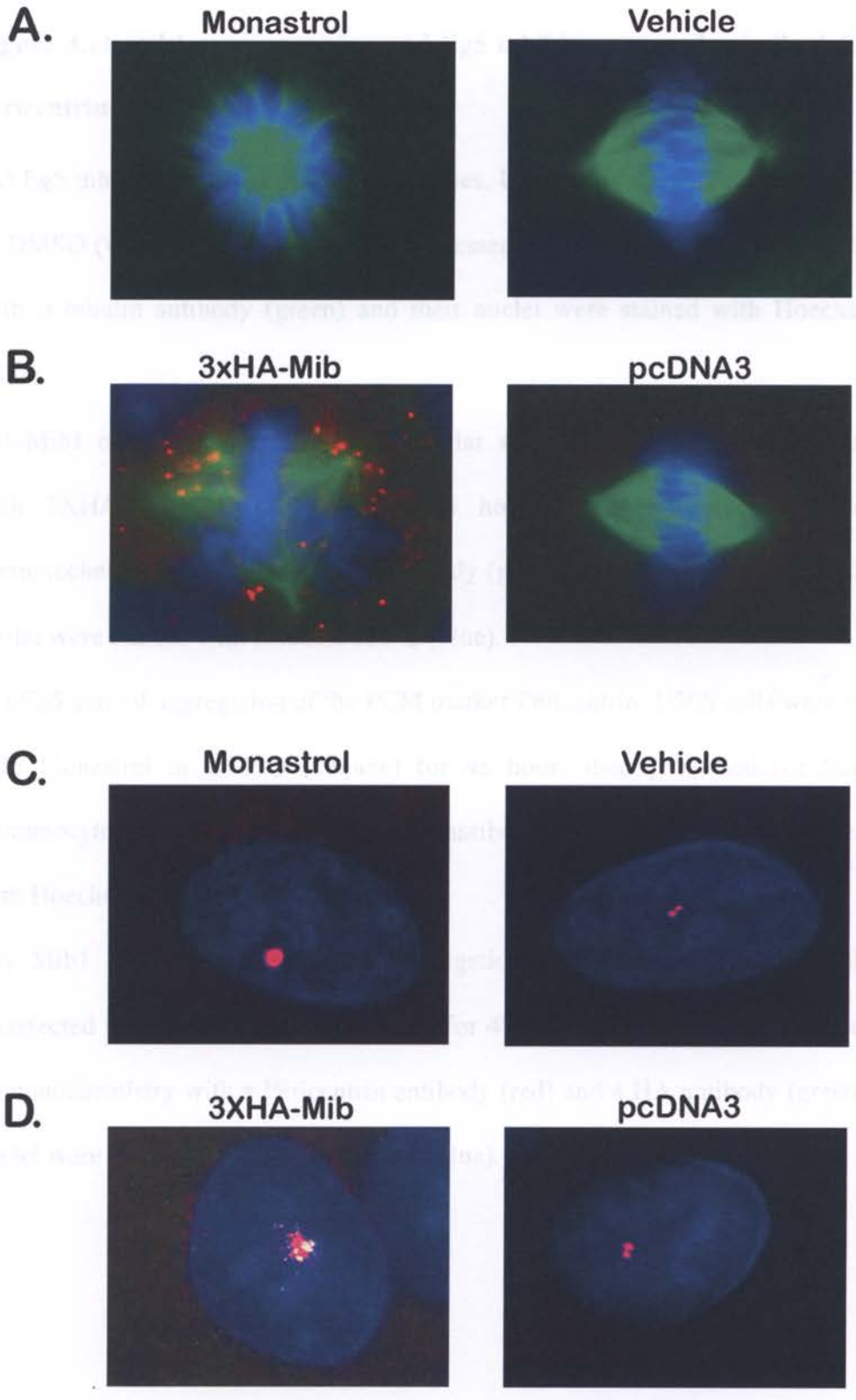
A.
Monastrol
Vehicle
B.
3xHA-Mib
pcDNA3
C.
Monastrol
Vehicle
D.
3XHA-Mib
pcDNA3

Figure 3.11 Mib1 overexpression and Eg5 inhibition caused spindle defects and pericentrin redistribution

(**A**) Eg5 inhibition caused monastral spindles. U20S cells were treated with Monastrol or DMSO (vehicle) for 48 hours then processed for fluorescent immunocytochemistry with α-tubulin antibody (green) and their nuclei were stained with Hoechst 33342 (blue).

(**B**) Mib1 overexpression caused multipolar spindles. U2OS cells were transfected with 3XHA-Mib1 or pcDNA3 for 48 hours, then processed for fluorescent immunochemistry with a α-tubulin antibody (green) and an HA antibody (red). Their nuclei were stained with Hoechst 33342 (blue).

(**C**) Eg5 caused aggregation of the PCM marker Pericentrin. U20S cells were treated with Monastrol or DMSO (vehicle) for 48 hours then processed for fluorescent immunocytochemistry with a Pericentrin antibody (red) and their nuclei were stained with Hoechst 33342 (blue).

(**D**) Mib1 overexpression caused aggregation of Pericentrin. U2OS cells were transfected with 3XHA-Mib or pcDNA3 for 48 hours, then processed for fluorescent immunochemistry with a Pericentrin antibody (red) and a HA antibody (green). Their nuclei were stained with Hoechst 33342 (blue).

CHAPTER FOUR

Conclusions and Future Directions

Conclusions

Summary of Findings

I began this dissertation with an overview of what is currently known about the RING finger E3 ubiquitin ligase, Mib1. Previously, there were only three known substrates of Mib1: the Notch ligands Delta and Serrate, and the serine-threonine kinase DAPK. These three substrates regulate different signaling pathways. Delta and Serrate regulate the Notch signaling pathway, whereas DAPK regulates apoptosis [1, 7, 55]. In an effort to determine whether Mib1 has additional substrates, I performed a proteomic screen for proteins that interact with Mib1. In this screen, I identified a number of substrates that are involved in ubiquitination, methylation, spindle formation, and centrosome regulation.

Based on preliminary evidence about the strength of the association, I decided to focus on one of the interacting-proteins, Eg5. Eg5 is a member of the kinesin-5 subclass, which is characterized by their homotetrameric structures [9, 69]. It is known to both stabilize and slide apart bipolar mitotic spindles by binding to antiparallel microtubules [9, 69]. I found that Mib1 could promote the monoubiquitination of Eg5. Monoubiquitination is a versatile post-translational modification and is known to regulate a diversity of cellular processes, such as protein trafficking, endocytosis, and DNA repair [139, 140]. However, this is the first time that monoubiquitination of a motor protein has been identified.

Modification with monoubiquitin is best known for regulating the distribution of a protein within a cell. To this end, I examined whether altering Mib1 expression

levels could affect Eg5 localization to the mitotic spindle in HEK-293 and HeLa cells, but I did not find Mib1 induced changes in Eg5 distribution. However, Mib1 may still regulate mitotic spindle function of Eg5 without affecting its localization to the spindle. Therefore, mitotic spindles were examined in cell culture with altered Mib1 expression levels. No defects in mitotic spindles were observed in HEK-293 or HeLa cells with overexpressed Mib1 or silenced Mib1. Consistent with these observations in cell culture, I also did not see spindle defects in *mib1*^{Hi904} zebrafish mutants. A recent discovery of an ortholog of Mib1, Mib2, could account for this absence. Mib2 could compensate for loss of Mib1 in these experiments and explain the lack of mitotic spindle defect. An alternative explanation for a Mib1-related spindle defect is that Mib1 and Eg5 function in some other cellular roles.

As the function of Eg5 was not previously examined *in vivo*, I characterized an *eg5*^{Hi3112A} insertional zebrafish mutant. In agreement with described phenotypes from Eg5 inhibition in cell culture, *eg5*^{Hi3112A} mutants form monastral mitotic spindles in the retina [66, 67]. Interestingly, the localization of these monastral spindles was not restricted to the apical membrane like normal spindles, but located throughout the retina. I then addressed whether *eg5*^{Hi3112A} mutants have cell fate specification defects similar to those observed in hindbrain and retina of *mib1*^{Hi904} zebrafish mutants. Examination of hindbrain and retina of *eg5*^{Hi3112A} mutants did not reveal any cell fate specification defects. These results suggest that Eg5, unlike Mib1, is not essential for cell fate specification. Furthermore, these results do not support a previously proposed

model that cell fate specification depends on the plane of cell division dictated by the mitotic spindle [170].

An indication of a shared function of Mib1 and Eg5 was revealed by their localization to the centrosome. Eg5 and Mib1 were present at the centriole in both single and duplicated centrosomes. I found that interfering with Mib1 expression levels or Eg5 activity affected centrosome number. In addition, both inhibition of Eg5 and overexpression of Mib1 could still promote centrosome amplification, even when the cells are blocked in S phase, which would rule out possible cytokinesis defects as the primary cause of excess centrosomes. However, these experiments do not differentiate whether this excess of centrosomes is caused by centriole splitting failure or centriole overduplication.

In sum, the novel finding of Mib1 and Eg5 as regulators of centrosome could promote greater understanding of how the centrosome is regulated.

Model for the role of Eg5 and Mib1 in centrosome regulation

In this dissertation, it was revealed that Mib1 and Eg5 modulated centrosome numbers. Furthermore, it was discovered that Mib1 inhibited Eg5-promoted centrosome and centriole production. Likely, Mib1 inhibited Eg5 through monoubiquitination. However, further experimentation will determine whether excess centrosome production is dependent on this monoubiquitination of Eg5. There are two possible outcomes of such monoubiquitination. One possibility is that it affects its the localization of Eg5 to the centrosome. However, from my studies in Chapter Two,

Mib1 did affect the localization of Eg5. Since the levels of some centrosome proteins are dynamic during the cell cycle and the immunofluorescent technique we used is not quantitative, it is possible that Mib1 could alter the amount of Eg5 recruited to the centrosome [185].

A second possibility is Mib1 regulates either the bundling activity or processivity of Eg5. The bundling activity of an ubiquitinated Eg5 could be determined by its crosslinking of purified microtubules. The processivity of Eg5 could be tested by two direct methods: optical trapping and ATPase end point assays [71]. However, all these methods are performed *in vitro* and require highly purified Eg5; making these approaches technically challenging.

A model for the role of Eg5 and Mib1 in promoting excess centrioles and centrosomes would depend whether they are involved in centriole duplication or centriole splitting. As both centriole duplication and centriole splitting could affect centrosome and centriole numbers, as described in Chapter 3, further experimentation would help differentiate between these two possibilities [12, 97, 98]. Therefore, I will describe a model for how Mib1 and Eg5 could be regulating each of these processes.

Based on current literature it is difficult to determine how Eg5 could affect centriole duplication, but one possible mechanism is that Eg5 could cross-link and stabilize the microtubules of centrioles and their growing pro-centrioles [13, 62]. In the absence of microtubule stabilization, centrioles could fragment and form multiple centrosome structures [189, 190]. Centriole duplication by fragmentation was previously observed when stabilization of microtubules, by polyglutamylated tubulin

and MAP215, was inhibited [189, 190]. These inhibited cells showed an apparent excess of centrioles and centrosomes with markers for Centrin and γ-tubulin, respectively [189, 190]. The destabilized centriole may present more than one site for procentriole assembly. However, it is unknown if these centrioles and centrosomes are fully developed and functional. It is also unknown whether a change in centriolar microtubule stability is involved in procentriole initiation.

Based on the current literature, it is more likely that Eg5 is promoting splitting of the intercentriolar bridge that links the parental centrioles. A mechanism that Eg5 could use to sever this bridge is suggested by studies on the *Saccharomyces cerevisiae* orthlog of Eg5, Cin8p [11]. Cin8p, through it microtubule-bundling activity, severs the bridge joining the analogous structure of the centrosome, the spindle pole body [11]. Likewise, Eg5 could use a similar mechanism to sever the intercentriolar filamentous bridge in vertebrates. Previously, it was demonstrated that severing of this intercentriolar bridge is required to prevent formation of excess centrioles and centrosomes [97]. Taken together, this would suggest a model in which Eg5 and Mib1 together split the intercentriolar bridge. Under normal conditions, Mib1 promotes ubiquitination of Eg5, thus inhibiting it. When this inhibition is relieved by some unknown factor, Eg5, through its microtubule-bundling activity, severs the intercentriolar bridge. The severing of this bridge prevents extraneous rounds of centriole duplication after S phase. Under experimental conditions, if Eg5 is inhibited, either directly or by overexpression of Mib1, this intercentriolar bridge does not sever and centriole duplication continues.

Future Directions

Do Mib1 and Eg5 promote centriole duplication or centrosome splitting?

In Chapter Three, I found that both Eg5 inhibition and Mib1 overexpression cause excess centrosomes and centrioles. I discussed several possible mechanisms for this observed phenotype, but demonstrated that only two of these, failure of centrioles to split or centriole overduplication, are likely to cause the observed excess centrosomes and centrioles.

Future studies should examine whether centriole splitting is the cause of observed centrosome defects. It was previously observed that enhanced centriole splitting results in greater percentage of cells with separated centriole [97, 98]. Therefore, methods employed in Chapter 3 could be expanded: Specifically, U2OS cells could be transfected with the V5-tagged version of Eg5 or Mib1 siRNA and the centriole distance observed with Centrin. U2OS cells would be used because their centrioles in interphase are less mobile than other cell lines; therefore, it may be easier to detect enhanced separation [97]. The percentage of cells with separated centrioles in the Eg5-transfected cells or Mib1-silenced cells could then be compared to pcDNA3-transfected cells.

If Eg5 or Mib1 has a role in centriole splitting, this function may also be revealed by their localization to the region of the intercentriolar bridge. Therefore, Eg5 localization at the centrosome should be defined by using markers to the intercentriolar bridge, C-NAP1 and Rootletin [98, 191].

Alternatively, centriole overduplication could be the cause of the excess centriole and centrosomes. This can be measured by determining the number of mature centrioles, which are characterized by their subdistal appendages [192]. For most of the centriole duplication cycle, only the mother centriole is mature, but in late G2/M, the daughter centriole will mature, acquiring these appendages [192]. Interestingly, excess centrioles formed from overduplication do not form subdistal appendages [192]. Conversely, centrioles that fail to segregate have two or more centrioles with subdistal appendages [192]. This phenomenon can be exploited to differentiate between centriole duplication and segregation effects using primary antibody against the subdistal protein, CEP170 [150, 192]. This antibody could be used to measure the number of mature centrioles produced by Eg5 inhibition or Mib1 overexpression to determine whether centriole overduplication or failed segregation occurs.

In addition, electron microscopy could be used to determine whether centrioles in Eg5-inhibited and Mib1-overexpressing cells are ultrastructurally similar to normal centrioles. If the centrosome overduplication is the result of fragmentation, these centrioles may differ from normal ones.

Is ubiquitination required for Eg5 and Mib1-mediated centrosome defects?

In Chapter 2, I demonstrated that Mib1 promoted ubiquitination of Eg5. The next step is to determine whether ubiquitin ligase activity of Mib1 is required for Eg5 and Mib1 to promote excess centriole formation.

First, it should be established whether the ubiquitin ligase activity of Mib1 is required to produce excess centrosomes. The ligase activity of the RING finger E3 ubiquitin ligases depends on their RING fingers [37]. I and other labs have shown that overexpression of a Mib1 RING finger deletion construct (Mib1ΔC) inhibits the ubiquitination activity of overexpressed full length-Mib1 [6]. Therefore, this Mib1ΔC construct can be used to ask whether ubiquitin ligase activity of Mib1 is critical for excess centrosome and centriole formation as previously described.

Next, it should be established whether ubiquitination is required for Eg5-mediated centrosome and centriole defects. This can be done through the creation of an Eg5 ubiquitin mutant once the sites of ubiquitination are mapped. These ubiquitination sites could be determined by mass spectrometry [193]. Alternatively, these sites could be determined by systematic site-directed mutagenesis of lysines in Eg5 to the non-ubiquitinatable arginines [194]. The necessity of each of these lysines for Mib1 ubiquitination could be tested in an ubiquitination assay. Once an Eg5 ubiquitin mutant is created, it would be possible to determine whether ubiquitination of Eg5 is required for the observed centrosome duplication or splitting defects. These mutants could be transfected into U2OS cells to examine whether they fail to induce centrosome duplication or splitting defects as observed with the wild type Eg5 constructs in the previous section. I could also examine whether these Eg5 lysine mutants are capable for rescuing Mib1-induced excess centrosomes.

How is Mib1 regulated during the centrosome duplication cycle?

The centrosome duplication cycle must be temporally regulated to coordinate with the DNA replication cycle [12, 15]. Therefore, centrosome regulators would have to be temporally regulated as well. As both Mib1 and Eg5 were found on single and duplicated centrosomes, this suggests their spatial localization is not critical for their generation of excess centrosomes and centrioles. Instead, this suggests that there is another potential regulator of Eg5 and Mib1 that is temporally regulated. One potential candidate revealed in my proteomic screen is the serine-threonine kinase, NDR1. Recently, NDR1 is a known regulator of the centrosome that localizes to the centrosome in a cell-cycle-specific manner [150]. These traits could implicate NDR1 as a potential temporal regulator of centrosome duplication [150]. However, despite extensive attempts to find the substrate of NDR1, none have been found. Hergovich and colleagues suggested that an NDR1 substrate would have to be localized to the centrosome, as a centrosome-anchored NDR1 could still promote centrosome duplication [150].

Mib1 could be this potential substrate. In preliminary experiments, I found Mib1 co-immunoprecipitates with NDR1. However, Mib1 does not ubiquitinate NDR1. Thus, a potential mechanism for how NDR1 and Mib1 interact is illustrated by RING finger containing protein Parkin and Cdk5 [195]. Phosphorylation of Parkin by Cdk5 decreases its autoubiquitination activity of Parkin. Furthermore, this phosphorylation enhances the ability of Parkin to ubiquitinate its substrates, synphilin-1 and p38 [195].

NDR1 and Mib1 could work in a similar manner as Parkin and Cdk5, where phosphorylation of Mib1 by NDR1 enhances the ubiquitin ligase activity of Mib1. First, it should be tested whether NDR1 phosphorylates Mib1 in an *in vitro* kinase assay. Purified NDR1 and Mib1 could be incubated in the presence of the radio-labeled phosphate, [γ-^{32} P] ATP, then examined for phospho-labeled Mib1 as compared to a control substrate [196]. If enhanced phosphorylation of Mib1 were observed, this would implicate NDR1 as a potential kinase for Mib1. Once NDR1 was verified as a potential kinase, it could be determined via ubiquitination assays whether NDR1 could promote Mib1 self-ubiquitination as well as Eg5 ubiquitination. In addition, NDR phosphorylation sites on Mib1 could be identified by phosphopeptide-mapping. A phosphorylation-deficient mutant of Mib1 could be created and used in the ubiquitination assay to test the necessity of these phosphorylation sites for self-ubiquitination and ubiquitination of Eg5.

Do Mib1 and Eg5 cause aneuploidy?

As I have detected a centrosome defect in U2OS cells, potential centrosome defects should be examined in *eg5*^{Hi3112A} and *mib1*^{Hi904} zebrafish mutants. As previously described, the centrosome marker γ-tubulin and centriole marker Centrin-3 could be employed to quantify the number of centrosomes and centrioles per cell. Cells could be identified with Hoechst 33342. Based on the cell culture experiments, I would predict the *eg5*^{Hi3112A} mutant to have an increase in the number of centrosomes and

centrioles, whereas the *mib1*^{Hi904} mutant would likely have a decrease in the number of centrosomes and centrioles.

Attempts to understand the consequence of Eg5 inhibition led to conflicting results. It was previously observed in mutants of the *Drosophila* ortholog Eg5, KLP61F, that the number of monastral cells is increased [157, 158]. Furthermore, an elevation in aneuploid cells is also observed. These results suggest that the cells with abnormal spindles can overcome the spindle assembly checkpoint and replicate despite misseggregated chromosomes [157, 158]. However, different conclusions were made from inhibition of Eg5 in vertebrate cancer cell lines. Treatment of the human multiple myeloma and ovarian cancer cells with the Eg5 inhibitors dimethylenastron and HR22C16 respectively caused apoptosis [197, 198]. These studies were limited to cell culture lines, which may not reflect the consequences of Eg5 inhibition *in vivo*. As Eg5 inhibitors are being explored for their therapeutic potential for cancer treatment, it is necessary to determine the consequences from the loss of Eg5 function [199-201]. In Chapter Two, I characterized the *eg5*^{Hi3112A} zebrafish mutant. However, it was not fully explored whether aneuploidy occurs in these mutants. Previously, I examined 48 hpf homozygous mutant embryos for aneuploidy by FACS analysis for DNA content. These results were inconclusive because the amount of tissue used for this study was inadequate for a robust FACS analysis. However, whether aneuploidy exists in these mutants could be determined by using G-banding of metaphase spreads or FISH [202, 203]. Similar experiments could also be performed in the *mib1*^{Hi904} mutant fish.

Aneuploidy and excess centrosomes are a common characteristic of cancer cells [122]. Whether tumor formation originates from aneuploidy or centrosome abnormalties is under much discussion [123]. Most of the current studies rely on the limited supply of biopsied tissue or on cell culture systems [122]. If *eg5*^{Hi3112A} mutants exhibit either aneuploidy or excess centrosomes, they could be used to examine whether the loss of Eg5 expression is tumorigenic. Further analysis of tumor progression could determine when aneuploidy, excess centrosomes, or both occur in these growths. Unfortunately, *eg5*^{Hi3112A} zebrafish mutants die at 6dpf from developmental abnormalities. As the embryos are unlikely to undergo tumorigenesis in this brief period, a chimera could be created by transplanting blastula cells from *eg5*^{Hi3112A} homozygous embryos into wild type blastula embryos [204]. To make identification of *eg5*^{Hi3112A} mutant cells easier, the *eg5*^{Hi3112A} mutants could be crossed to the Xenopus EF1α driven GFP transgenic fish [205]. Possible tumors formed in these adult chimeras could then be analyzed by standard histological methods [206]. The development of aneuploidy or centrosome defects could be analyzed using cytogenetic methods or labeling with γ-tubulin as described above [202, 203]. Similar chimera experiments could also be done with the *mib*^{Hi904} zebrafish mutants to examine the significance of this gene in tumorigenesis.

REFERENCES

1. Bray, S.J., *Notch signalling: a simple pathway becomes complex.* Nat Rev Mol Cell Biol, 2006. **7**(9): p. 678-89.
2. Artavanis-Tsakonas, S., M.D. Rand, and R.J. Lake, *Notch signaling: cell fate control and signal integration in development.* Science, 1999. **284**(5415): p. 770-6.
3. Wang, W. and G. Struhl, *Distinct roles for Mind bomb, Neuralized and Epsin in mediating DSL endocytosis and signaling in Drosophila.* Development, 2005. **132**(12): p. 2883-94.
4. Itoh, M., et al., *Mind bomb is a ubiquitin ligase that is essential for efficient activation of Notch signaling by Delta.* Developmental Cell, 2003. **4**(1): p. 67-82.
5. Chen, W. and D. Casey Corliss, *Three modules of zebrafish Mind bomb work cooperatively to promote Delta ubiquitination and endocytosis.* Developmental Biology, 2004. **267**(2): p. 361-73.
6. Lai, E.C., et al., *The ubiquitin ligase Drosophila Mind bomb promotes Notch signaling by regulating the localization and activity of Serrate and Delta.* Development, 2005. **132**(10): p. 2319-32.
7. Jin, Y., et al., *A death-associated protein kinase (DAPK)-interacting protein, DIP-1, is an E3 ubiquitin ligase that promotes tumor necrosis factor-induced*

15. Doxsey, S., W. Zimmerman, and K. Mikule, *Centrosome control of the cell cycle.* Trends Cell Biol, 2005. **15**(6): p. 303-11.

16. Kramer, A., K. Neben, and A.D. Ho, *Centrosome aberrations in hematological malignancies.* Cell Biol Int, 2005. **29**(5): p. 375-83.

17. Kramer, A., *Centrosome aberrations--hen or egg in cancer initiation and progression?* Leukemia, 2005. **19**(7): p. 1142-4.

18. Baron, M., et al., *Multiple levels of Notch signal regulation (review).* Mol Membr Biol, 2002. **19**(1): p. 27-38.

19. Haddon, C., et al., *Hair cells without supporting cells: further studies in the ear of the zebrafish mind bomb mutant.* Journal of Neurocytology, 1999. **28**(10-11): p. 837-50.

20. Schier, A.F., et al., *Mutations affecting the development of the embryonic zebrafish brain.* Development, 1996. **123**: p. 165-78.

21. Jiang, Y.J., et al., *Mutations affecting neurogenesis and brain morphology in the zebrafish, Danio rerio.* Development, 1996. **123**: p. 205-16.

22. Louvi, A. and S. Artavanis-Tsakonas, *Notch signalling in vertebrate neural development.* Nat Rev Neurosci, 2006. **7**(2): p. 93-102.

23. Yoo, K.W., et al., *Snx5, as a Mind bomb-binding protein, is expressed in hematopoietic and endothelial precursor cells in zebrafish.* FEBS Lett, 2006. **580**(18): p. 4409-16.

24. Liu, Y., et al., *Notch signaling controls the differentiation of transporting epithelia and multiciliated cells in the zebrafish pronephros.* Development, 2007. **134**(6): p. 1111-22.

25. Bernardos, R.L., et al., *Notch-Delta signaling is required for spatial patterning and Muller glia differentiation in the zebrafish retina.* Developmental Biology, 2005. **278**(2): p. 381-95.

26. Crosnier, C., et al., *Delta-Notch signalling controls commitment to a secretory fate in the zebrafish intestine.* Development, 2005. **132**(5): p. 1093-104.

27. Fang, S. and A.M. Weissman, *A field guide to ubiquitylation.* Cell Mol Life Sci, 2004. **61**(13): p. 1546-61.

28. Jackson, P.K., et al., *The lore of the RINGs: substrate recognition and catalysis by ubiquitin ligases.* Trends Cell Biol, 2000. **10**(10): p. 429-39.

29. Pickart, C.M. and M.J. Eddins, *Ubiquitin: structures, functions, mechanisms.* Biochim Biophys Acta, 2004. **1695**(1-3): p. 55-72.

30. Zheng, N., et al., *Structure of the Cul1-Rbx1-Skp1-F boxSkp2 SCF ubiquitin ligase complex.* Nature, 2002. **416**(6882): p. 703-9.

31. Zheng, N., et al., *Structure of a c-Cbl-UbcH7 complex: RING domain function in ubiquitin-protein ligases.* Cell, 2000. **102**(4): p. 533-9.

32. Miura, T., et al., *Characterization of the binding interface between ubiquitin and class I human ubiquitin-conjugating enzyme 2b by multidimensional heteronuclear NMR spectroscopy in solution.* J Mol Biol, 1999. **290**(1): p. 213-28.

33. Orlicky, S., et al., *Structural basis for phosphodependent substrate selection and orientation by the SCFCdc4 ubiquitin ligase.* Cell, 2003. **112**(2): p. 243-56.

34. VanDemark, A.P. and C.P. Hill, *Structural basis of ubiquitylation.* Curr Opin Struct Biol, 2002. **12**(6): p. 822-30.

35. Hershko, A., et al., *Components of ubiquitin-protein ligase system. Resolution, affinity purification, and role in protein breakdown.* J Biol Chem, 1983. **258**(13): p. 8206-14.

36. Mukhopadhyay, D. and H. Riezman, *Proteasome-independent functions of ubiquitin in endocytosis and signaling.* Science, 2007. **315**(5809): p. 201-5.

37. Passmore, L.A. and D. Barford, *Getting into position: the catalytic mechanisms of protein ubiquitylation.* Biochem J, 2004. **379**(Pt 3): p. 513-25.

38. Baboshina, O.V. and A.L. Haas, *Novel multiubiquitin chain linkages catalyzed by the conjugating enzymes E2EPF and RAD6 are recognized by 26 S proteasome subunit 5.* J Biol Chem, 1996. **271**(5): p. 2823-31.

39. Liu, Z., et al., *Characterization of a novel keratinocyte ubiquitin carrier protein.* J Biol Chem, 1996. **271**(5): p. 2817-22.

40. Johnson, E.S., et al., *A proteolytic pathway that recognizes ubiquitin as a degradation signal.* J Biol Chem, 1995. **270**(29): p. 17442-56.

41. Huang, F., et al., *Differential regulation of EGF receptor internalization and degradation by multiubiquitination within the kinase domain.* Mol Cell, 2006. **21**(6): p. 737-48.

42. Hofmann, R.M. and C.M. Pickart, *Noncanonical MMS2-encoded ubiquitin-conjugating enzyme functions in assembly of novel polyubiquitin chains for DNA repair.* Cell, 1999. **96**(5): p. 645-53.

43. Deng, L., et al., *Activation of the IkappaB kinase complex by TRAF6 requires a dimeric ubiquitin-conjugating enzyme complex and a unique polyubiquitin chain.* Cell, 2000. **103**(2): p. 351-61.

44. Wang, C., et al., *TAK1 is a ubiquitin-dependent kinase of MKK and IKK.* Nature, 2001. **412**(6844): p. 346-51.

45. Galan, J.M. and R. Haguenauer-Tsapis, *Ubiquitin lys63 is involved in ubiquitination of a yeast plasma membrane protein.* Embo J, 1997. **16**(19): p. 5847-54.

46. Seugnet, L., P. Simpson, and M. Haenlin, *Requirement for dynamin during Notch signaling in Drosophila neurogenesis.* Dev Biol, 1997. **192**(2): p. 585-98.

47. Wang, W. and G. Struhl, *Drosophila Epsin mediates a select endocytic pathway that DSL ligands must enter to activate Notch.* Development, 2004. **131**(21): p. 5367-80.

48. Horvath, C.A., et al., *Epsin: Inducing membrane curvature.* Int J Biochem Cell Biol, 2007.

49. Pitsouli, C. and C. Delidakis, *The interplay between DSL proteins and ubiquitin ligases in Notch signaling.* Development, 2005. **132**(18): p. 4041-50.

50. Le Borgne, R. and F. Schweisguth, *Notch signaling: endocytosis makes delta signal better*. Current Biology, 2003. **13**(7): p. R273-5.

51. Le Borgne, R., et al., *Two distinct E3 ubiquitin ligases have complementary functions in the regulation of delta and serrate signaling in Drosophila*. PLoS Biol, 2005. **3**(4): p. e96.

52. Koo, B.K., et al., *Mind bomb-2 is an E3 ligase for Notch ligand*. Journal of Biological Chemistry, 2005. **280**(23): p. 22335-42.

53. Zhang, C., Q. Li, and Y.J. Jiang, *Zebrafish Mib and Mib2 are mutual E3 ubiquitin ligases with common and specific delta substrates*. J Mol Biol, 2007. **366**(4): p. 1115-28.

54. Bialik, S. and A. Kimchi, *The death-associated protein kinases: structure, function, and beyond*. Annu Rev Biochem, 2006. **75**: p. 189-210.

55. Bialik, S. and A. Kimchi, *The Death-Associated Protein Kinases: Structure, Function, and Beyond*. Annu Rev Biochem, 2006.

56. Gingras, A.C., R. Aebersold, and B. Raught, *Advances in protein complex analysis using mass spectrometry*. J Physiol, 2005. **563**(Pt 1): p. 11-21.

57. Aebersold, R. and M. Mann, *Mass spectrometry-based proteomics*. Nature, 2003. **422**(6928): p. 198-207.

58. Domon, B. and R. Aebersold, *Mass spectrometry and protein analysis*. Science, 2006. **312**(5771): p. 212-7.

59. Chang, I.F., *Mass spectrometry-based proteomic analysis of the epitope-tag affinity purified protein complexes in eukaryotes.* Proteomics, 2006. **6**(23): p. 6158-66.

60. Knuesel, M., et al., *Identification of novel protein-protein interactions using a versatile mammalian tandem affinity purification expression system.* Mol Cell Proteomics, 2003. **2**(11): p. 1225-33.

61. O'Connell, C.B. and A.L. Khodjakov, *Cooperative mechanisms of mitotic spindle formation.* J Cell Sci, 2007. **120**(Pt 10): p. 1717-22.

62. Bornens, M., *Centrosome composition and microtubule anchoring mechanisms.* Curr Opin Cell Biol, 2002. **14**(1): p. 25-34.

63. Luders, J. and T. Stearns, *Microtubule-organizing centres: a re-evaluation.* Nat Rev Mol Cell Biol, 2007. **8**(2): p. 161-7.

64. Rogers, G.C., S.L. Rogers, and D.J. Sharp, *Spindle microtubules in flux.* J Cell Sci, 2005. **118**(Pt 6): p. 1105-16.

65. Sharp, D.J., et al., *The bipolar kinesin, KLP61F, cross-links microtubules within interpolar microtubule bundles of Drosophila embryonic mitotic spindles.* Journal of Cell Biology, 1999. **144**(1): p. 125-38.

66. Kapoor, T.M., et al., *Probing spindle assembly mechanisms with monastrol, a small molecule inhibitor of the mitotic kinesin, Eg5.* Journal of Cell Biology, 2000. **150**(5): p. 975-88.

67. Zhu, C., et al., *Functional analysis of human microtubule-based motor proteins, the kinesins and dyneins, in mitosis/cytokinesis using RNA interference*. Mol Biol Cell, 2005. **16**(7): p. 3187-99.

68. Valentine, M.T. and S.P. Gilbert, *To step or not to step? How biochemistry and mechanics influence processivity in Kinesin and Eg5*. Curr Opin Cell Biol, 2007. **19**(1): p. 75-81.

69. Kapitein, L.C., et al., *The bipolar mitotic kinesin Eg5 moves on both microtubules that it crosslinks*. Nature, 2005. **435**(7038): p. 114-8.

70. Kwok, B.H., J.G. Yang, and T.M. Kapoor, *The rate of bipolar spindle assembly depends on the microtubule-gliding velocity of the mitotic kinesin Eg5*. Current Biology, 2004. **14**(19): p. 1783-8.

71. Endow, S.A. and D.S. Barker, *Processive and nonprocessive models of kinesin movement*. Annu Rev Physiol, 2003. **65**: p. 161-75.

72. Crevel, I.M., A. Lockhart, and R.A. Cross, *Kinetic evidence for low chemical processivity in ncd and Eg5*. J Mol Biol, 1997. **273**(1): p. 160-70.

73. Sawin, K.E. and T.J. Mitchison, *Poleward microtubule flux mitotic spindles assembled in vitro*. J Cell Biol, 1991. **112**(5): p. 941-54.

74. Jiang, W. and D.D. Hackney, *Monomeric kinesin head domains hydrolyze multiple ATP molecules before release from a microtubule*. J Biol Chem, 1997. **272**(9): p. 5616-21.

75. Valentine, M.T., et al., *Individual dimers of the mitotic kinesin motor Eg5 step processively and support substantial loads in vitro.* Nat Cell Biol, 2006. **8**(5): p. 470-6.

76. Kwok, B.H., et al., *Allosteric inhibition of kinesin-5 modulates its processive directional motility.* Nat Chem Biol, 2006. **2**(9): p. 480-5.

77. Mallik, R. and S.P. Gross, *Molecular motors: strategies to get along.* Curr Biol, 2004. **14**(22): p. R971-82.

78. Shirasu-Hiza, M., et al., *Eg5 causes elongation of meiotic spindles when flux-associated microtubule depolymerization is blocked.* Current Biology, 2004. **14**(21): p. 1941-5.

79. Crasta, K. and U. Surana, *Disjunction of conjoined twins: Cdk1, Cdh1 and separation of centrosomes.* Cell Div, 2006. **1**: p. 12.

80. de Gramont, A., et al., *The spindle midzone microtubule-associated proteins Ase1p and Cin8p affect the number and orientation of astral microtubules in Saccharomyces cerevisiae.* Cell Cycle, 2007. **6**(10): p. 1231-41.

81. Blangy, A., et al., *Phosphorylation by p34cdc2 regulates spindle association of human Eg5, a kinesin-related motor essential for bipolar spindle formation in vivo.* Cell, 1995. **83**(7): p. 1159-69.

82. Ou, Y., M. Zhang, and J.B. Rattner, *The centrosome: The centriole-PCM coalition.* Cell Motil Cytoskeleton, 2004. **57**(1): p. 1-7.

83. Ou, Y.Y., et al., *Higher order structure of the PCM adjacent to the centriole.* Cell Motil Cytoskeleton, 2003. **55**(2): p. 125-33.

84. Leidel, S. and P. Gonczy, *Centrosome duplication and nematodes: recent insights from an old relationship.* Dev Cell, 2005. **9**(3): p. 317-25.

85. Bettencourt-Dias, M. and D.M. Glover, *Centrosome biogenesis and function: centrosomics brings new understanding.* Nat Rev Mol Cell Biol, 2007. **8**(6): p. 451-63.

86. Andersen, J.S., et al., *Proteomic characterization of the human centrosome by protein correlation profiling.* Nature, 2003. **426**(6966): p. 570-4.

87. Sluder, G., F.J. Miller, and C.L. Rieder, *Reproductive capacity of sea urchin centrosomes without centrioles.* Cell Motil Cytoskeleton, 1989. **13**(4): p. 264-73.

88. Nigg, E.A., *Centrosome duplication: of rules and licenses.* Trends Cell Biol, 2007. **17**(5): p. 215-21.

89. Paintrand, M., et al., *Centrosome organization and centriole architecture: their sensitivity to divalent cations.* J Struct Biol, 1992. **108**(2): p. 107-28.

90. Jean, C., et al., *The mammalian interphase centrosome: two independent units maintained together by the dynamics of the microtubule cytoskeleton.* Eur J Cell Biol, 1999. **78**(8): p. 549-60.

91. Adams, I.R. and J.V. Kilmartin, *Spindle pole body duplication: a model for centrosome duplication?* Trends Cell Biol, 2000. **10**(8): p. 329-35.

92. Dippell, R.V., *The development of basal bodies in paramecium.* Proc Natl Acad Sci U S A, 1968. **61**(2): p. 461-8.

93. Gould, R.R., *The basal bodies of Chlamydomonas reinhardtii. Formation from probasal bodies, isolation, and partial characterization.* J Cell Biol, 1975.

93. Gould, R.R., *The basal bodies of Chlamydomonas reinhardtii. Formation from probasal bodies, isolation, and partial characterization.* J Cell Biol, 1975. **65**(1): p. 65-74.

94. Maniotis, A. and M. Schliwa, *Microsurgical removal of centrosomes blocks cell reproduction and centriole generation in BSC-1 cells.* Cell, 1991. **67**(3): p. 495-504.

95. Tsou, M.F. and T. Stearns, *Mechanism limiting centrosome duplication to once per cell cycle.* Nature, 2006. **442**(7105): p. 947-51.

96. Agarwal, R. and O. Cohen-Fix, *Mitotic regulation: the fine tuning of separase activity.* Cell Cycle, 2002. **1**(4): p. 255-7.

97. Faragher, A.J. and A.M. Fry, *Nek2A kinase stimulates centrosome disjunction and is required for formation of bipolar mitotic spindles.* Mol Biol Cell, 2003. **14**(7): p. 2876-89.

98. Mayor, T., et al., *The centrosomal protein C-Nap1 is required for cell cycle-regulated centrosome cohesion.* J Cell Biol, 2000. **151**(4): p. 837-46.

99. Sankaran, S., et al., *Identification of domains of BRCA1 critical for the ubiquitin-dependent inhibition of centrosome function.* Cancer Res, 2006. **66**(8): p. 4100-7.

100. Lotti, L.V., et al., *Subcellular localization of the BRCA1 gene product in mitotic cells.* Genes Chromosomes Cancer, 2002. **35**(3): p. 193-203.

101. Hsu, L.C. and R.L. White, *BRCA1 is associated with the centrosome during mitosis.* Proc Natl Acad Sci U S A, 1998. **95**(22): p. 12983-8.

102. Starita, L.M., et al., *BRCA1-dependent ubiquitination of gamma-tubulin regulates centrosome number.* Mol Cell Biol, 2004. **24**(19): p. 8457-66.

103. Kemp, C.A., et al., *Suppressors of zyg-1 define regulators of centrosome duplication and nuclear association in Caenorhabditis elegans.* Genetics, 2007. **176**(1): p. 95-113.

104. O'Connell, K.F., *The ZYG-1 kinase, a mitotic and meiotic regulator of centriole replication.* Oncogene, 2002. **21**(40): p. 6201-8.

105. O'Connell, K.F., et al., *The C. elegans zyg-1 gene encodes a regulator of centrosome duplication with distinct maternal and paternal roles in the embryo.* Cell, 2001. **105**(4): p. 547-58.

106. Ko, M.A., et al., *Plk4 haploinsufficiency causes mitotic infidelity and carcinogenesis.* Nat Genet, 2005. **37**(8): p. 883-8.

107. Kleylein-Sohn, J., et al., *Plk4-induced centriole biogenesis in human cells.* Dev Cell, 2007. **13**(2): p. 190-202.

108. Delattre, M., C. Canard, and P. Gonczy, *Sequential protein recruitment in C. elegans centriole formation.* Curr Biol, 2006. **16**(18): p. 1844-9.

109. Wang, W., et al., *Temporal and spatial control of nucleophosmin by the Ran-Crm1 complex in centrosome duplication.* Nat Cell Biol, 2005. **7**(8): p. 823-30.

110. Budhu, A.S. and X.W. Wang, *Loading and unloading: orchestrating centrosome duplication and spindle assembly by Ran/Crm1.* Cell Cycle, 2005. **4**(11): p. 1510-4.

111. Hinchcliffe, E.H., et al., *The coordination of centrosome reproduction with nuclear events of the cell cycle in the sea urchin zygote.* J Cell Biol, 1998. **140**(6): p. 1417-26.

112. Sluder, G., et al., *Protein synthesis and the cell cycle: centrosome reproduction in sea urchin eggs is not under translational control.* J Cell Biol, 1990. **110**(6): p. 2025-32.

113. Balczon, R., et al., *Dissociation of centrosome replication events from cycles of DNA synthesis and mitotic division in hydroxyurea-arrested Chinese hamster ovary cells.* J Cell Biol, 1995. **130**(1): p. 105-15.

114. Hinchcliffe, E.H., et al., *Requirement of Cdk2-cyclin E activity for repeated centrosome reproduction in Xenopus egg extracts.* Science, 1999. **283**(5403): p. 851-4.

115. Hinchcliffe, E.H. and G. Sluder, *Two for two: Cdk2 and its role in centrosome doubling.* Oncogene, 2002. **21**(40): p. 6154-60.

116. Lacey, K.R., P.K. Jackson, and T. Stearns, *Cyclin-dependent kinase control of centrosome duplication.* Proc Natl Acad Sci U S A, 1999. **96**(6): p. 2817-22.

117. Matsumoto, Y., K. Hayashi, and E. Nishida, *Cyclin-dependent kinase 2 (Cdk2) is required for centrosome duplication in mammalian cells.* Curr Biol, 1999. **9**(8): p. 429-32.

118. Meraldi, P., et al., *Centrosome duplication in mammalian somatic cells requires E2F and Cdk2-cyclin A.* Nat Cell Biol, 1999. **1**(2): p. 88-93.

119. Peter, M., et al., *Identification of major nucleolar proteins as candidate mitotic substrates of cdc2 kinase.* Cell, 1990. **60**(5): p. 791-801.

120. Tokuyama, Y., et al., *Specific phosphorylation of nucleophosmin on Thr(199) by cyclin-dependent kinase 2-cyclin E and its role in centrosome duplication.* J Biol Chem, 2001. **276**(24): p. 21529-37.

121. Wong, C. and T. Stearns, *Centrosome number is controlled by a centrosome-intrinsic block to reduplication.* Nat Cell Biol, 2003. **5**(6): p. 539-44.

122. Nigg, E.A., *Centrosome aberrations: cause or consequence of cancer progression?* Nat Rev Cancer, 2002. **2**(11): p. 815-25.

123. Nigg, E.A., *Origins and consequences of centrosome aberrations in human cancers.* Int J Cancer, 2006. **119**(12): p. 2717-23.

124. Lingle, W.L., et al., *Centrosome amplification drives chromosomal instability in breast tumor development.* Proc Natl Acad Sci U S A, 2002. **99**(4): p. 1978-83.

125. Salisbury, J.L., A.B. D'Assoro, and W.L. Lingle, *Centrosome amplification and the origin of chromosomal instability in breast cancer.* J Mammary Gland Biol Neoplasia, 2004. **9**(3): p. 275-83.

126. D'Assoro, A.B., W.L. Lingle, and J.L. Salisbury, *Centrosome amplification and the development of cancer.* Oncogene, 2002. **21**(40): p. 6146-53.

127. Pihan, G.A., et al., *Centrosome abnormalities and chromosome instability occur together in pre-invasive carcinomas.* Cancer Res, 2003. **63**(6): p. 1398-404.

128. Pihan, G.A., et al., *Centrosome defects can account for cellular and genetic changes that characterize prostate cancer progression.* Cancer Res, 2001. **61**(5): p. 2212-9.

129. Pihan, G.A., et al., *Centrosome defects and genetic instability in malignant tumors.* Cancer Res, 1998. **58**(17): p. 3974-85.

130. Fukasawa, K., *Introduction. Centrosome.* Oncogene, 2002. **21**(40): p. 6140-5.

131. Boveri, T., *The origin of malignant tumors.* 1914, Baltimore: Waverly Press.

132. Duensing, S. and K. Munger, *Centrosome abnormalities and genomic instability induced by human papillomavirus oncoproteins.* Prog Cell Cycle Res, 2003. **5**: p. 383-91.

133. Duensing, S., et al., *Human papillomavirus type 16 E7 oncoprotein-induced abnormal centrosome synthesis is an early event in the evolving malignant phenotype.* Cancer Res, 2001. **61**(6): p. 2356-60.

134. Duensing, S., et al., *The human papillomavirus type 16 E6 and E7 oncoproteins cooperate to induce mitotic defects and genomic instability by uncoupling centrosome duplication from the cell division cycle.* Proc Natl Acad Sci U S A, 2000. **97**(18): p. 10002-7.

135. Couch, F.J., *Genetic epidemiology of BRCA1.* Cancer Biol Ther, 2004. **3**(6): p. 509-14.

136. Claus, E.B., et al., *Prevalence of BRCA1 and BRCA2 mutations in women diagnosed with ductal carcinoma in situ.* Jama, 2005. **293**(8): p. 964-9.

137. Meraldi, P., R. Honda, and E.A. Nigg, *Aurora-A overexpression reveals tetraploidization as a major route to centrosome amplification in p53-/- cells.* Embo J, 2002. **21**(4): p. 483-92.

138. Itoh, M., et al., *Mind bomb is a ubiquitin ligase that is essential for efficient activation of Notch signaling by Delta.* Dev Cell, 2003. **4**(1): p. 67-82.

139. Welchman, R.L., C. Gordon, and R.J. Mayer, *Ubiquitin and ubiquitin-like proteins as multifunctional signals.* Nat Rev Mol Cell Biol, 2005. **6**(8): p. 599-609.

140. Kirkin, V. and I. Dikic, *Role of ubiquitin- and Ubl-binding proteins in cell signaling.* Curr Opin Cell Biol, 2007. **19**(2): p. 199-205.

141. Hurlbut, G.D., et al., *Crossing paths with Notch in the hyper-network.* Curr Opin Cell Biol, 2007. **19**(2): p. 166-75.

142. Amsterdam, A., et al., *A large-scale insertional mutagenesis screen in zebrafish.* Genes Dev, 1999. **13**(20): p. 2713-24.

143. Golling, G., et al., *Insertional mutagenesis in zebrafish rapidly identifies genes essential for early vertebrate development.* Nat Genet, 2002. **31**(2): p. 135-40.

144. Koo, B.K., et al., *Mind bomb 1 is essential for generating functional Notch ligands to activate Notch.* Development, 2005. **132**(15): p. 3459-70.

145. Koo, B.K., et al., *Mind bomb-2 is an E3 ligase for Notch ligand.* J Biol Chem, 2005. **280**(23): p. 22335-42.

146. Kimmel, C.B., et al., *Stages of embryonic development of the zebrafish.* Dev Dyn, 1995. **203**(3): p. 253-310.

147. *Zebrafish.* Pratical Approach, ed. C. Nusslein-Volhard and D. R. 2002, New York: Oxford University Press. 303.

148. Nijman, S.M., et al., *A genomic and functional inventory of deubiquitinating enzymes.* Cell, 2005. **123**(5): p. 773-86.

149. Overstreet, E., E. Fitch, and J.A. Fischer, *Fat facets and Liquid facets promote Delta endocytosis and Delta signaling in the signaling cells.* Development, 2004. **131**(21): p. 5355-66.

150. Hergovich, A., et al., *Centrosome-associated NDR kinase regulates centrosome duplication.* Mol Cell, 2007. **25**(4): p. 625-34.

151. Sawin, K.E., et al., *Mitotic spindle organization by a plus-end-directed microtubule motor.[see comment].* Nature, 1992. **359**(6395): p. 540-3.

152. Uzbekov, R., C. Prigent, and Y. Arlot-Bonnemains, *Cell cycle analysis and synchronization of the Xenopus laevis XL2 cell line: study of the kinesin related protein XlEg5.* Microsc Res Tech, 1999. **45**(1): p. 31-42.

153. Houliston, E., et al., *The kinesin-related protein Eg5 associates with both interphase and spindle microtubules during Xenopus early development.* Dev Biol, 1994. **164**(1): p. 147-59.

154. Mayer, T.U., et al., *Small molecule inhibitor of mitotic spindle bipolarity identified in a phenotype-based screen.* Science, 1999. **286**(5441): p. 971-4.

155. Amsterdam, A., et al., *Identification of 315 genes essential for early zebrafish development.* Proc Natl Acad Sci U S A, 2004. **101**(35): p. 12792-7.

156. Furutani-Seiki, M., et al., *Neural degeneration mutants in the zebrafish, Danio rerio*. Development, 1996. **123**: p. 229-39.

157. Wilson, P.G., M.T. Fuller, and G.G. Borisy, *Monastral bipolar spindles: implications for dynamic centrosome organization*. Journal of Cell Science, 1997. **110**(Pt 4): p. 451-64.

158. Heck, M.M., et al., *The kinesin-like protein KLP61F is essential for mitosis in Drosophila*. Journal of Cell Biology, 1993. **123**(3): p. 665-79.

159. Wagner, D.S., et al., *Maternal control of development at the midblastula transition and beyond: mutants from the zebrafish II*. Dev Cell, 2004. **6**(6): p. 781-90.

160. Dosch, R., et al., *Maternal control of vertebrate development before the midblastula transition: mutants from the zebrafish I*. Dev Cell, 2004. **6**(6): p. 771-80.

161. Link, B.A., et al., *The perplexed and confused mutations affect distinct stages during the transition from proliferating to post-mitotic cells within the zebrafish retina*. Dev Biol, 2001. **236**(2): p. 436-53.

162. Bingham, S., et al., *Neurogenic phenotype of mind bomb mutants leads to severe patterning defects in the zebrafish hindbrain*. Dev Dyn, 2003. **228**(3): p. 451-63.

163. Bingham, S., et al., *Neurogenic phenotype of mind bomb mutants leads to severe patterning defects in the zebrafish hindbrain*. Developmental Dynamics, 2003. **228**(3): p. 451-63.

164. Bilotta, J. and S. Saszik, *The zebrafish as a model visual system.* Int J Dev Neurosci, 2001. **19**(7): p. 621-9.

165. Sawin, K.E. and T.J. Mitchison, *Mutations in the kinesin-like protein Eg5 disrupting localization to the mitotic spindle.* Proceedings of the National Academy of Sciences of the United States of America, 1995. **92**(10): p. 4289-93.

166. Reilein, A.R., et al., *Regulation of molecular motor proteins.* Int Rev Cytol, 2001. **204**: p. 179-238.

167. Punga, T., M.T. Bengoechea-Alonso, and J. Ericsson, *Phosphorylation and ubiquitination of the transcription factor sterol regulatory element-binding protein-1 in response to DNA binding.* J Biol Chem, 2006. **281**(35): p. 25278-86.

168. Dada, L.A., et al., *Phosphorylation and ubiquitination are necessary for Na,K-ATPase endocytosis during hypoxia.* Cell Signal, 2007.

169. Wu, R.C., et al., *SRC-3 Coactivator Functional Lifetime Is Regulated by a Phospho-Dependent Ubiquitin Time Clock.* Cell, 2007. **129**(6): p. 1125-40.

170. Buchman, J.J. and L.H. Tsai, *Spindle regulation in neural precursors of flies and mammals.* Nat Rev Neurosci, 2007. **8**(2): p. 89-100.

171. Das, T., et al., *In vivo time-lapse imaging of cell divisions during neurogenesis in the developing zebrafish retina.* Neuron, 2003. **37**(4): p. 597-609.

172. Badano, J.L., T.M. Teslovich, and N. Katsanis, *The centrosome in human genetic disease.* Nat Rev Genet, 2005. **6**(3): p. 194-205.

173. Parvin, J.D. and S. Sankaran, *The BRCA1 E3 ubiquitin ligase controls centrosome dynamics.* Cell Cycle, 2006. **5**(17): p. 1946-50.

174. Sankaran, S. and J.D. Parvin, *Centrosome function in normal and tumor cells.* J Cell Biochem, 2006. **99**(5): p. 1240-50.

175. Young, A., et al., *Cytoplasmic dynein-mediated assembly of pericentrin and gamma tubulin onto centrosomes.* Mol Biol Cell, 2000. **11**(6): p. 2047-56.

176. Purohit, A., et al., *Direct interaction of pericentrin with cytoplasmic dynein light intermediate chain contributes to mitotic spindle organization.* J Cell Biol, 1999. **147**(3): p. 481-92.

177. Christodoulou, A., et al., *Motor protein KIFC5A interacts with Nubp1 and Nubp2, and is implicated in the regulation of centrosome duplication.* J Cell Sci, 2006. **119**(Pt 10): p. 2035-47.

178. Goshima, G. and R.D. Vale, *The roles of microtubule-based motor proteins in mitosis: comprehensive RNAi analysis in the Drosophila S2 cell line.* J Cell Biol, 2003. **162**(6): p. 1003-16.

179. Barton, N.R., A.J. Pereira, and L.S. Goldstein, *Motor activity and mitotic spindle localization of the Drosophila kinesin-like protein KLP61F.* Molecular Biology of the Cell, 1995. **6**(11): p. 1563-74.

180. Uzbekov, R. and C. Prigent, *Clockwise or anticlockwise? Turning the centriole triplets in the right direction!* FEBS Lett, 2007. **581**(7): p. 1251-4.

181. Paoletti, A., et al., *Most of centrin in animal cells is not centrosome-associated and centrosomal centrin is confined to the distal lumen of centrioles.* J Cell Sci, 1996. **109 (Pt 13)**: p. 3089-102.

182. DeBonis, S., et al., *Interaction of the mitotic inhibitor monastrol with human kinesin Eg5.* Biochemistry, 2003. **42**(2): p. 338-49.

183. Krzysiak, T.C., et al., *A structural model for monastrol inhibition of dimeric kinesin Eg5.* Embo J, 2006. **25**(10): p. 2263-73.

184. Maliga, Z., T.M. Kapoor, and T.J. Mitchison, *Evidence that monastrol is an allosteric inhibitor of the mitotic kinesin Eg5.* Chemistry & Biology, 2002. **9**(9): p. 989-96.

185. Zimmerman, W. and S.J. Doxsey, *Construction of centrosomes and spindle poles by molecular motor-driven assembly of protein particles.* Traffic, 2000. **1**(12): p. 927-34.

186. Cho, J.H., et al., *Depletion of CPAP by RNAi disrupts centrosome integrity and induces multipolar spindles.* Biochem Biophys Res Commun, 2006. **339**(3): p. 742-7.

187. Doxsey, S., D. McCollum, and W. Theurkauf, *Centrosomes in cellular regulation.* Annu Rev Cell Dev Biol, 2005. **21**: p. 411-34.

188. Doxsey, S.J., *Centrosomes as command centres for cellular control.* Nat Cell Biol, 2001. **3**(5): p. E105-8.

189. Abal, M., G. Keryer, and M. Bornens, *Centrioles resist forces applied on centrosomes during G2/M transition.* Biol Cell, 2005. **97**(6): p. 425-34.

190. Cassimeris, L. and J. Morabito, *TOGp, the human homolog of XMAP215/Dis1, is required for centrosome integrity, spindle pole organization, and bipolar spindle assembly.* Mol Biol Cell, 2004. **15**(4): p. 1580-90.

191. Bahe, S., et al., *Rootletin forms centriole-associated filaments and functions in centrosome cohesion.* J Cell Biol, 2005. **171**(1): p. 27-33.

192. Guarguaglini, G., et al., *The forkhead-associated domain protein Cep170 interacts with Polo-like kinase 1 and serves as a marker for mature centrioles.* Mol Biol Cell, 2005. **16**(3): p. 1095-107.

193. Xu, P. and J. Peng, *Dissecting the ubiquitin pathway by mass spectrometry.* Biochim Biophys Acta, 2006. **1764**(12): p. 1940-7.

194. Cottrell, G.S., et al., *Ubiquitin-dependent down-regulation of the neurokinin-1 receptor.* J Biol Chem, 2006. **281**(38): p. 27773-83.

195. Avraham, E., et al., *Phosphorylation of Parkin by the cyclin-dependent kinase 5 at the linker region modulates its ubiquitin-ligase activity and aggregation.* J Biol Chem, 2007. **282**(17): p. 12842-50.

196. Berwick, D.C. and J.M. Tavare, *Identifying protein kinase substrates: hunting for the organ-grinder's monkeys.* Trends Biochem Sci, 2004. **29**(5): p. 227-32.

197. Liu, M., et al., *Inhibition of the mitotic kinesin Eg5 up-regulates Hsp70 through the phosphatidylinositol 3-kinase/Akt pathway in multiple myeloma cells.* J Biol Chem, 2006. **281**(26): p. 18090-7.

198. Marcus, A.I., et al., *Mitotic kinesin inhibitors induce mitotic arrest and cell death in Taxol-resistant and -sensitive cancer cells.* Journal of Biological Chemistry, 2005. **280**(12): p. 11569-77.

199. Carter, B.Z., et al., *Regulation and targeting of Eg5, a mitotic motor protein in blast crisis CML: overcoming imatinib resistance.* Cell Cycle, 2006. **5**(19): p. 2223-9.

200. Muller, C., et al., *Inhibitors of kinesin Eg5: antiproliferative activity of monastrol analogues against human glioblastoma cells.* Cancer Chemother Pharmacol, 2007. **59**(2): p. 157-64.

201. Duhl, D.M. and P.A. Renhowe, *Inhibitors of kinesin motor proteins--research and clinical progress.* Curr Opin Drug Discov Devel, 2005. **8**(4): p. 431-6.

202. Shepard, J.L., et al., *A zebrafish bmyb mutation causes genome instability and increased cancer susceptibility.* Proc Natl Acad Sci U S A, 2005. **102**(37): p. 13194-9.

203. Shepard, J.L., et al., *A mutation in separase causes genome instability and increased susceptibility to epithelial cancer.* Genes Dev, 2007. **21**(1): p. 55-9.

204. Carmany-Rampey, A. and C.B. Moens, *Modern mosaic analysis in the zebrafish.* Methods, 2006. **39**(3): p. 228-38.

205. Linney, E., et al., *Transgene expression in zebrafish: A comparison of retroviral-vector and DNA-injection approaches.* Dev Biol, 1999. **213**(1): p. 207-16.

206. Kufe, D.W.e.a., *Cancer Medicine. 6th ed.* 2003, Hamilton: BC Decker Inc.